CHALMERS

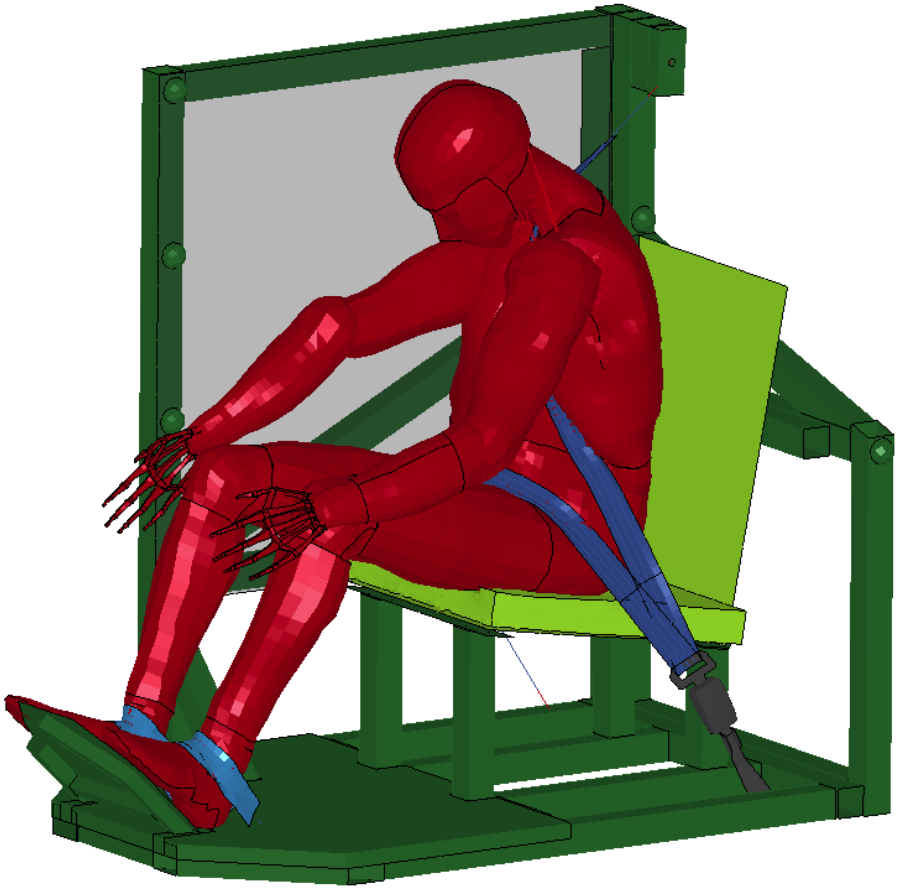

# Evaluation of THUMS Human FE Model in Oblique Frontal Sled Tests against Post Mortem Human Subject Test Data

*Master's thesis in Solid and Structural Mechanics*

ELIN SIBGÅRD
SOFIE WISTRAND

Department of Applied Mechanics
*Division of Vehicle Safety*
CHALMERS UNIVERSITY OF TECHNOLOGY
Gothenburg, Sweden 2012
Master's thesis 2012:23

MASTER'S THESIS IN SOLID AND STRUCTURAL MECHANICS

# Evaluation of THUMS Human FE Model in Oblique Frontal Sled Tests against Post Mortem Human Subject Test Data

ELIN SIBGÅRD
SOFIE WISTRAND

Department of Applied Mechanics

*Division of Vehicle Safety*

CHALMERS UNIVERSITY OF TECHNOLOGY

Gothenburg, Sweden 2012

Evaluation of THUMS Human FE Model in Oblique Frontal Sled Tests against Post Mortem Human Subject Test Data
ELIN SIBGÅRD
SOFIE WISTRAND



Master's thesis 2012:23
ISSN 1652-8557
Department of Applied Mechanics
Division of Vehicle Safety
Chalmers University of Technology
SE-412 96 Gothenburg
Sweden
Telephone: +46 (0)31-772 1000

Cover:
A simulation of THUMS in a model of the Graz test sled.

Chalmers Reproservice
Gothenburg, Sweden 2012

Evaluation of THUMS Human FE Model in Oblique Frontal Sled Tests against Post Mortem Human Subject Test Data
Master's thesis in Solid and Structural Mechanics
ELIN SIBGÅRD
SOFIE WISTRAND
Department of Applied Mechanics
Division of Vehicle Safety
Chalmers University of Technology

# Abstract

Last year 319 people were killed in traffic accidents in Sweden. The majority of these were car drivers and passengers. In order to minimize the number of people killed in traffic, vehicle safety is very important.

Crash tests are frequently used to develop safety systems in cars. Both mechanical testing with crash dummies and simulations with mathematical models of the crash dummies are used. However, a disadvantage with the crash dummies is that they have limited biofidelity in order to be durable for repeatable testing. Therefore there is a difference between their kinematics in a collision compared to the kinematics of humans.

To be able to predict the response of a human body, mathematical human body models have recently been developed, e.g. the Total HUman Model for Safety (THUMS). Since THUMS is a relatively new model there have been limited validation done to establish its kinematic performance. In pure frontal impact some validations have been done, by means of pendulum and sled tests, but in oblique frontal impacts, a rather common crash situation, no evaluation have been done.

The aim of this project is to evaluate the kinematics of THUMS version 2.21 against Post Mortem Human Subjects (PMHS) in oblique frontal collisions. Two sled test series with belted PMHS and Hybrid III 50th percentile male (HIII) dummies have been used in the project. The velocities in the tests were approximately 30 km/h and the acceleration pulses in the sleds were approximately 13 g.

The two sled setups have been modelled and simulated with an HIII dummy model and with THUMS. The HIII simulations were used to validate the sled environment and then THUMS was evaluated against the PMHS data. The results consist of belt force, acceleration and displacement comparisons between the mechanical test results and the mathematical model predictions. The results from the HIII simulations shows good conformity with the HIII dummy test results for both sled environments.

In the THUMS evaluation there are issues with THUMS interaction with the simulated seat belt. The belt elements entangle with the elements in the neck and the chest of THUMS and the belt therefore get stuck. However, THUMS replicates post mortem human kinematics even though THUMS appears to be somewhat stiffer than the PMHS.

Keywords: THUMS, PMHS, Hybrid III 50th percentile male, Oblique frontal collision, Sled test

# Preface

This master thesis is the final part of a Master of Science in Applied Mechanics at Chalmers University of Technology. The work reported in this thesis was carried out at Epsilon AB in Göteborg, Sweden, during the spring of 2012. The work was supervised by Johan Iraeus at Epsilon AB. Examiner was Karin Brolin at the Division of Vehicle Safety at Chalmers University of Technology.

# Acknowledgements

We want to express our gratitude to Johan Iraeus who helped make this thesis possible. We also want to thank Bengt Pipkorn and Mats Lindquist for their knowledge and insight on the thesis subject. Thanks to Karin Brolin who agreed to be our examiner. Thanks to Fredrik Törnvall, Johan Davidsson, Kristian Holmkvist and Mats Y. Svensson who have helped us to get the information we have needed.

Göteborg, June 2012

Elin Sibgård, Sofie Wistrand

# Definitions and Abbrevations

**Accelerometers** Measuring equipment that measures the acceleration in 1, 2 or 3 directions.

**Acromion** A bone, part of the scalpula, in the shoulder, see figure 0.0.1.

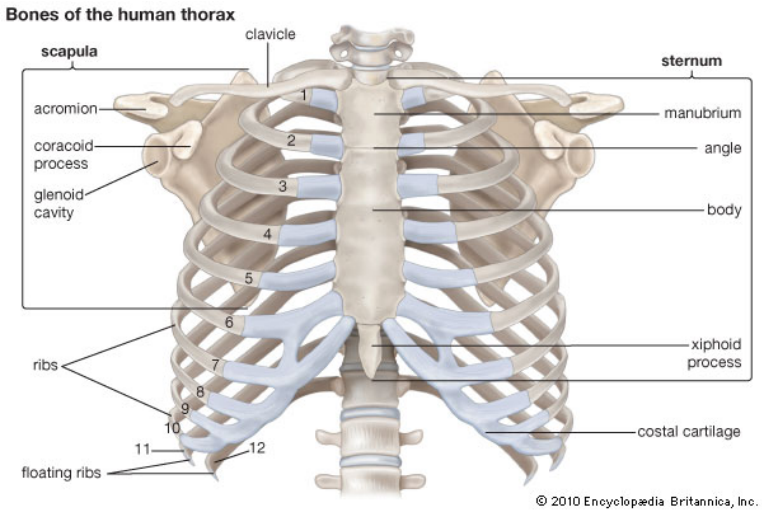


Figure 0.0.1: *Bones of the human thorax.* Britannica *(2012a)*

.

**ANSA** A pre-processing tool for model build-up. Includes CAD and meshing tools as well as material and property information used in LS-DYNA and other simulation software. (*ANSA* 2011).

**Biofidelity** Lifelike in appearance or response.

**CAD** Computer Aided Design.

**Depenetrate** A tool in ANSA that can adjust geometry to remove intersections between parts.

**HIII** Hybrid III 50th percentile male crash test dummy. The most widely used crash test dummy in the world for the evaluation of automotive safety restraint systems in frontal crash testing.

**HyperGraph** A data analysing tool. (*HyperGraph* 2011).

**LS-DYNA** A general-purpose finite element program capable of simulating complex real world problems. (*LS-DYNA* 2012).

**MetaPost** A general purpose post-processor used, in this project, for tracking movements in a video. (*MetaPost* 2011).

**PHMS** Post Mortem Human Subject.

**sbtout** Seat belt output file in LS-DYNA which includes seat belt forces, elongation and slipring slip.

**Shape factor** A material property in MAT 57 in LS-DYNA. The factor determines the hysteresis effect of the force-deflection curve

**Slipring** A point where the belt is angled.

**T1** Thoracic vertebrae 1, the bone connecting the first set of ribs in the spine, counted from the top, see figure 0.0.2.

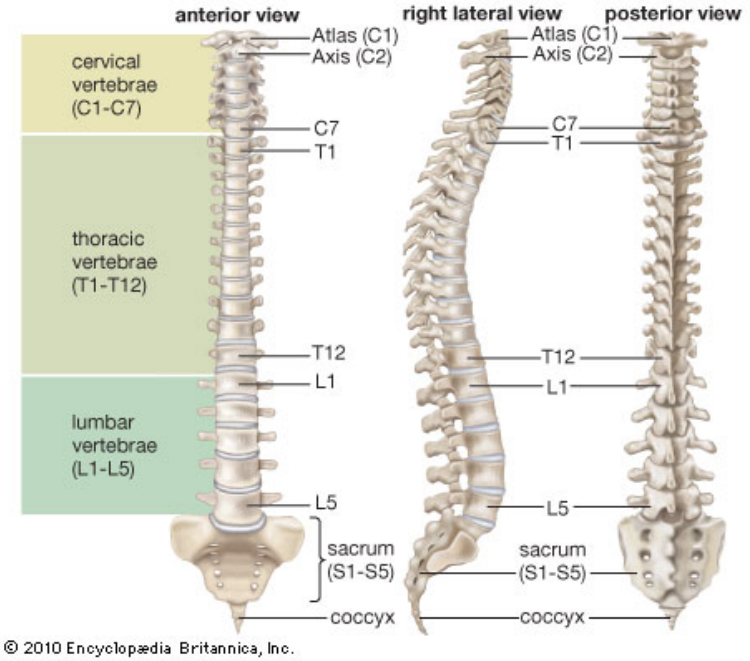


Figure 0.0.2: *The human vertebral column.* Britannica *(2012b)*

.

**T6** Thoracic vertebrae 6, the bone connecting the 6th set of ribs, counted from the top, see figure 0.0.2.

**T12** Thoracic vertebrae 12, the bone connecting the 12th set of ribs, counted from the top, see figure 0.0.2.

**THUMS** Total HUman Model for Safety, an advanced injury-simulation software that measures injury to parts of the body not measurable with conventional crash test dummies.

**Video tracking** Measuring the movement by following a point in a video.

# Contents

# 1 Introduction

## 1.1 Purpose

Evaluate the kinematics of Total HUman Model for Safety (THUMS) against Post Mortem Human Subjects (PMHS) in oblique frontal sled tests.

## 1.2 Problem Definition

The evaluation focuses on oblique frontal collisions with impact angles between 0° and 45°, where 0° is a pure frontal impact. The initial velocity in which the kinematics is evaluated is approximately 30 km/h in all angles. Both near and far sided belt systems are included in the evaluation. In a near sided crash the subject moves towards the door and in a far sided crash the subject moves away from the door, see figure 1.2.1.

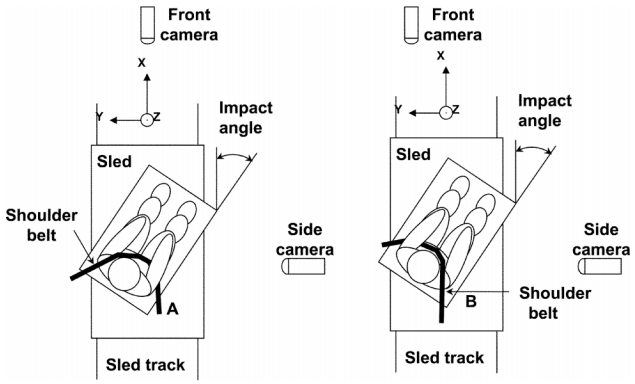


Figure 1.2.1: *Near and far side belt system. From Törnvall et al. (2008a).*

## 1.3 Background

The safety of vehicles today has increased dramatically in recent years. Last year 319 people were killed in traffic accidents in Sweden (*Transportstyrelsen* 2012), the majority of these, 175 people, were car drivers and passengers. This can be compared to 1970 when the fatalities were 1307. Both mechanical testing as well as mathematical simulations has contributed to the increased occupant safety. In the mechanical testing, crash test dummies are often used as occupant substitutes. In the mathematical simulations, mathematical models of the mechanical crash dummies are maily used.

The biofidelity of the mechanical crash test dummies is limited, partly due to the fact that the dummies need to be durable and reliable for repeatable testing and partly due to other reasons like cost and manufacturing. The mathematical models of the crash test dummies are developed to predict the behavior of the mechanical crash test dummies and not the behavior of humans in a crash. Therefore the mathematical crash test dummy models has the same problems with biofidelety as the mechanical counterpart.

In car occupant safety research sled tests are often used to create mechanical crash situations in order to investigate the biomechanical response of a human in a car crash. In a sled test a car, or part of a car, is placed on a track and is either given an initial velocity which is then decelerated or is accelerated backward from 0 velocity. In some tests PMHS are used as occupant substitutes. However there are some issues with these human cadavers that do not make them ideal when evaluating human kinematics of a specific size of

persons, like the 50th percentile male. The PMHS differ in age, weight and length and it is complicated to estimate the kinematic of a medium person using them. The kinematics of a PMHS also differs some to that of a living human. Apart from the physical issues, it is very expensive to perform PMHS tests and there is a lack of PMHS to use. When it comes to research performed that is commercially founded it might not be considered ethical to use them.

To develop a tool with a wide field of application within safety research, detailed mathematical human body models are being developed e.g. the THUMS model. These mathematical models are made to predict the behaviour of the human body in a crash and would therefore be more useful than crash dummies and easier and less expensive to use than the PMHS.

More than 70% of the frontal collisions are oblique impacts according to Ragland et al. (2001). Up till now, some work has been done on validation of the THUMS model in frontal and rear collisions, by means of both pendulum and sled tests (Oshita et al. (2002) and Chawla et al. (2005)), but to our knowledge nothing has been published on oblique frontal collisions.

# 2 Method

Data from two test series of oblique frontal collision sled tests are used in this project. They are described in Kallieris (1982), Törnvall et al. (2005), Törnvall et al. (2008a) and Törnvall et al. (2008b). Both tests include PMHS and HIII dummy test data.

The two sled environments are reconstructed in the pre-processor *ANSA* (2011), as will be described in chapter 2.2.1 and 2.2.2. The sleds are simulated with a mathematical HIII 50th percentile male dummy model, created by *LSTC*, which is described in chapter 2.3. The simulation data are compared to accelerometer data and videos from the mechanical HIII tests in order to validate the sled environments. As the HIII dummy is well defined it is expected that the error from the HIII model is small. Unknown parameters in the sled models are optimized to create conformity between test data and simulation data.

When the sled environment is validated, a human mathematical model, THUMS, replaces the HIII model in the sleds and oblique frontal collisions are simulated. This is described in chapter 2.4. The simulation data is compared to the data and videos from the PMHS tests and the results are analyzed. A flow chart showing the procedure is seen in figure 2.0.1.

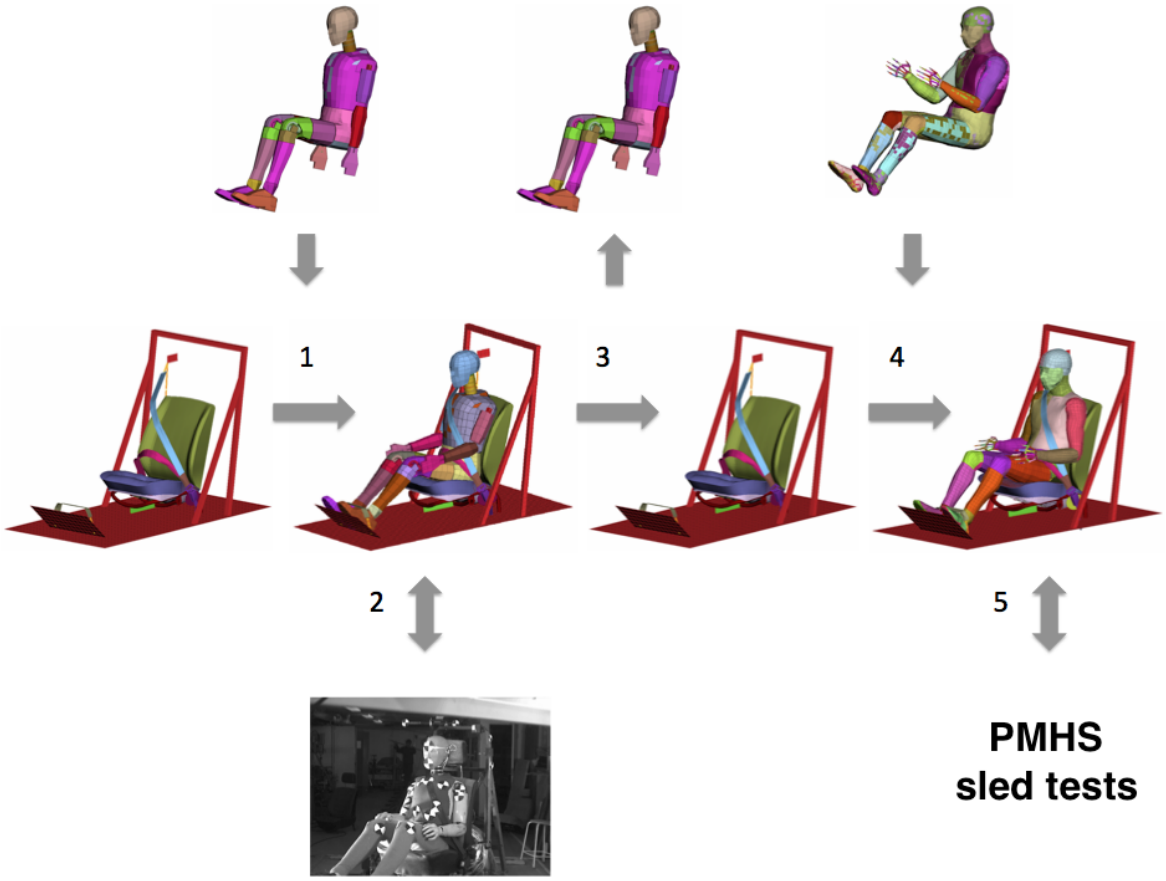


Figure 2.0.1: *Method: 1. HIII simulation dummy is inserted into the sled model and the collisions are simulated. 2. The HIII simulated kinematic response is validated against HIII dummy test data. 3. HIII is removed from the sled when the validation is complete. 4. THUMS is inserted into the validated sled and the collisions are simulated. 5. THUMS simulated kinematic response is evaluated against PMHS test data.*

## 2.1 Mechanical Sled Tests

The two test series used in the project were performed in Heidelberg, Germany and Graz, Austria and will further on be referred to as Heidelberg respectively Graz. The Heidelberg tests are described in Kallieris (1982) and Törnvall et al. (2005) while the Graz tests are described in Törnvall et al. (2008a) and Törnvall et al. (2008b).

The mechanical tests were performed within 0°-45° angle from pure longitudinal direction. The tests were run as both near and far sided collisions and a three-point seat belt was used.

### 2.1.1 Graz Test Setup

In 2006 Törnvallet al. performed frontal oblique crash tests in Graz, Austria, using PMHS and dummies. This work is reported in Törnvall et al. (2008a) and Törnvall et al. (2008b). Three PMHS were used and they were each tested in three angles, 0°, 30° near sided and 45° far sided. A HIII dummy was also tested in the same three angles, once in each angle. The average velocity was 26.6 km/h and the mean acceleration was 13.9 g. Table 2.1.1 shows the test subjects in the Graz test.

Table 2.1.1: The test subjects used in the Graz test. Redrawn from Törnvall et al. (2008a).

| Test subject | sex | Age [years] | Weight [kg] | Length [m] | Chest depth [m] |
|---|---|---|---|---|---|
| PMHS 1 | F | 84 | 62 | 1.64 | 0.21 |
| PMHS 2 | M | 59 | 61 | 1.66 | 0.21 |
| PMHS 3 | M | 71 | 94 | 1.79 | 0.30 |
| HIII | M | 30-45 | 78 | 1.79 | 0.22 |

According to Törnvall et al. (2008a) and Törnvall et al. (2008b) the PMHS were fully clothed in cotton whilst the HIII dummy did not wear any clothing. All test subjects were positioned in the sled with their backs leaning on the backrest, their hands on their knees and with their feet put together, strapped to a footrest.

According to Törnvall et al. (2008b) the PMHS torsos were hard to position so there might be some differences in their positions. The upper body of PMHS 3 was, in contrast to PMHS 1 and 2, held up with a band that was released when the sled started to move. Also the heads, for all PMHS, were held up with a band and released.

In the mechanical tests tri-axial accelerometers measuring x, y and z linear acceleration were attached to the test subjects, both PMHS and HIII. Two were placed on the head; front and rear, one on T1 and two were placed on the upper arms, see figure 2.1.1. The sled accelerations were also measured during the tests as well as the force responses in both shoulder and lap belt. It is unknown where the force measuring devices were situated.

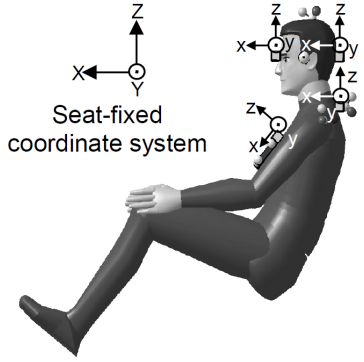


Figure 2.1.1: *The positions of the accelerometers. From Törnvall et al. (2008a)*

The mechanical tests were recorded using three video cameras in order to make 3D tracking possible. PMHS 3 was impacted twice in 0° angle since the top camera did not function properly the first test. Tracking of the displacements of the head, T1 and shoulders were performed on all test subjects. The accelerometer signals, belt forces and displacements are included in Törnvall et al. (2008a) for both PMHS and HIII.

Videos from the tests (*Unpublished material from the Graz test* 2012) have been studied during this project. In the first test with PMHS 1 in 0°, the seat foam was not attached to the seat which caused the foam to slide. In all the following tests the seat foam was strapped to the seat.

#### Graz Sled

The sled in the Graz test was a steel rig with a simplified car seat, a footrest and a generic door. It was drawn up in CAD, which can be seen in figure 2.1.2. The seat and back was made out of plywood of unspecified quality and polyethylene foam was used as seat couching. The foam was an ETHAFOAM $220 - E$, which was produced by Dow Plastics. It has a closed cell structure and a density of 35 kg/m$^3$. The compressive strength is 40 kPa at 10%, 55 kPa at 25% and 110 kPa at 50%. A 10 mm MAKROCLEAR polycarbonate board was used to replace the door window according to *Plastmästarn* (2012).

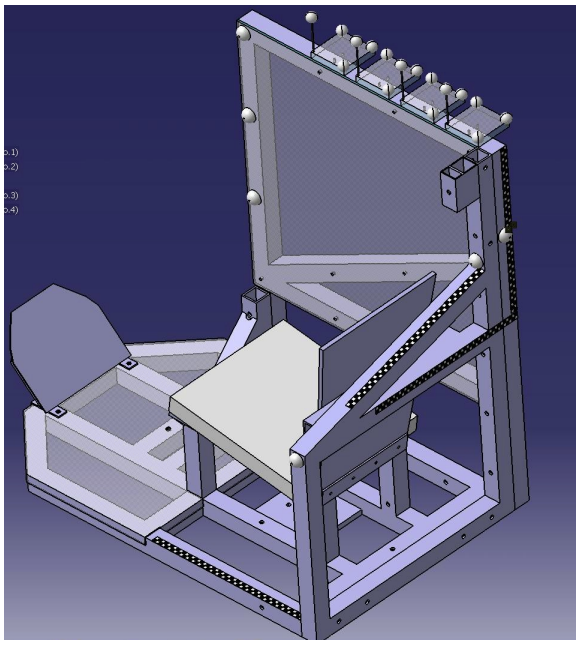

Figure 2.1.2: *CAD image of the Graz sled. From* Unpublished material from the Graz test *(2012).*

The belt was a three-point belt with a standard buckle and conveyer belt without force limitation. The positions and distances to the belt attachments are according to Törnvall et al. (2008a), see figure 2.1.3. The upper end of the belt was attached to a Aluminium box that was fixed on to the rig with a bolt. At the upper and the lower attachment points the belt was tied to the rig using a simple knot. The belt was a high stretch belt with 16% stretch at 10 kN. It was produced by Autoliv (production number 570 419 00H) according to Törnvall et al. (2008a). A new belt and seat padding was used for each test.

### 2.1.2 Heidelberg Test Setup

Kallieris performed frontal oblique sled tests using PMHS in Heidelberg, Germany. The work is reported in Kallieris (1982). In August 2000 Chalmers replicated these tests using an HIII dummy. This work is partly reported in Törnvall et al. (2005).

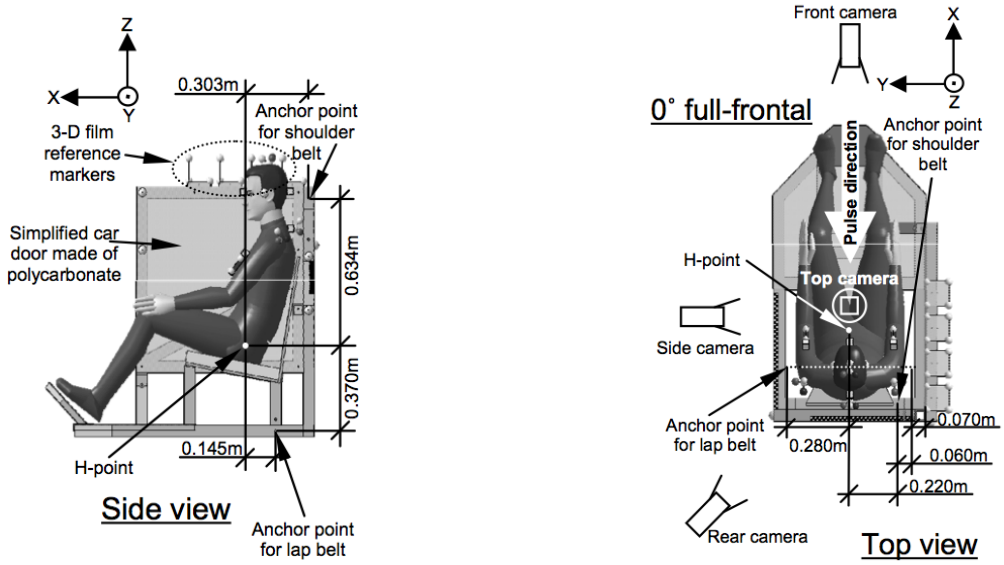


Figure 2.1.3: *Test subject position in the Graz sled and the belt anchor locations. From Törnvall et al. (2008a).*

Thirteen PMHS were used in Kallieris test series and they were each tested once in one of 6 angles. Tests were performed in ±15°, ±30° and ±45° angle. The belt setup was changed between near and far sided collision in each angle since the sled was only rotated in one direction. Figure 1.2.1 shows the belt position. The tests were performed using a moving sled, which was decelerated to stop using steel band brakes. The mean velocity in the collisions was 30.3 km/h in all tests according to *Unpublished material from the Heidelberg test* (2012). Table 2.1.2 shows the test subjects in the Heidelberg test.

Table 2.1.2: The test subjects used in the Heidelberg tests. Redrawn from Törnvall et al. (2005).

| Test subject | sex | Age [years] | Weight [kg] | Length [m] | Chest depth [m] | Test angle [°] | Belt geometry |
|---|---|---|---|---|---|---|---|
| 79/14 | F | 56 | 64 | 1.67 | 0.22 | 15 | Near |
| 79/20 | M | 59 | 57 | 1.62 | 0.20 | 15 | Near |
| 79/21 | M | 52 | 89 | 1.69 | 0.24 | 15 | Far |
| 79/22 | M | 23 | 75 | 1.70 | 0.22 | 30 | Near |
| 79/23 | M | 39 | 81 | 1.80 | 0.25 | 30 | Near |
| 79/26 | M | 24 | 72 | 1.85 | 0.23 | 30 | Far |
| 79/29 | F | 35 | 70 | 1.70 | 0.22 | 30 | Far |
| 80/07 | M | 69 | 69 | 1.67 | 0.21 | 45 | Near |
| 80/09 | M | 45 | 73 | 1.68 | 0.25 | 45 | Near |
| 80/16 | M | 56 | 88 | 1.64 | 0.28 | 45 | Near |
| HIII | M | 30-45 | 78 | 1.79 | 0.22 | 15, 30, 45 | Both |

The PMHS were wearing clothing of unspecified material. However the arms and legs were not covered. The heads were attached to the seat with tape that broke as the deceleration started. According to Törnvall et al. (2005) the PMHS were postured in a normal car occupant posture. But the report also states that "It was difficult to position the test subjects in exactly the same position for each test".

Accelerometers measuring x and z linear accelerations were mounted on the sled, on T6 and on the left respectively right side of the head. The forces originating in the shoulder and lap belts were measured as well but it is uncertain where the force measuring devices were located. Accelerometer data from the tests were scanned from paper copies by Fredrik Törnvall according to Törnvall et al. (2005). Accelerometer signals and belt forces are included in *Unpublished material from the Heidelberg test* (2012) but some of the data are missing. The T6 accelerometer signals and shoulder belt forces are only found on 10 PMHS, none of which were tested in 45° far side collision.

The tests were filmed using high speed film and photos were taken before and after each test. Some of these films and photos are included in *Unpublished material from the Heidelberg test* (2012). Törnvall performed 3D tracking on the displacement of the shoulders using videos from the tests. The contours of the shoulders were used in the tracking. The tracking was done on the loaded shoulder in 30° far side and the unloaded shoulder in 30° and 45° near side. This tracking was done on 7 PMHS and the results are reported in Törnvall et al. (2005).

When Chalmers replicated the test in August 2000 (Törnvall et al., 2005) a HIII 50th percentile male dummy was used. A sled similar to Kallieris sled was built and the HIII dummy was tested in the same angles as the PMHS in Kallieris test. The dummies were dressed in cotton clothing according to Törnvall et al. (2005). Their hands were placed on the knees and their feet were strapped to the footrest.

Accelerometers were mounted on the dummy along the spine at the corresponding level of T1, T6, T12 and the pelvis. The back and front of the head as well as the sled were also measured by accelerometers. Unfortunately the accelerometers were not zeroed out before the tests started. The belt forces on the lap and shoulder belt were also measured. This data are included in *Unpublished material from the Heidelberg test* (2012). These tests were also filmed using a video camera (1000 fps). However only the video from the test in 30° far side was included in *Unpublished material from the Heidelberg test* (2012).

The dummy accelerometer coordinate systems appear to be inconsistent. The accelerometer on T1 appears to have a right hand coordinate system but the ones on T6, T12 and pelvis a left hand coordinate systems. All systems have x in the frontal direction of the test subject, and z downwards. During the sled validation in chapter 2.3 the accelerometer data is rotated so that the coordinate systems are right hand coordinate systems with z upwards and x in the frontal direction of the test subject.

### Heidelberg Sled

The original Heidelberg sled was a steel rig with a brand new Volkswagen Golf Mk1 seat attached. The seat had an adherent three-point seat belt system including a retractor. The seat belt was a high streched belt with 17% stretch at 10 kN. A new seat and belt were used for each test. The sled geometry and belt anchor positions are documented in Törnvall et al. (2005), see figure 2.1.5. The golf seat has a metal plate attached to the buckle side of the seat. This plate limits the buckle to move more than 15 mm inward the seat, see figure 2.1.4. Material data for the Golf seat are not specified in Kallieris (1982), Törnvall et al. (2005) or any other document known to this project.

Figure 2.1.4: *The Golf Mk1 seat buckle.*

For the HIII dummy tests performed at Chalmers a reproduction of the original sled was used. However, unused Volkswagen Golf Mk1 seats could not be found and used passenger seats and belts from Volkswagen golf Mk1 were used instead according to Törnvall et al. (2005). The seats and belts were replaced between each test.

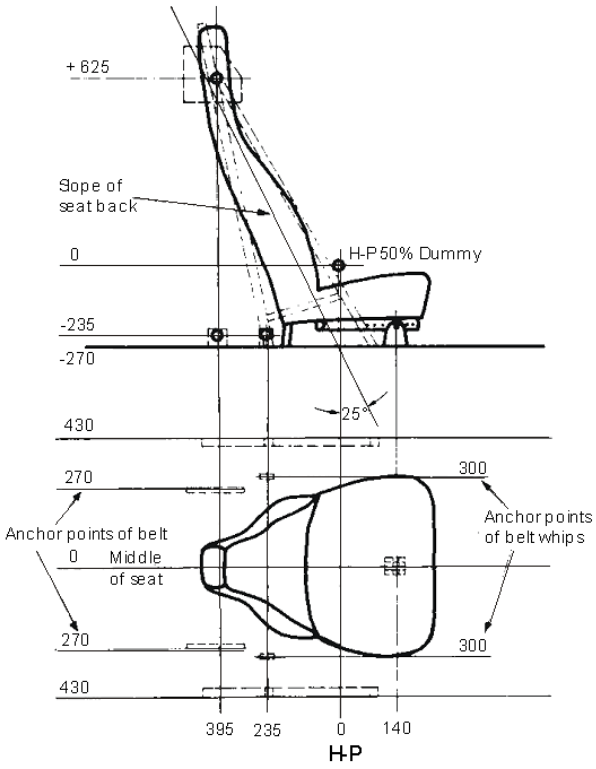


Figure 2.1.5: *Belt anchor positions and H-point of the Heidelberg sled. From Törnvall et al. (2005).*

## 2.2 Simulation Models

In order to simulate the mechanical sled tests, the sleds used in the tests are created as FE models. This is done in the pre-processor *ANSA* (2011). The creation of the sled simulation models are described in chapter 2.2.1 for the Graz sled and in chapter 2.2.2 for the Heidelberg sled.

The FE models of the test subjects used in this project are also presented below. In chapter 2.2.3 the HIII simulation model used is presented and in chapter 2.2.4 THUMS is presented.

### 2.2.1 Graz Sled Simulation Model

A simulation model of the Graz sled is created using the CAD model of the original sled. The CAD model is used as input in ANSA to create the FE model. The rig, plywood seat and polycarbonate window are modelled as shells. The shells are modelled at the centre of the original thickness. The majority of the shell elements in the sled are quadratic, see table 2.2.1. The seat foam is modelled as solid with volume hexa elements. The rig is meshed with an element length about 20 mm and the foot plate and the seat foam with an element length around 15 mm.

Table 2.2.1: The element types in the Graz sled simulation model.

| Element kind | Number of Elements |
|---|---|
| Shell Quads | 10402 |
| Shell Trias | 82 |
| Volume Hexas | 4860 |

The sled rig and footrest are assumed to be rigid. Data used for the MAKROCLEAR polycarbonate is taken from *MAKROCLEAR* (2012). The material for the aluminium box is chosen as the alloy AlMg1SiCu and the bolt holding the aluminium in place is a 10 mm 8.8 bolt. The material model in LS-DYNA choosen for the aluminium and the bolt, require a load curve defining effective stress versus effective plastic strain, see figure 2.2.1. The data in the figure are taken from from Mattson (2001) and *Bultens teknikhandbok* (1999).

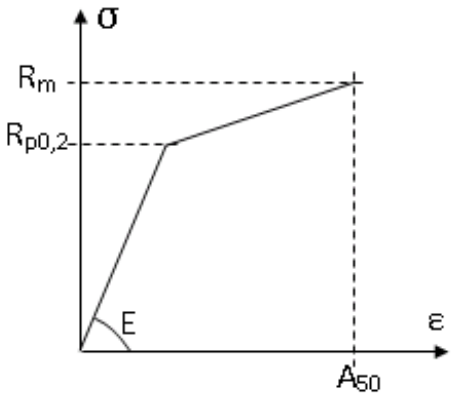


| | Aluminium | Bolt |
|---|---|---|
| Tensile stress $R_m$ [MPa] | 280 | 800 |
| Yield stress $R_{p0.2}$ [MPa] | 230 | 640 |
| Ultimate strain $A_{50\%}$ [MPa] | 8 | 12 |

Figure 2.2.1: *A stress strain diagram with the parameters needed for defining the load curve.*

For the seat padding material, data of polyethylene foam from Mills and Lyn (2001) is used. The foam in Mills and Lyn (2001) is a polyethylene foam with unknown cell structure and a density of $35kg/m^3$. The stress-strain curve is measured for a velocity of $4.4m/s$ and it reaches up to 50% strain. The curve is extrapolated using Equation 2 in Serifi et al. (2008) and put into the material model for low density foam (MAT57) in LS-DYNA.

An experimental material test is performed in Mills and Lyn (2001) resulting in a force-deflection curve. To determine the unloading properties of the foam, this test is simulated in LS-DYNA, see figure 2.2.2. Different shape factors are used in the material model in the simulation test, in order to find the correct angle of the unloading curve. The shape factor is chosen as 7.

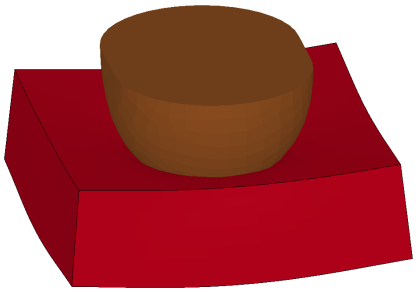

Figure 2.2.2: *Simulation of impact test.*

To get the density of the plywood seat it is measured and weighted. The plywood seat has the mass $m = 1.240kg$, the width $w = \frac{386+293}{2} = 339.5mm$, the length $l = 400mm$ and the height $h = 16mm$. The volume is, $V = w * l * h = 339.5 * 400 * 16 = 2172800mm^3$ and the density, $\rho = \frac{m}{V} = 5.71 * 10^{-7} kg/mm^3$.

To get the Young's modulus, E, a test is performed. The plywood seat is piled up on bricks and a weight is placed on the seat and the deflection, $\delta$, is measured. We have $P = mg = 0.95kN$, $\delta \approx 8.9mm$, $\alpha = \beta = 0.5$. Using the equations $I = \frac{bh^3}{12}$ and $\delta = \frac{Pl^3}{3EI}\alpha^2\beta^2$ we get:

$$I = \frac{bh^3}{12} = \frac{339.5 * 16^3}{12} = 115883$$

$$E = \frac{Pl^3}{3\delta I}\alpha^2\beta^2 = \frac{0.95 * 400^3}{3 * 8.9 * 115883} * 0.5^2 * 0.5^2 = 1.22812 \approx 1.23GPa.$$

The belt is modelled as a three-point 2D belt with a 100 mm long 1D belt at the upper belt end and a 200 mm long 1D belt at the lower end. The load curve for the seat belt is given by Autoliv, see figure 2.2.7. The material data used in the Graz sled are listed in table 2.2.2.

Table 2.2.2: The material data in the Graz simulation model.

| Material | Density $[kg/m^3]$ | Young's modulus [MPa] | HU | Beta | Shape factor | Load Curve |
|---|---|---|---|---|---|---|
| Steel | 7850 | 210 000 | | | | See A.2 |
| Plywood | 571 | 1230 | | | | See A.2 |
| Window | 1 200 | 3 200 | | | | See A.2 |
| Aluminium | 2700 | 69 000 | | | | See A.2 |
| Belt | | | | | | See figure 2.2.7 |
| Foam | 35 | | 0.01 | - | 7 | See figure 2.2.8 |

The belt is attached over the right shoulder and it is strapped over the chest, through the buckle slipring and then over the lap and fastened at the lower anchor point, see figure 2.1.3. Spring elements are added at the ends of the belt to represent the slack in the belt and the stretch in the belt anchors. The positioning of the belts on the HIII model and THUMS are described in chapter 2.3 and 2.4 respectively.

An automatic_surface_to_surface contact is applied between the window and the steel rig and an automatic_single_surface contact in the belt attachment. The contact between the plywood seat and the foam, which in the tests were kept in place with straps, is a tied_surface_to_surface offset. The simulated Graz sled is seen in figure 2.2.3. For more information on the material and contact cards see appendix A.

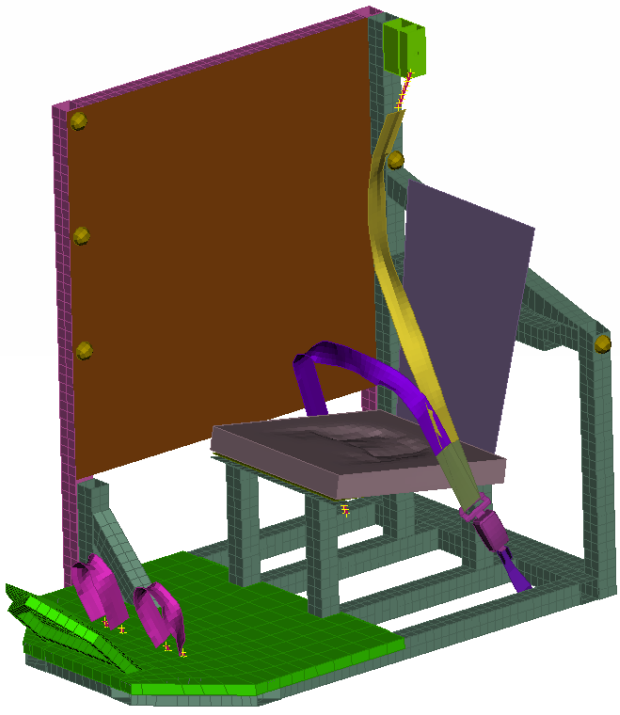

Figure 2.2.3: *Simulation model of the Graz sled.*

### 2.2.2 Heidelberg Sled Simulation Model

In order of creating the Heidelberg sled simulation model, a Volkswagen golf Mk1 seat is obtained, see figure 2.2.4. The seat geometry is measured using a FARO arm, a measuring equipment that gives coordinates for selected points on the measured object, see figure 2.2.5. The measured points are used as input in ANSA and the seat shape is created using these points. To obtain the seat H-point, measurements with an H-point dummy is also made, which can be seen in figure 2.2.6. From figure **??** and 2.1.5 the sled geometry and belt anchor positions are obtained.

Figure 2.2.4: *The golf seat used for geometry and material data.*

Figure 2.2.5: *Measuring the geometry of the seat structure.*

Figure 2.2.6: *Measuring of the H-point with an H-point dummy.*

The sled is modelled with shell elements apart from the foam, which is modelled with solid hexa volume elements. The majority of the shell elements are quadratic elements. The rig is modelled with an average element length of 30 mm, the steel seat with an average element length of 12 mm and the foam with an average element lengths of 15 mm. Table 2.2.3 shows the types of elements the sled consists of.

Table 2.2.3: The element types in the Heidelberg sled simulation model.

| Element kind | Number of Elements |
|---|---|
| Shell Quads | 8760 |
| Shell Trias | 286 |
| Volume Hexas | 8407 |

The sled and the seat back are modelled as rigid material. The plate preventing the belt buckle from penetrating into the seat is modelled as a rigid plate 15 mm from the buckle. The seat belt is modelled as a 1D belt from the retractor through the upper slipring and 100 mm towards the shoulder. Along the chest, through the buckle slipring and along the lap the belt is a 2D seat belt. The last 100 mm towards the lower belt anchor the belt is 1D. As an approximation for the belt curve, the Graz belt data is scaled in the y-direction (strain) by 17/16=1.06, see figure 2.2.7. The materials used in the Heidelberg sled are listed in the material data table 2.2.4.

Table 2.2.4: The material data in the Heidelberg simulation model.

| Material | Density $[kg/m^3]$ | Young's modulus [MPa] | HU | Beta | Shape factor | Load Curve |
|---|---|---|---|---|---|---|
| Steel | 7800 | 210 000 | | | | See figure B.2.1 |
| Belt | | | | | | See figure 2.2.7 |
| Foam | 67 | | 0.1 | 8000 | 2 | See figure 2.2.8 |

Spring elements are inserted at the anchors of the belts to represent the stretch in the belt attachment points and the film spool effect from the retractor. The spring elements are also used as slack in the belts. The position of the belts on the HIII model and THUMS are described in chapter 2.3 and 2.4 respectively.

Contacts are defined between the steel seat and the foam. Automatic_surface_to_surface contact type is chosen for the contacts. The Heidelberg sled is seen in figure 2.2.9. For more information on the material cards and sled contacts see appendix B.

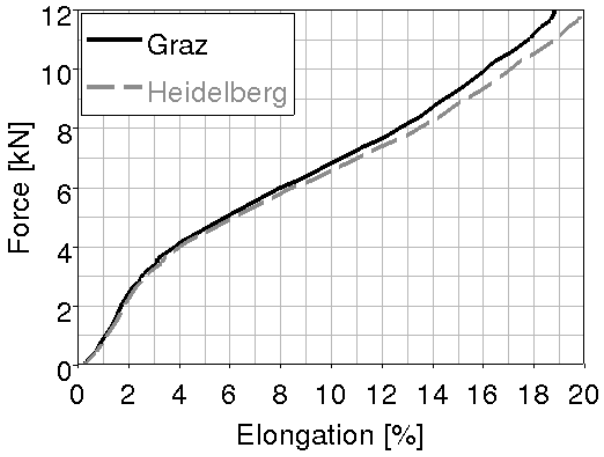


Figure 2.2.7: *Load curves for the seat belts in the Graz and Heidelberg sleds.*

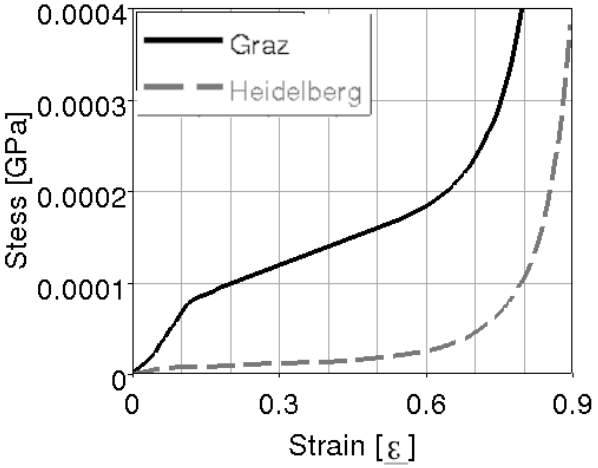


Figure 2.2.8: *Stress strain curves for the foams in the Graz and Heidelberg sleds.*

### 2.2.3 HIII simulation model

The HIII simulation model is a mathematical model of the physical HIII dummy. The HIII simulation model has rotational joints between all limbs which are used when HIII is positioned during the sled validation in chapter 2.3.

The simulation model is a FE-model with large elements with an average element side length of 24.5 mm. The version used is LSTC.H3.103008.V1.0.RigidFE.50th (Guha et al., 2008), see figure 2.2.10. The model has been validated in Kang and Xiao (2008).

### 2.2.4 THUMS

THUMS is a mathematical human body model of a 50% adult American male (Iwarmoto et al., 2002). The model is produces by *Toyota Central R&D Labs*. The model includes skeleton, muscle, organs and other internal structures. It simulates injuries sustained in actual car crashes. When THUMS is positioned for the simulation in chapter 2.4 only the arms are moved from their original position. THUMS limbs cannot be moved using the tools for crash dummies in *ANSA* (2011).

The THUMS used is *Version 2.21-040407* (2005) with changes according to Pipkorn and Kent (2011). THUMS has an average element side length of 6.8 mm, see figure 2.2.11.

## 2.3 Validation of the Sled Environments

The sled environments are validated using an HIII simulation model. The description of how this is done follows in this chapter. The HIII model is positioned as in the mechanical HIII dummy tests, in a normal car occupant posture (Törnvall et al., 2005). Contacts are defined between the dummy and the sleds and nodes corresponding to the accelerometers from the mechanical tests are located. The sled is rotated to the collision angle in which the tests were performed and the sled pulse used is the same as in the respective test angle. The mathematical model predications are compared with the mechanical test results and unknown parameters such as the seat material data, friction and belt properties are varied to see how these affect the result. The spring belt elements are varied in length in order for the belt forces to start loading similarly.

Figure 2.2.9: *Simulation model of the Heidelberg sled.*

### 2.3.1 Positioning of HIII

The HIII model is placed with its H-point at the seat H-point in the two sled model. The HIII model is rotated backwards to a normal car occupant posture, in the Heidelberg model the rotation is 21.2° and in the Graz model it is 17°. The HIII model's elbows are moved inwards the ribcage and the hands are moved as far towards the knees as possible. The legs are positioned along the seat foam and the feet are strapped on the footrest with a belt of fabric material. In the Graz model the HIII legs are moved close together before the feet are strapped to the footrest. Table 2.3.1 shows the rotation of the limbs.

Table 2.3.1: The positioning of limbs on HIII. Symmetry about the dummy H-point.

| Limb | Joint | Rotation direction | Angle [°] in Heidelberg | Angle [°] in Graz |
|---|---|---|---|---|
| Upper arm | Shoulder | Up | 11.913 | 28 |
| Lower arm | Elbow | Up | 52.109 | 30 |
| Hand | Wrist | Twist | 0 | 41 |
| Thigh | Hip | Up | 0.15 | -6.918 |
| Thigh | Hip | Inwards | 0 | 2.65 |
| Lower leg | Knee | Up | 21.593 | 32.211 |
| Feet | Ankle | Up | -0.823 | -4.955 |

When the HIII model is positioned it penetrates the seat foam, see figure 2.3.1. The seat depenetrate function in ANSA is therefore used to modify the seat foam elements as if compressed by the HIII bottom, see figure 2.3.2. The foam is modelled to return to its original shape when the simulation starts. When the seat foam is depenetrated by the HIII bottom the force in the compressed foam might become larger, or smaller, than the mass of the HIII. When the simulation starts this can cause the dummy to accelerate upwards or sink down into the foam. Before the HIII in the Graz model is rotated backwards it is moved 18.5 mm down into the foam until force balance occurs between the HIII weight and the foam.

When the HIII is positioned the seat belt is routed over the chest and lap. It is not specified how the belt is routed in the mechanical tests and the belt is therefore positioned according to the best guess on the HIII. The HIII is positioned according to figure 2.3.3 and 2.3.4.

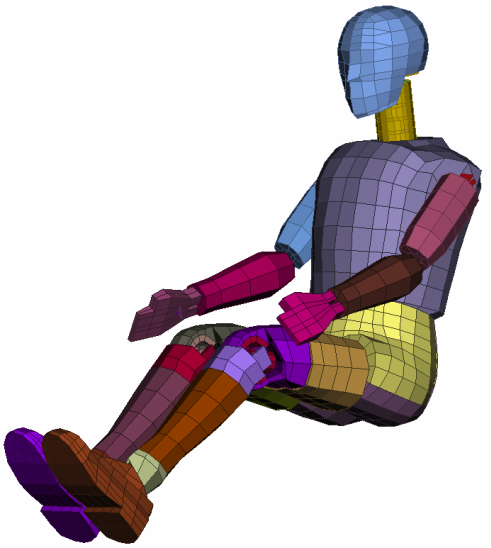

Figure 2.2.10: *HIII simulation model.*

Figure 2.2.11: *THUMS.*

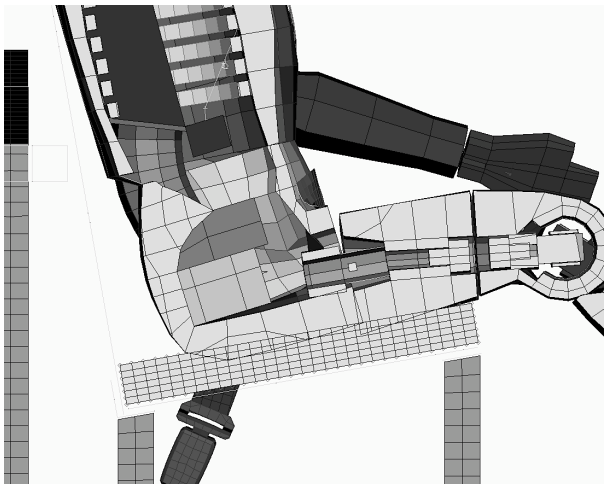

Figure 2.3.1: *Foam before seat depenetration.*

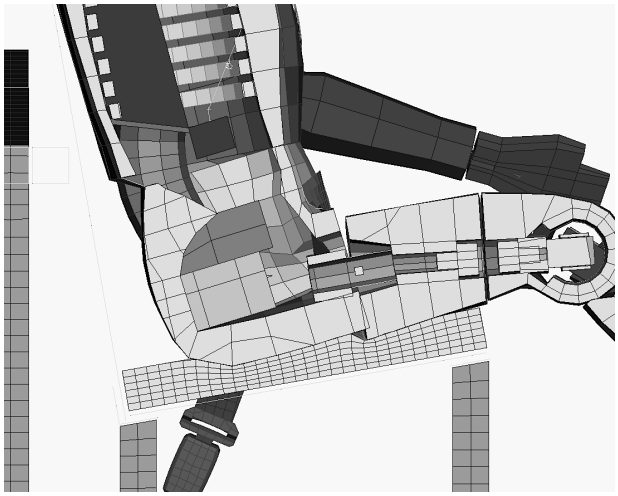

Figure 2.3.2: *Foam after seat depenetration.*

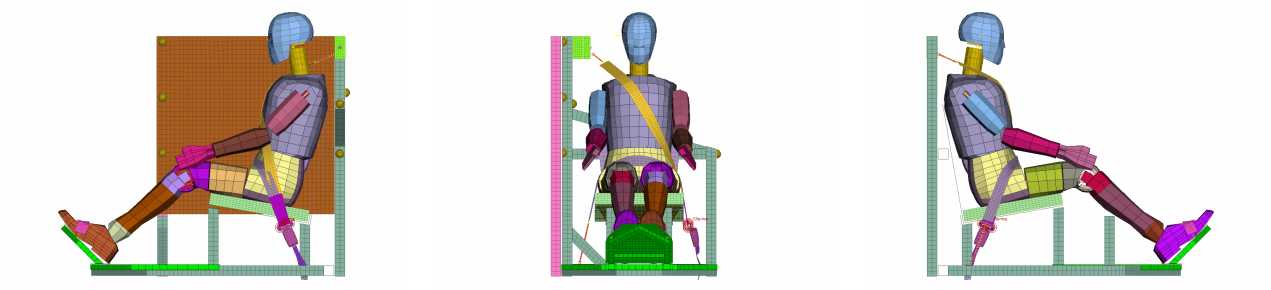

Figure 2.3.3: *Position of the HIII simulation model in the Graz sled.*

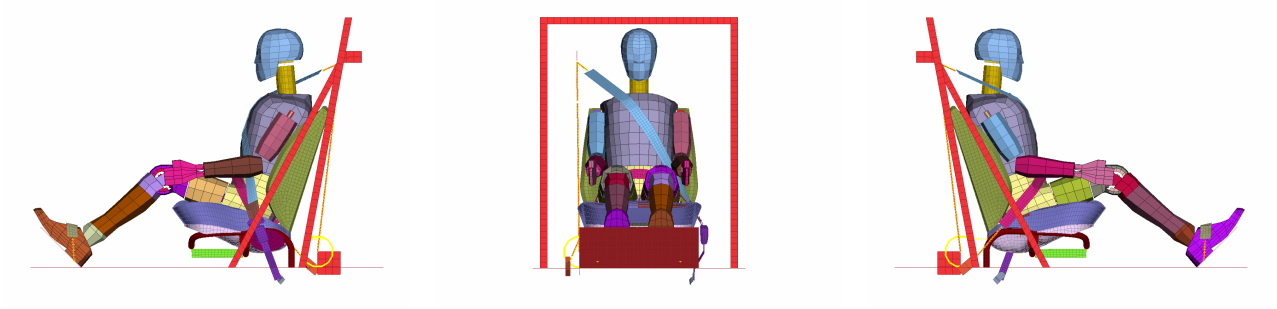

Figure 2.3.4: *Position of the HIII simulation model in the Heidelberg sled.*

### 2.3.2 Definition of Contacts

Contacts are defined between HIII, the seat and the belt. Contacts are also added between the legs of the model and between the feet and the sled. In the Graz model a contact is added between HIII and the door. The automatic_surface_to_surface contact type is chosen for all contacts.

Frictions differ between the two models. The HIII dummy did not wear any clothing during the Graz dummy test. Rubber has a higher friction coefficient than clothing and the Graz model frictions are therefore higher than the Heidelberg model frictions. In the Graz model the friction between the HIII model and the seat is 0.3, between the HIII model and the belt it is 0.9 and in the slipring is it 0.4. In the Heidelberg model the friction between the HIII model and the seat is 0.23 and between the HIII and the belt it is 0.1. In the sliprings the frictions are set to 0. For more information on the contact cards see appendix A for Graz and appendix B for Heidelberg.

### 2.3.3 Measuring Equipment

Nodes corresponding to the test accelerometers are located on the dummy. They are positioned according to the respective test. The node accelerometers are placed on T1 for the Graz model and on T1, T6, T12 and pelvis for the Heidelberg model. Local coordinate systems are created using a right hand system where x is in the frontal direction of HIII and z is upwards, see figure 2.4.3. The accelerations are measured as node accelerations in the local coordinate systems.

The corresponding belt forces are also measured. The shoulder belt force is measured in the 1D belt over the shoulder and the lap belt force in the 1D belt near the lower anchor point. The belt forces are measured as belt forces using the output file sbtout in LS-DYNA.

### 2.3.4 Loads

The sleds are rotated to the respective test angles. The Graz sled is rotated -45°, 0° and 30° and the Heidelberg sled is rotated ±15° and ±30° around the positive z axis. Finally the sled pulse from the tests in each angle is filtered using SAE60 and applied to the sleds in negative x direction in the corresponding angle. The simulated time span is from 0 to 150 ms and it takes 15-20 minutes to simulate on an Intel Xeon 12 Cores 3.33GHz computer using 4 cores.

### 2.3.5 Post-processing

The test data from the Heidelberg test is modified in order to be comparable. All of the PMHS in table 2.1.2 are used in the validation except for 80/07 and 80/09. The inconsistent test coordinate systems are changed into right hand systems with x in the HIII frontal direction and z up. For the near sided collisions the y

direction accelerometers are changed in sign as the near side simulations are rotated positive about the positive z axis while the mechanical tests are rotated negative about the positive z axis.

For the Graz sled evaluation a tracking is performed on the pelvis. The videos of the tests are imported into *MetaPost* (2011) where a point on pelvis on the HIII dummy is tracked, see figure 2.3.5. This tracking record the movement in the approximate x and y direction but not in the z direction, as it is an overhead view. In the tracking x is in the direction of the sled displacement. The resultant xy displacement is used when comparing. Corridors are created in the hip tracking due to measuring errors during the tracking. The tracking differs up to 20 mm from the tracking point.

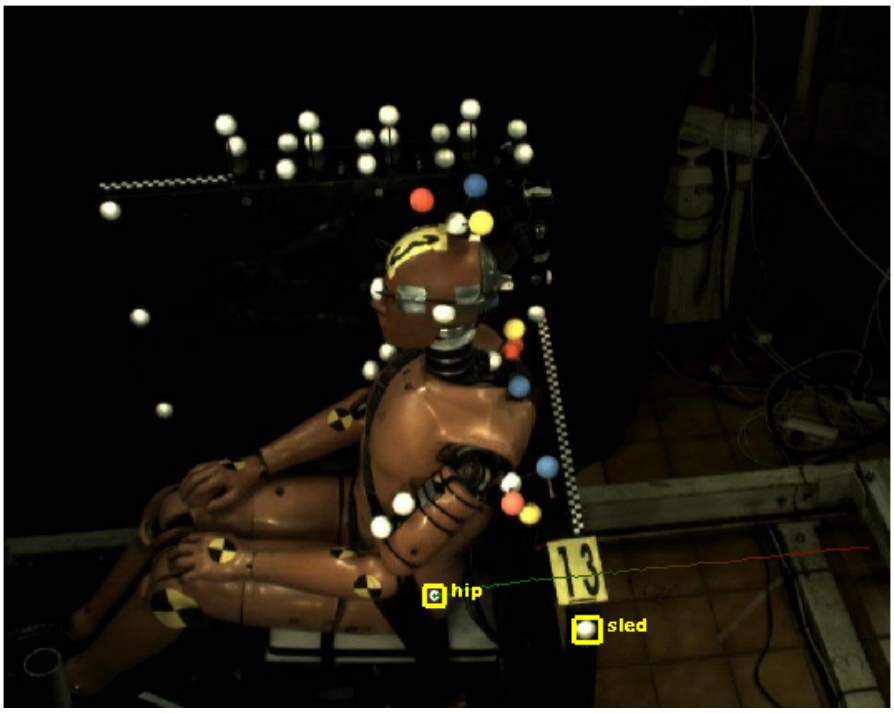


Figure 2.3.5: *Video tracking of the movement of the hip.*

The force, acceleration and displacement curves from the simulations and the HIII tests are put into the post-processor *HyperGraph* (2011) and filtered with SAE60 filter. The unknown material parameters in the sled models are varied in order to see how they affect the kinematic response.

Then the frictions from the mechanical tests are unknown and they are therefore optimized to create best possible conformity between the belt forces and accelerometer signals in the test data and the simulation data. The parameters varied in the validations are:

- Friction between HIII and the seat foam. (0.1-0.6)
- Friction between HIII and the seat belt. (0-locked)
- Friction in the sliprings. (0-locked)
- The anchor springs in the seat belt. (0-50mm)
- The seat foam loading curve. (Varied between 50-200% of nominal value)
- The seat structure. (Heidelberg seat steel: varied between 50-200% and Graz seat plywood: 100-1000% of nominal value)

The spring elements modelled in the seat belt differ between the sled models and the test angles. In the Graz model the springs are adapted in order for the simulated belt forces curve to reach 1 kN at the same time as the test curves. In the Heidelberg model the springs are adapted in order for the simulated belt forces to coincide with the test belt forces during the loading phase. The elongation of the chosen springs in the different angles can be seen in table 2.3.2.

Table 2.3.2: The maximum elongation in the belt springs.

| Test setup | Angle | Upper spring [mm] | Lower spring [mm] |
|---|---|---|---|
| Graz | 45° far | 0 | 0 |
| | 0° | 0 | 15 |
| | 30° near | 15 | 15 |
| Heidelberg | 30° Far | 0 | 29 |
| | 15° Far | 0 | 14.5 |
| | 15° Near | 45 | 14.5 |
| | 30° Near | 0 | 29 |

## 2.4 Evaluation of THUMS

The validated sled environments are used to evaluate THUMS. The description of how this is done follows in this chapter. THUMS is positioned as in the mechanical PMHS tests, in a normal car occupant posture (Törnvall et al., 2005). Contacts are defined between THUMS and the sleds and nodes corresponding to where the accelerometers from the mechanical tests are located. The sled is rotated to the collision angle in which the tests were performed and the sled pulse used is the same as in the respective test angle. The simulation data are compared with the test data and the belt springs are varied in length in order for the belt forces to start loading similarly.

THUMS is evaluated against PMHS test data using both sled models. It is evaluated in 45° far, 0° and 30° near side collision in the Graz sled model and in 30° far/near, 15° far/near and 45° near side collision in the Heidelberg sled model.

### 2.4.1 Positioning of THUMS

As for the HIII simulation model, the THUMS model is placed with its H-point in the seat H-point in both sleds. THUMS is rotated backwards so that the feet are resting on the sled and the back is in a normal car occupant posture. The rotation is 13° in the Graz sled and 18.5° in the Heidelberg sled. The feet are strapped to the sled using a fabric belt. The arms are rotated down 29 °, about the shoulder joint, so that the hands are positioned beside the legs. As for the HIII, the seat foams are depenetrated by the THUMS bottom and they are modelled to return to their initial shapes when the simulations start. At last, the seat belts are routed over the chest and lap. It is not specified how the belt is positioned in the mechanical tests and the belt is therefore positioned according to the best guess on THUMS. THUMS is positioned according to figure 2.3.3 and 2.3.4.

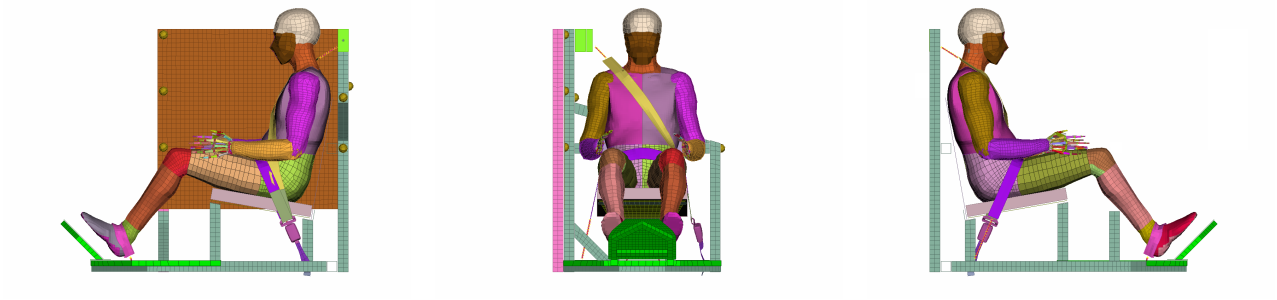

Figure 2.4.1: *Position of THUMS in the Graz sled.*

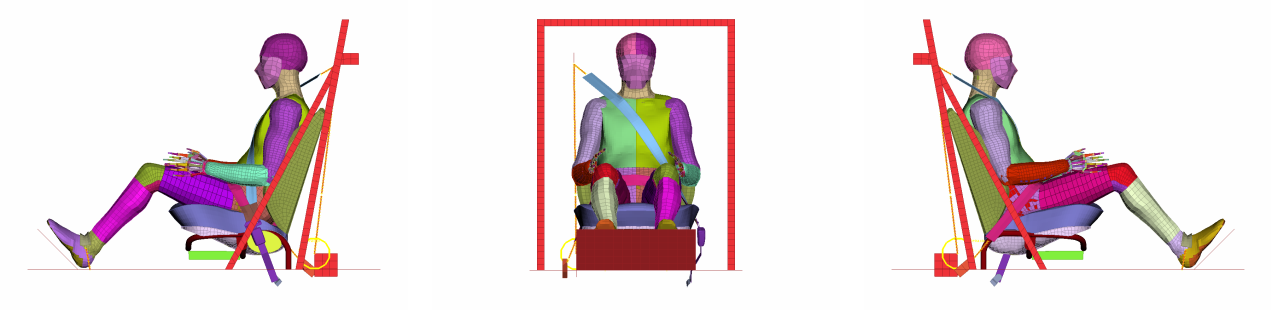

Figure 2.4.2: *Position of THUMS in the Heidelberg sled.*

### 2.4.2 Definition of Contacts

Contacts are created, the same as for the HIII simulation, between THUMS, the belt and the seat. One is added between THUMS head and arms and one between the feet and the sled. A contact between THUMS and the door is also added in Graz. The automatic_surface_to_surface contacts type is used for all contacts.

The frictions are the same as in the HIII simulations, except for two of the frictions in the Graz simulation; the frictions between THUMS and the seat and between THUMS and the belt, which are both set to 0.6. For more information on the contact cards see appendix A for Graz and appendix B for Heidelberg.

### 2.4.3 Measuring Equipment

Seat belt accelerometers are added in the nodes corresponding to the accelerometers positions in the test setup, on T1 in Graz and on T6 in Heidelberg. The shoulder nodes used for 3D tracking are output and the corresponding belt forces are measured. The shoulder belt force is measured in the 1D belt over the shoulder and the lap belt force in the 1D belt near the lower anchor. In the accelerometers the x direction is in the frontal direction of THUMS, see figure 2.4.3, while in the shoulder tracking x is in the direction of the sled displacement, see figure 2.4.4.

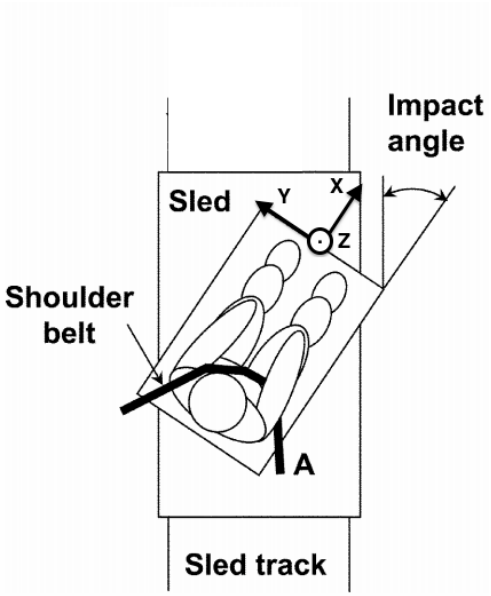


Figure 2.4.3: *Coordinate system of the accelerations.*

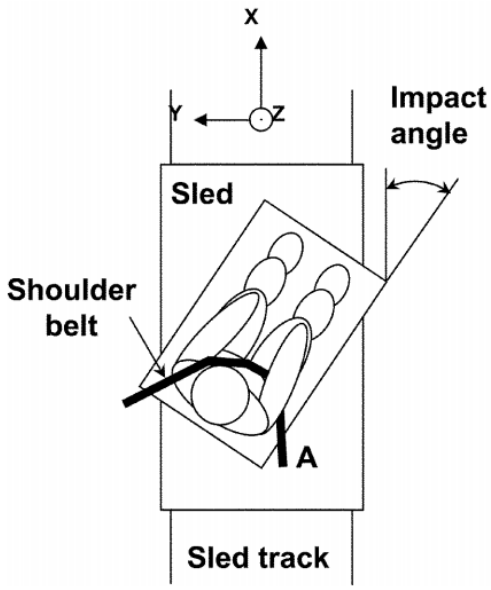


Figure 2.4.4: *Coordinate system of the displacements.*

### 2.4.4 Loads

The sleds are rotated to respective test angles. An average of the sled accelerations from the PMHS tests are calculated in each angle and applied in negative x direction in the corresponding angle. The simulated time is 0-150 ms and the simulation takes about 1 hour and 40 minutes to simulate on an Intel Xeon 12 Cores 3.33GHz computer using 6 cores.

### 2.4.5 Post-processing

The force and accelerometer curves from the simulations and the tests are imported into Hypergraph and filtered with SAE60 filter.

The test data is modified before the comparison. The test data from the PMHS tests are scaled based on weight and chest depth according to Mertz (1984). The parameters scaled are time, force, acceleration and displacement and their scale factors are $R_t$, $R_f$, $R_a$ and $R_x$ respectively. The scale factors are listed in table 2.4.1. Figure 2.4.5 and 2.4.6 show an example of how the test data is changed.

Table 2.4.1: The scale factors for the PMHS, Graz.

| Test Setup | Test Subject | $R_t = R_x$ | $R_a$ | $R_f$ |
|---|---|---|---|---|
| Graz | PMHS 1 | 1.065 | 0.939 | 1.166 |
| | PMHS 2 | 1.074 | 0.931 | 1.176 |
| | PMHS 3 | 1.034 | 0.967 | 0.792 |
| Heidelberg | 79/14 | 1.073 | 0.932 | 1.122 |
| | 79/20 | 1.084 | 0.923 | 1.246 |
| | 79/21 | 0.950 | 1.052 | 0.911 |
| | 79/22 | 0.991 | 1.009 | 1.036 |
| | 79/23 | 1.017 | 0.984 | 0.935 |
| | 79/26 | 1.034 | 0.967 | 1.034 |
| | 79/29 | 1.026 | 0.975 | 1.072 |
| | 80/07 | 1.009 | 0.991 | 1.106 |
| | 80/09 | 1.071 | 0.934 | 0.985 |
| | 80/16 | 1.032 | 0.969 | 0.848 |

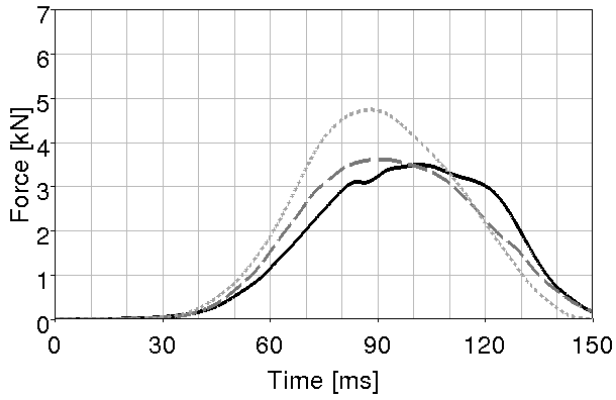


Figure 2.4.5: *Unscaled PMHS shoulder belt force test data.*

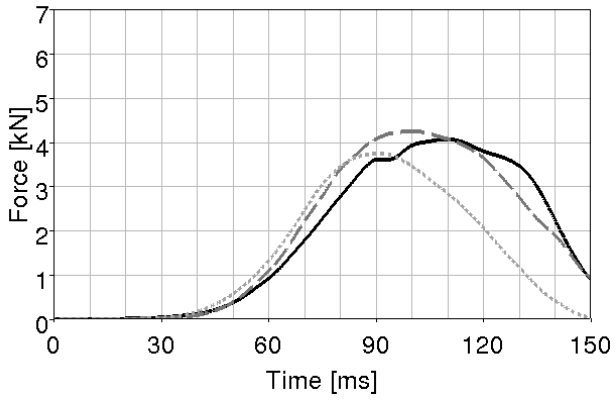


Figure 2.4.6: *Scaled PMHS shoulder belt force test data.*

In most angles there are more than one PMHS tested. In these angles corridors are created. The average and the standard deviation of the PMHS curves in each collision angle are calculated. The standard deviation is calculated in each time step and then fitted with an $8^{th}$ grade polynomial. The standard deviation is fluctuating and by replacing it with a polynomial it becomes more even and realistic, for an example see figure 2.4.7.

Corridors are then created by taking the average ±1 standard deviation. Figure 2.4.8 shows an example of the corridors and the scaled PMHS data.

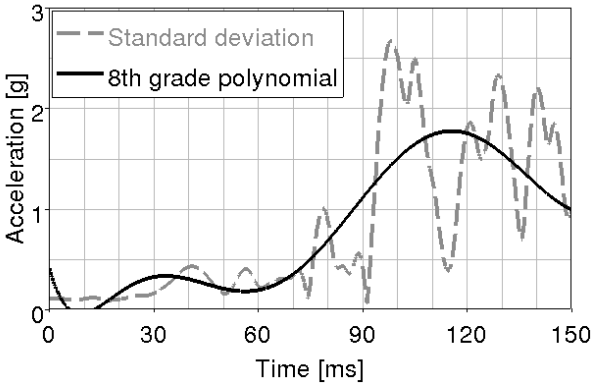


Figure 2.4.7: *The standard deviation and the polynomial.*

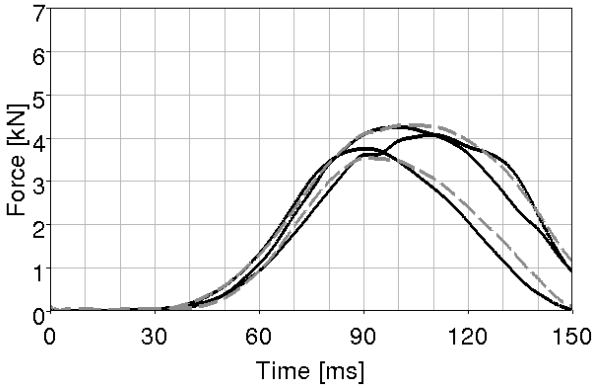


Figure 2.4.8: *The grey dashed lines are the corridors and the black curves are the PMHS data.*

In the 30° near side collision in the Heidelberg setup, four PMHS were tested. Two of these were very small and differs much compared to a 50 percentile American male. These two tests are therefore removed and not used when corridors and sled accelerations are created.

The Heidelberg test data is modified further in order to be comparable. The PMHS in table 2.1.2 are used in the validation. 80/07 and 80/09 are only used for shoulder tracking. All coordinate systems of the tests are changed into right hand coordinate systems where z is directed upwards and x is directed in the frontal direction of THUMS.

The frictions between THUMS and the sled are optimized in the Graz sled model since frictions between THUMS and the sled does not coincide with the frictions between an undressed HIII and the sled, as used in chapter 2.3. Frictions varied in the Graz sled are:

- Friction between HIII and the seat foam. (0.1-0.6)
- Friction between HIII and the seat belt. (0-locked)

In the Graz sled model the springs in the belt ends are adapted in order for the belt force curves to reach 1 kN at the same time as the PMHS test curves. The springs in the Heidelberg seat belt are given a length that makes the simulation belt curves coincide with the test belt curves during loading. In some cases that is not possible and the springs are then chosen so that the maximum forces coincides in time. The elongation of the springs is listed in table 2.4.2.

Table 2.4.2: The maximum elongation in the belt springs.

| Test setup | Angle | Upper spring [mm] | Lower spring [mm] |
|---|---|---|---|
| Graz | 45° far | 30 | 35 |
| | 0° | 30 | 45 |
| | 30° near | 30 | 35 |
| Heidelberg | 30° far | 85 | 14.5 |
| | 15° far | 115 | 45 |
| | 15° near | 115 | 14.5 |
| | 30° near | 145 | 0 |
| | 45° near | 165 | 29 |

# 3 Result

In this chapter the results from the simulations and test comparisons are found. All of the test and simulation data are filtered with SAE60 filter to simplify and clarify the comparison. Using filters according to *SAE J211* (1970) leaves too much noise for comparison. The results from the simulated foam test is presented in chapter 3.1. In chapter 3.2 the validation of the sled environments are presented and the results from the evaluation of THUMS is presented in chapter 3.3.

## 3.1 Material Test for the Graz Sled

The result from the foam test simulation, described in chapter 2.2.1, is compared to the force-deflection curve from the test, see figure 3.1.1. Shape factor 7 gives an unloading curve similar to the experimentally obtained curve.

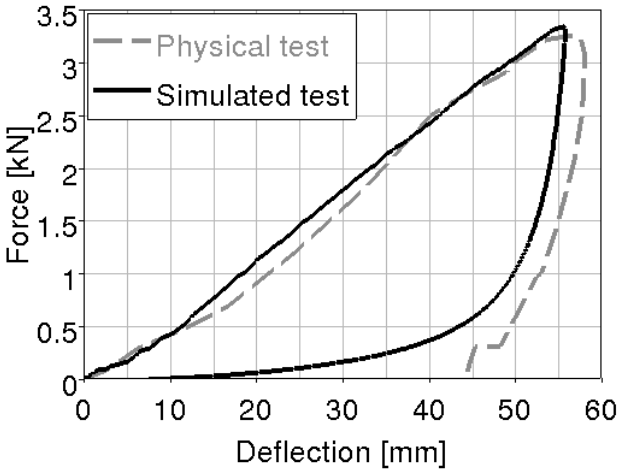


Figure 3.1.1: *Experimental and simulated impact test data from the foam test.*

## 3.2 Validation of the Sled Environments

The results from the sled validation are shown in this section. The validation of the Graz sled is presented in 3.2.1 and the validation of the Heidelberg sled in 3.2.2.

All figures show the simulated results compared to the measured mechanical test results. The black continuous curves are from the HIII simulation, while the grey dashed lines shows the measured data from the tests.

### 3.2.1 Graz

The belt forces, T1 acceleration and the displacement of the hip from the HIII simulations are compared with the ones from the physical tests. The forces are shown in figure 3.2.1, the resultant accelerations can be seen in figure 3.2.2 and the displacement are found in figure 3.2.3. All responses can be seen in appendix C.

In 45° the shoulder belt slips off the shoulder in the simulation but not in the test. This happens after approximately 80 ms. This is seen in the figure where the simulated shoulder belt force curve and the tested one are alike the first 70 ms but then the simulated curve levels out. In the decreasing phase they are alike

again. The simulated lap belt force is around 5 ms later than in the test and it start to decrease 15-20 ms too early. The maximum force is 0.5 kN to low in the lap belt. The acceleration response are similar, maximum 5 ms too early, until 80 ms. The simulated displacement is in the test corridor the first 80 ms. Then the simulation model moves 20 mm longer relative the test.

The shoulder belt force in 0° are alike the first 70 ms. Then the simulated force are lower than the force measured in the test, the maximum difference is 1 kN. The simulated curve then decreases earlier and faster than the test curve. The lap belt force from the simulation is maximum 5 ms later than the test force the first 110 ms. After that the simulation curve decreases faster than the test curve. The resultant acceleration for the simulation is 3 g higher than the test acceleration in the increasing part. But they start to decrease at the same time, after 80 ms. The simulated displacement is outside the test corridor from 70 ms to 120 ms where the maximum displacement is 30 mm too long.

In 30° the shoulder belt force is alike the first 80 ms. Then the simulated curve is 0.3 kN lower than the test curve for 30 ms. Then the simulation force decrease faster than the test force. The lap belt forces are similar the first 80 ms then the simulated force increase to around the double value of the test force. As in the other angles, the simulated acceleration in T1 is earlier than the measured test acceleration in the increasing phase. Then the simulation curve is right above the test curve. The simulated hip displacement is approximately ms delayed the first 110 ms. Then the simulation starts to go back while the test displacement continues and turns first after 135 ms.

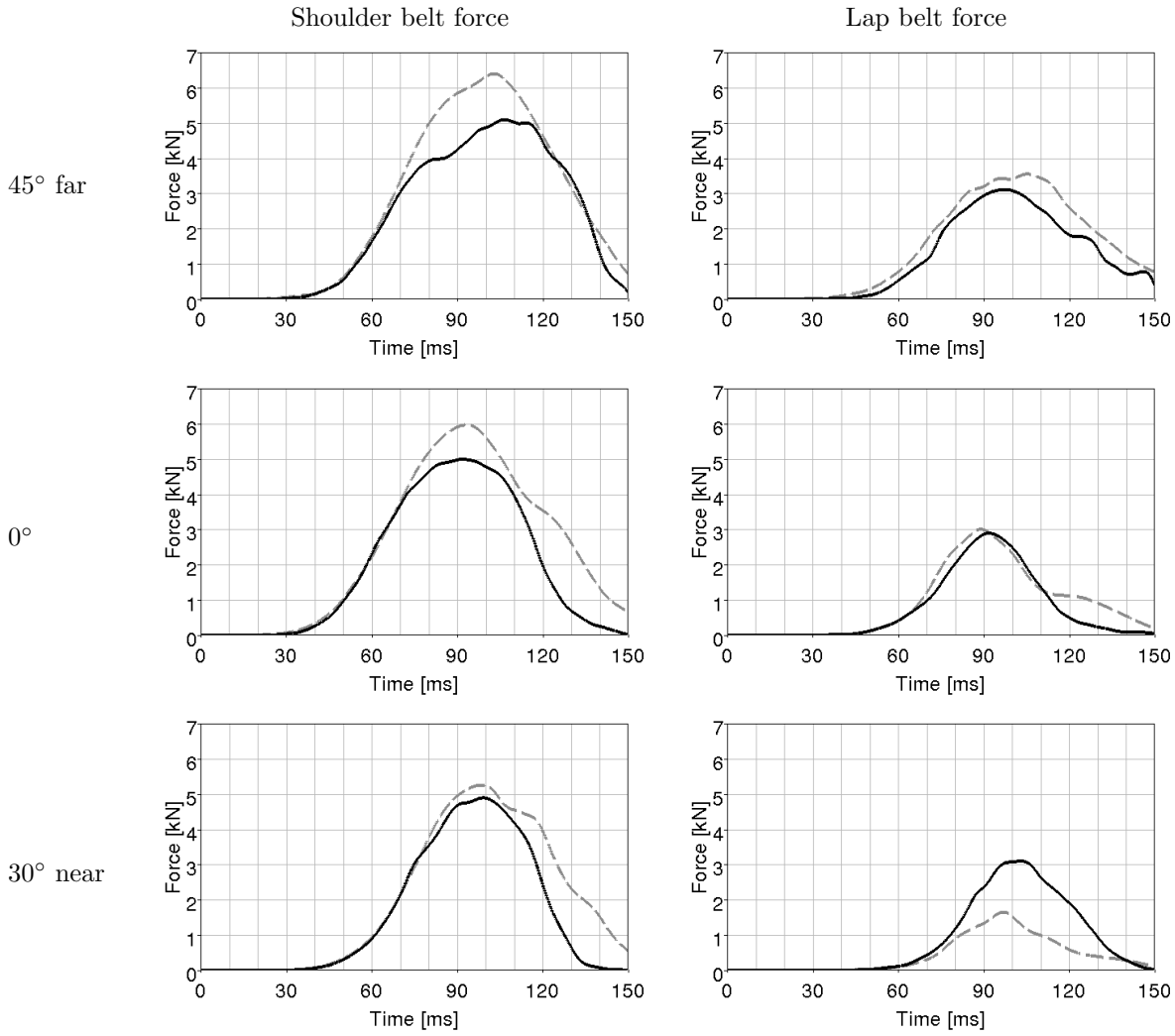


Figure 3.2.1: *The seat belt forces in the Graz simulation with HIII compared to the measured data from the mechanical test (Törnvall et al., 2008a).*

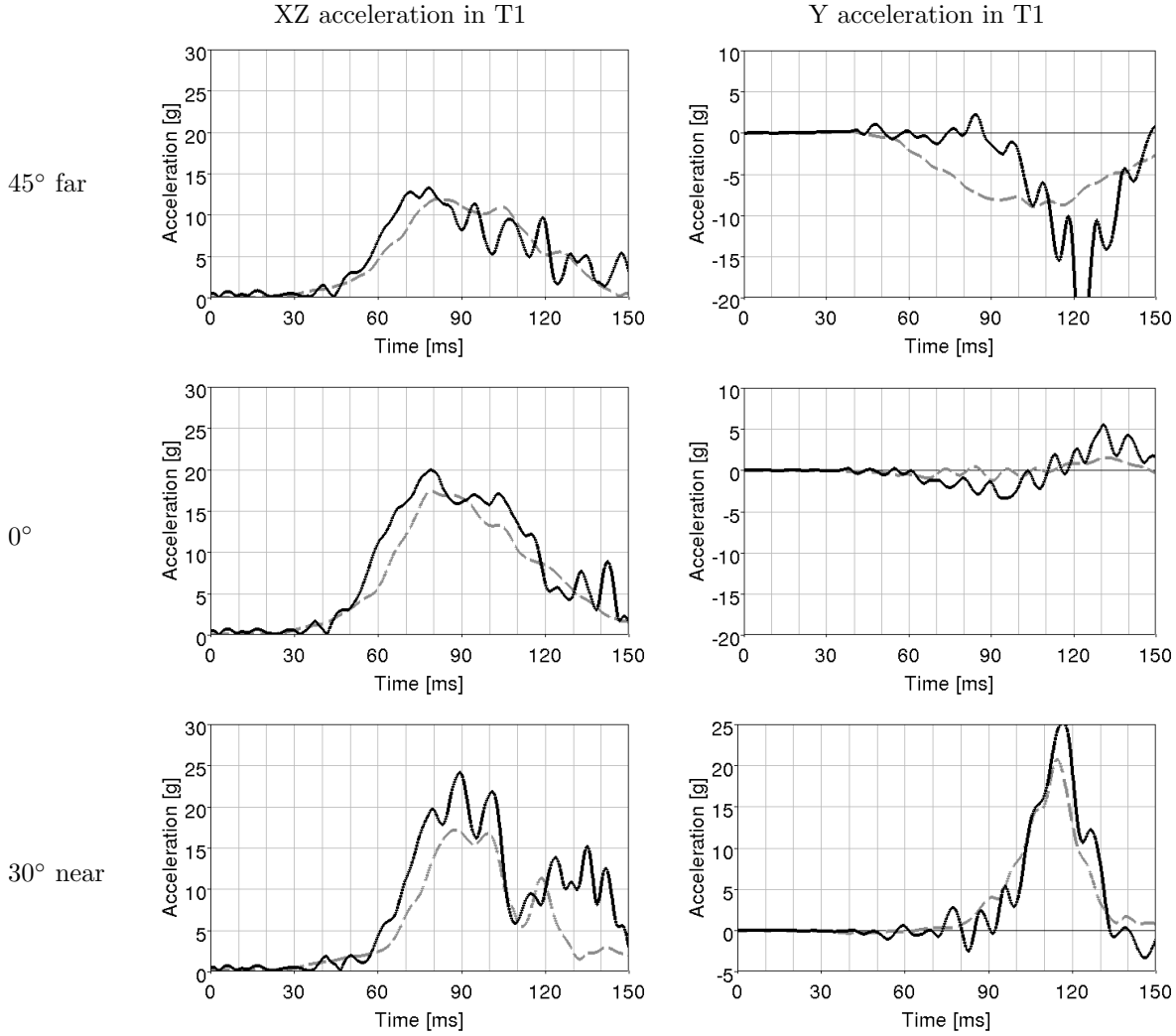


Figure 3.2.2: *The accelerations of HIII in the Graz simulation compared to the measured data from the mechanical test (Törnvall et al., 2008a).*

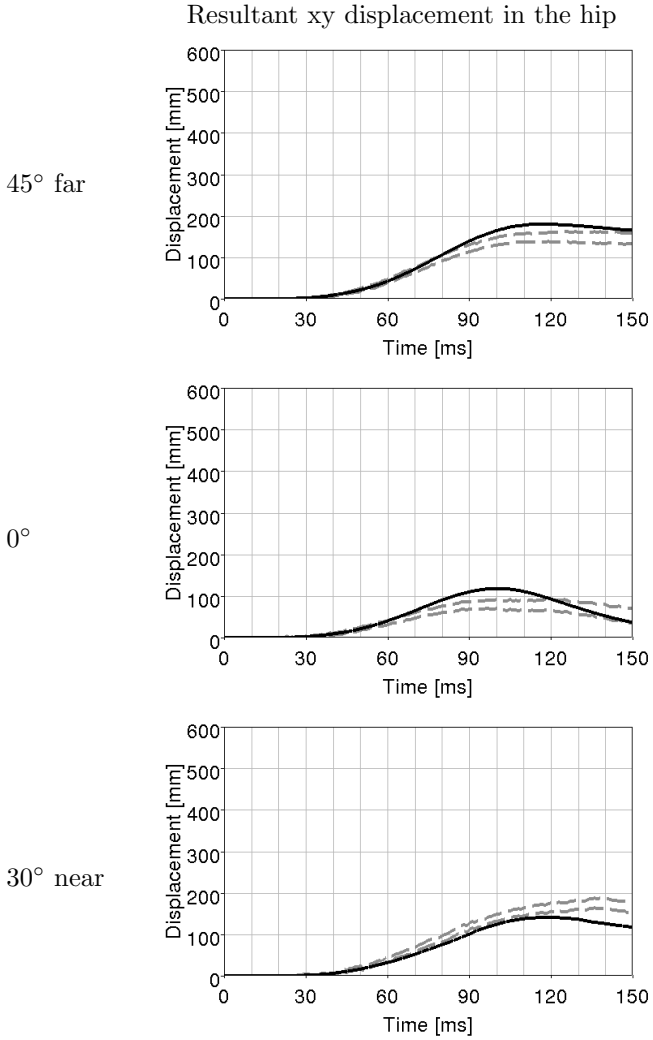


Figure 3.2.3: *The displacements of HIII in the Graz simulation compared to the measured data from the mechanical test (Törnvall et al., 2008a).*

### 3.2.2 Heidelberg

The kinematic response from the simulations is compared to the response from the Heidelberg tests. The comparisons are made in ±15° and ±30°.

Figure 3.2.4 shows the comparison of the belt forces and figure 3.2.5 and 3.2.6 shows the resultant acceleration of T6 and pelvis. All the kinematic data is showed in appendix D.

In the 30° far side simulation the shoulder belt slips off the HIII shoulder after approximately 75 ms. It can be seen in the shoulder belt force that the force loading flattens out when this occurs. In the dummy test the belt does not slip off the shoulder and it is therefore not useful to compare the kinematics after 75 ms in this angle. Both the shoulder belt force and the lap belt force differs less than approximately 0.3 kN compared to test belt forces during the first 75 ms. The belt slip can be seen in the accelerations of the spine. The resultant acceleration in T6 especially since it is located close to where the slip occurs. The first 75 ms the accelerations follow the acceleration data from the test but after that the acceleration decreases. The pelvis acceleration is a few ms early but has a parallel loading.

The shoulder belt force in the 15° far side simulation differs less than 0.35 kN during the entire loading and offloading phase. Both belts has the maximum force of approximately 4 kN which is approximately 0.1 kN less than the maximum forces from the test. However, the lap belt force in the simulation increases faster than in the test so that the maximum force is reached approximately 14 ms earlier in the simulation than in the test. This time difference is kept during the offloading.

In the 15° near side simulation the shoulder belt and the lap belt reaches approximately 4.2 respectively approximately 3.5 kN. The curves differ less than approximately 0.4 kN from 0 to 90 ms compared to the test curves. After 90 ms the lap belt force starts to decrease while the shoulder belt force increases for 10 ms more. The opposite situations occur in the test data.

In the 30° near side simulation the shoulder belt from the simulation has approximately the same maximum force as the test data, approximately 4.35 kN. However, this occurs approximately 14 ms later in the simulation. The two curves starts to increase at the same time but the simulated force increases slower after 70 ms. The lap belt force from the simulation increases approximately 3 ms earlier than the test data. After 75ms it flattens out some, reaches a maximum of approximately 3.4 kN and decreases after 95 ms.

In both 15° far/near and 30 ° near the acceleration of T6 and pelvis follows the test data within a few g's until approximately 120 ms, where the acceleration in the simulation starts to increase. This is due to an increase of acceleration in the positive z direction, which does not occur in the test.

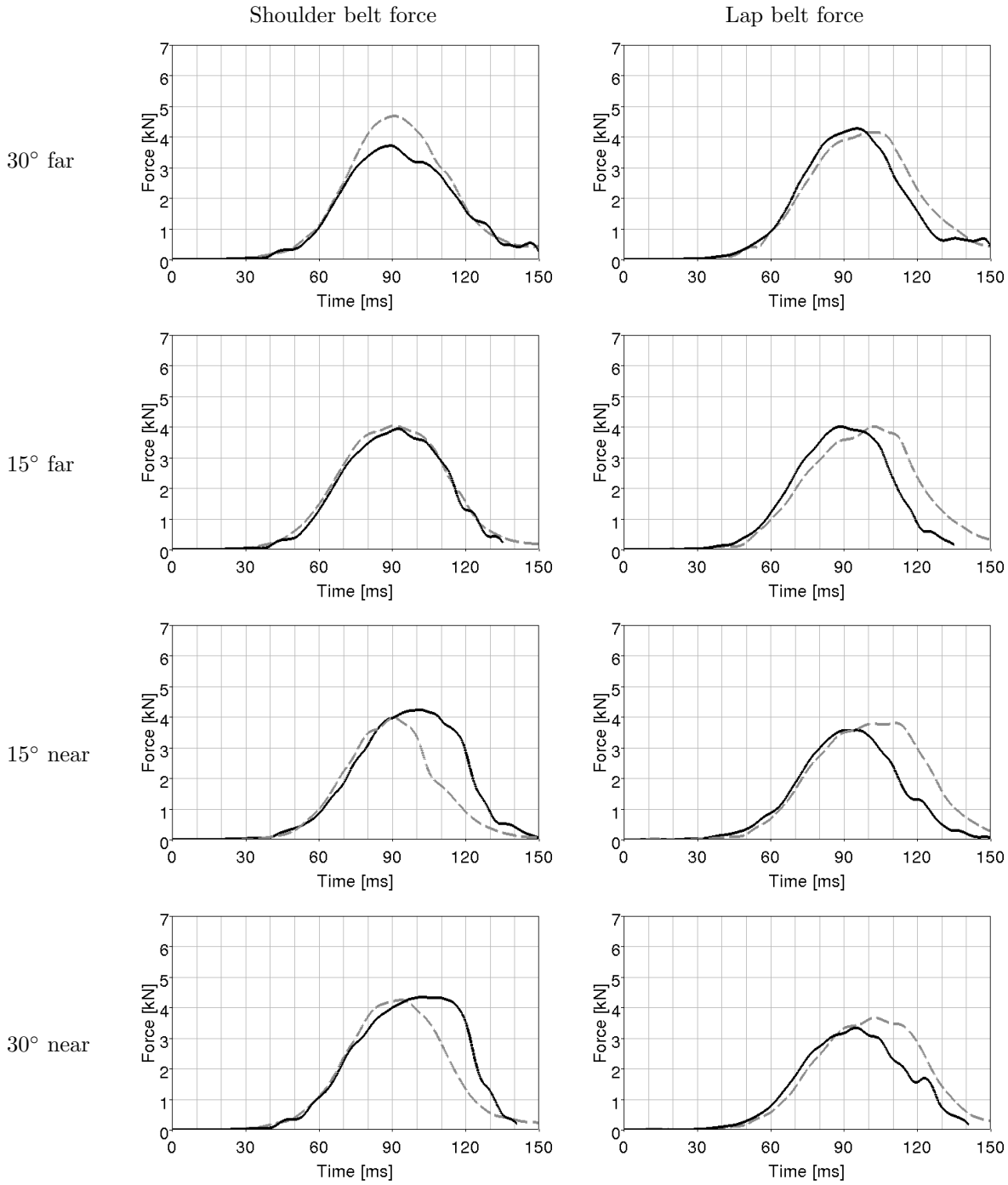


Figure 3.2.4: *The seat belt forces in the Heidelberg simulation with HIII compared to the measured data from the mechanical test (*Unpublished material from the Heidelberg test *2012).*

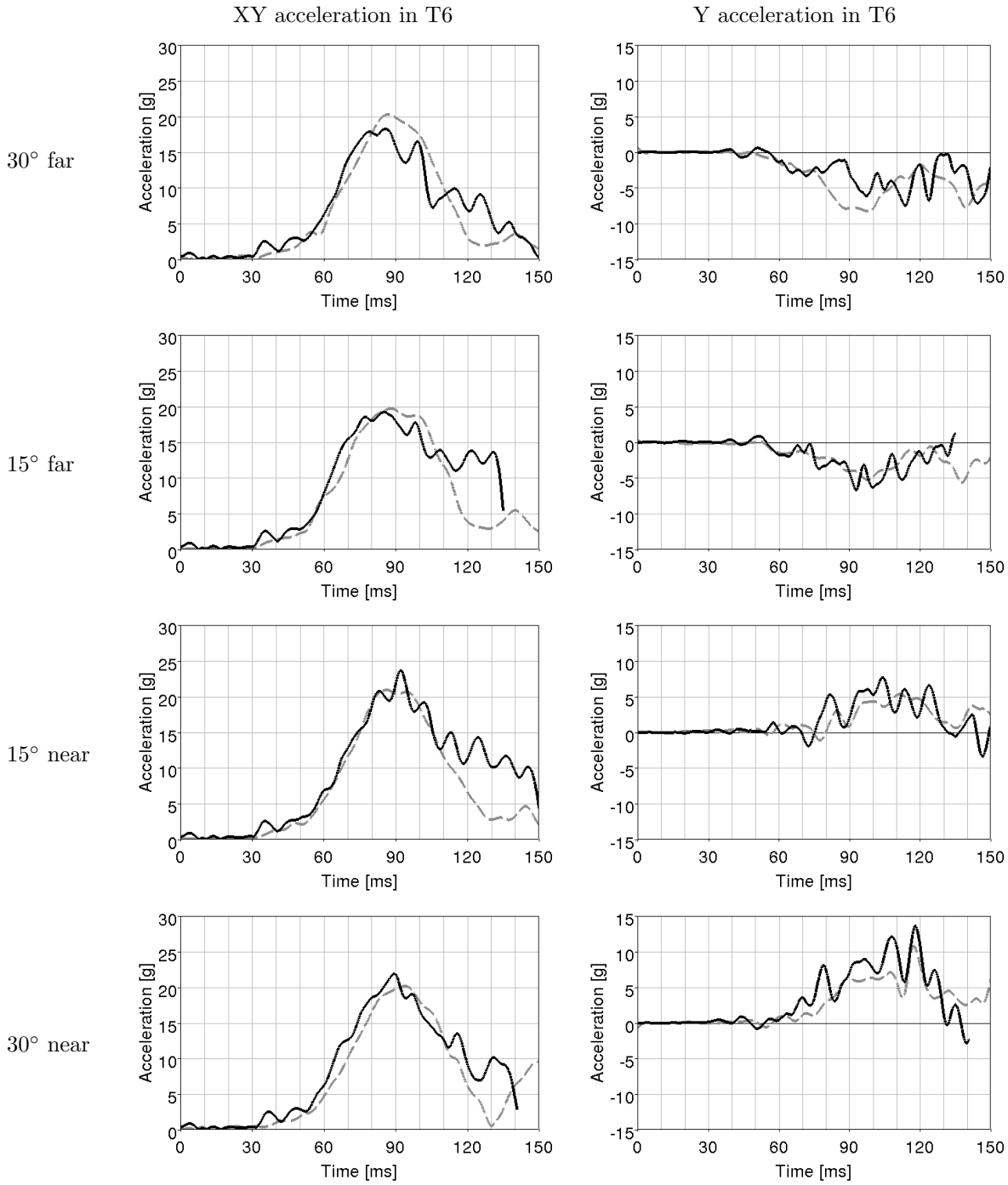


Figure 3.2.5: *The accelerations of HIII in the Heidelberg simulation compared to the measured data from the mechanical test (*Unpublished material from the Heidelberg test *2012).*

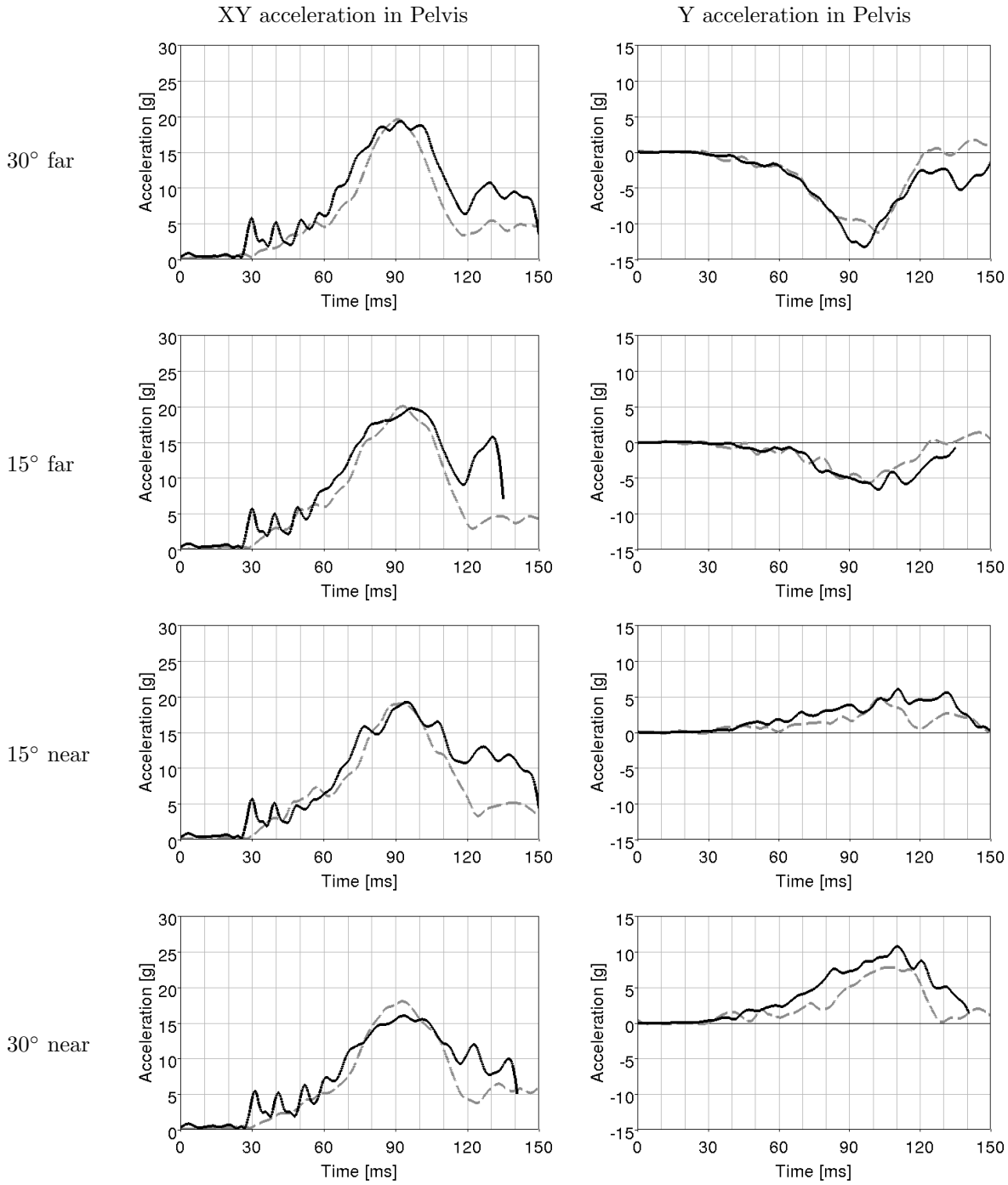


Figure 3.2.6: *The accelerations of HIII in the Heidelberg simulation compared to the measured data from the mechanical test (*Unpublished material from the Heidelberg test *2012).*

## 3.3 Evaluation of THUMS

In this section the results of the THUMS simulation is presented. The force and acceleration responses are compared to the responses from the mechanical tests. The black continuous curves in are from the THUMS simulation, while the grey dashed lines shows the PMHS data from the tests.

### 3.3.1 Graz

The belt force responses from the THUMS simulation are compared to the corridors gained from the PMHS data in figure 3.3.1 and the resultant T1 acceleration and the resultant shoulder displacements are compared in figure 3.3.2 and 3.3.3. All responses can be seen in appendix E. As for the HIII, the accelerometers in the simulations and in the tests are mounted with x in the frontal direction of the test subject. However there might be a difference in the rotation around the y axis. Therefore it is more relevant to look at the resultant xz acceleration and y acceleration.

In all three angles, the shoulder belt force responses from THUMS increase more rapidly than the test data and the peak is approximately 10 ms too early.

In 45° the simulated lap belt force follows the test corridors in the loading phase but the peak is 10 ms too early. Then the simulated curve decreases approximately 15 ms earlier than the test curve. The shoulder displacements are within the corridors. In the simulation the resultant acceleration for T1 is up to 1 g higher the first 80 ms than in the test. The maximum acceleration on the other hand is 1 g lower in the simulation relative the test.

The simulated lap belt force in 0° increase too rapidly and it reaches the peak 12 ms earlier than the test. Then it decreases faster than the test and lies around 10 ms too early in the unloading phase. In 0° the THUMS shoulders moves shorter than the PMHSs, approximately 100 mm shorter. It is the same for the unloaded shoulder in 30° but the loaded shoulder is within the corridor.

The simulated acceleration in 30° is within the corridor the first 95 ms. THUMS lap belt force follows the corridor in 85 ms then it starts to decrease while the test corridor continues and has its maximum at 105 ms before it decreases. The unloading phase is 25 ms earlier for the lap belt force for THUMS relative the test. In the simulations THUMS hit the door window after approximately 90 ms, which is seen as peak in the resultant acceleration.

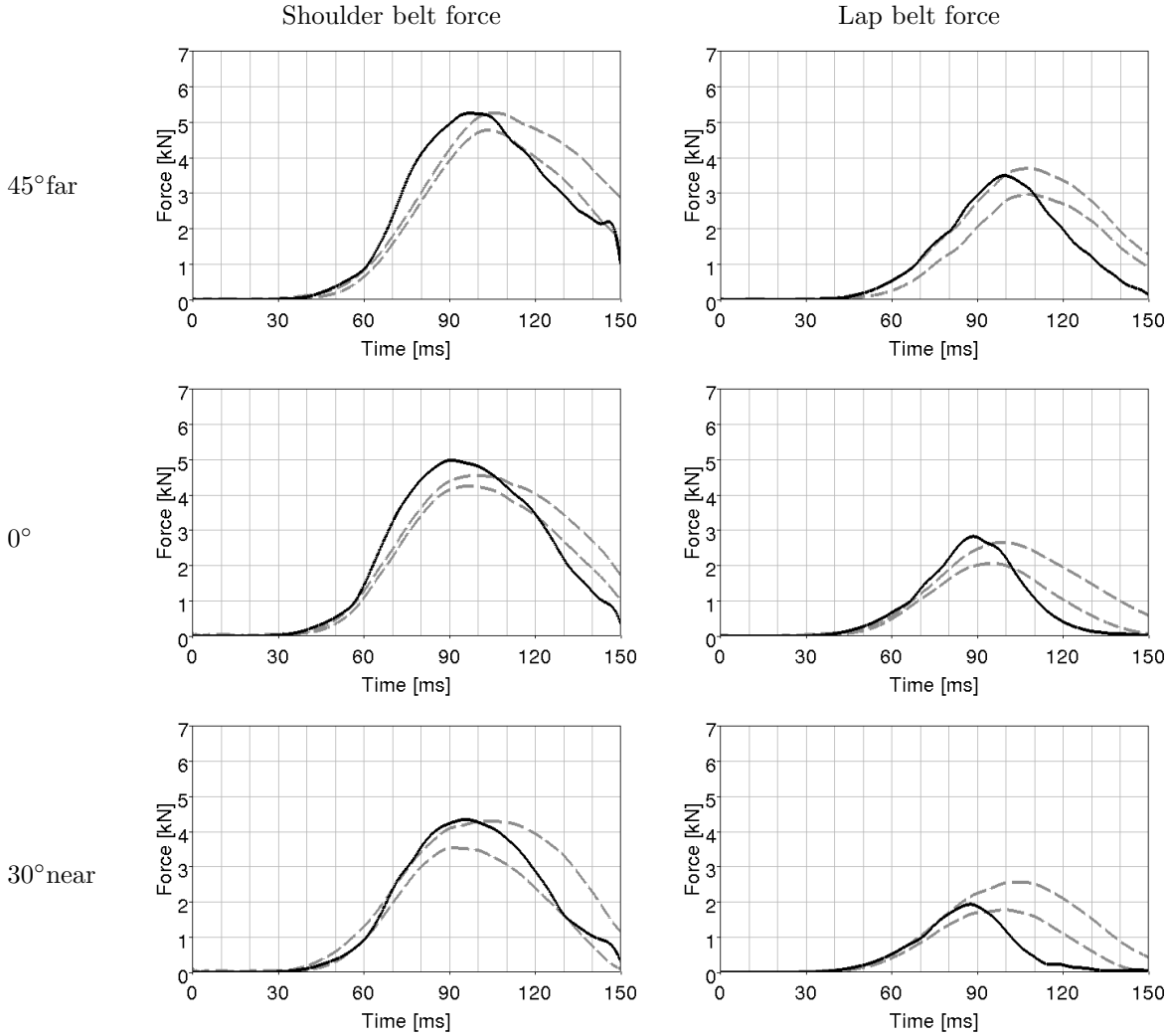


Figure 3.3.1: *The seat belt forces in the Graz simulation with THUMS compared to the measured data from the mechanical test (Törnvall et al., 2008b).*

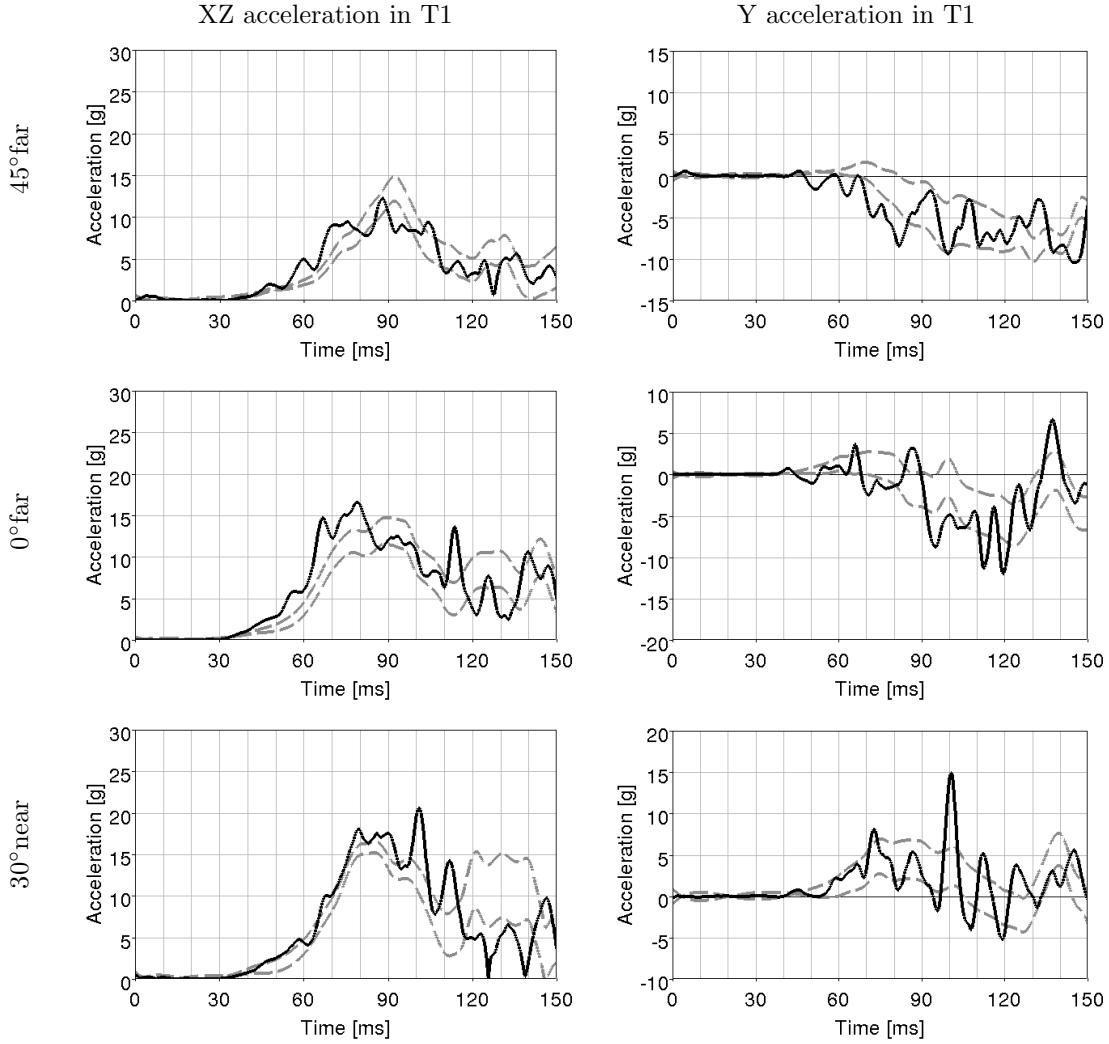


Figure 3.3.2: *The accelerations of THUMS in the Graz simulation compared to the measured data from the mechanical test (Törnvall et al., 2008b).*

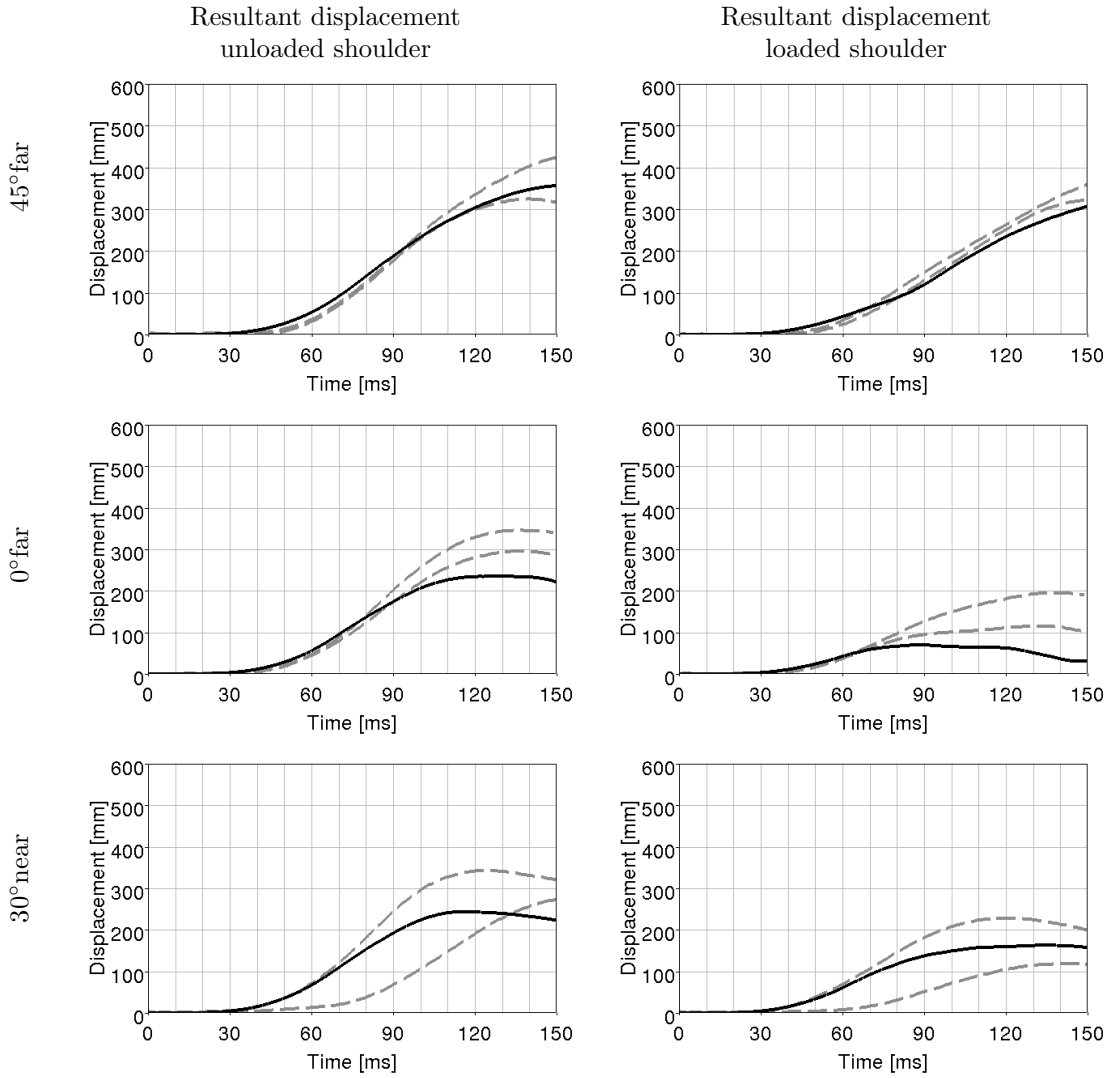


Figure 3.3.3: *The displacements of THUMS in the Graz simulation compared to the measured data from the mechanical test (Törnvall et al., 2008b).*

### 3.3.2 Heidelberg

The kinematic response from THUMS in the simulations is compared to the response from the Heidelberg tests. The comparisons are made in ±15°, ±30° and +45°.

Figure 3.3.4 shows the comparison of the belt forces and figure 3.3.5 shows the resultant acceleration of T6 and the displacement of the shoulder. The accelerometers on THUMS in the simulations might be rotated around the y axis differently than the accelerometers in the test and it is therefore useful to look at the resultants. There are no y acceleration signals in the test data and the resultant is therefore an xz resultant. Notice that the accelerometer signals from THUMS are noisy. All the kinematic data is showed in appendix F.

The shoulder belt forces in all angles increases steeper than the tests. The shoulder and lap belts forces from the 30° far side simulation differ less than 0.4 kN from the test corridors. The maximum force in the shoulder and lap belt is approximately 4 and 3.6 kN respectively. The maximum force in the shoulder belt is reached approximately 10 ms earlier in the simulation than in the test. The acceleration in T6 from the simulation differs less than 3 g from the test corridor during the first 80 ms. After that the acceleration increases towards 20g while the test corridor decreases toward 5 g. The total displacement of the loaded shoulder in the simulation is approximately 30 mm farther than the test data.

In the 15° far side comparison the maximum shoulder belt force in the simulation is approximately 1 kN lower than the force from the test. The lap belt force is within 0.5 kN from the test data. The acceleration in T6 from the simulation differs less than 5 g during the entire collision.

The simulated shoulder belt force in 15° near side differs less than 0.3 kN from the test corridors. However, the lap belt maximum force is 1 kN lower than the test force. In the loading and unloading phase the simulation force is approximately 4 ms later than the test force. The maximum acceleration in T6 from the simulation is approximately 5 g higher than the maximum value of the test corridor. The maximum value also occurs approximately 17 ms earlier than in the test.

In 30° near side the simulated shoulder belt maximum force is 1 kN higher than the test corridor. From the start until 60 ms the simulation force differ less than 0.1 kN from the corridor. At 60 ms the loading force steepens and it stays between 0.5 and 1 kN higher than the test corridor. The lap belt is within the test corridor during loading but it is approximately 5 ms later on the unloading. The acceleration in T6 from the simulation differs approximately 8 g from the test corridor. The total displacement of the loaded shoulder in the simulation is within the test corridor.

In the 45° near side simulation the belt forces from the simulations differ less than 0.5 ms from the test belt forces during the entire loading and unloading phase. The acceleration in T6 from the simulation differs approximately 10 g from the test data. The total displacement of the loaded shoulder in the simulation is approximately 20 mm shorter than the test data.

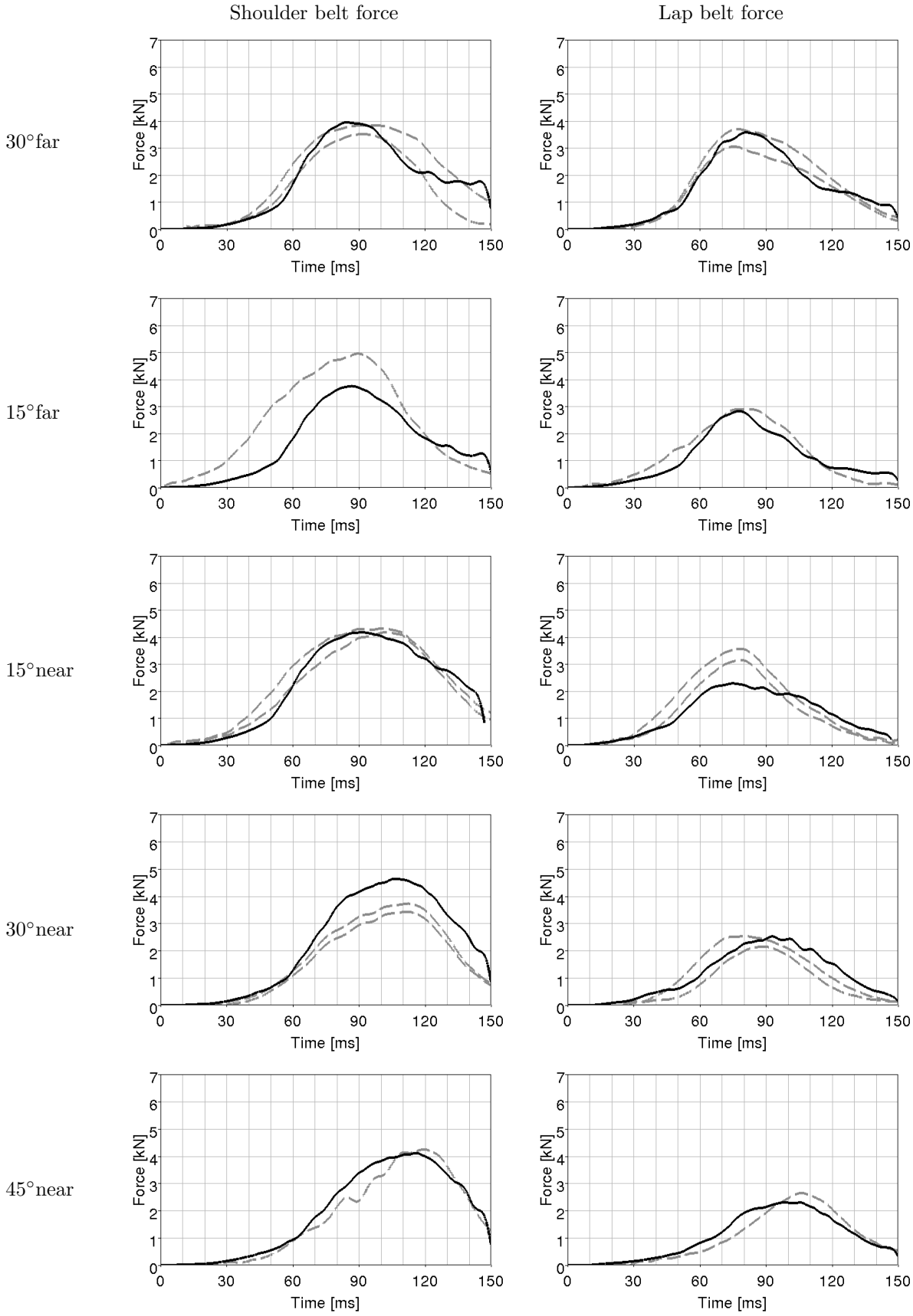


Figure 3.3.4: *The seat belt forces in the Heidelberg simulation with THUMS compared to the measured data from the mechanical test (*Unpublished material from the Heidelberg test *2012).*

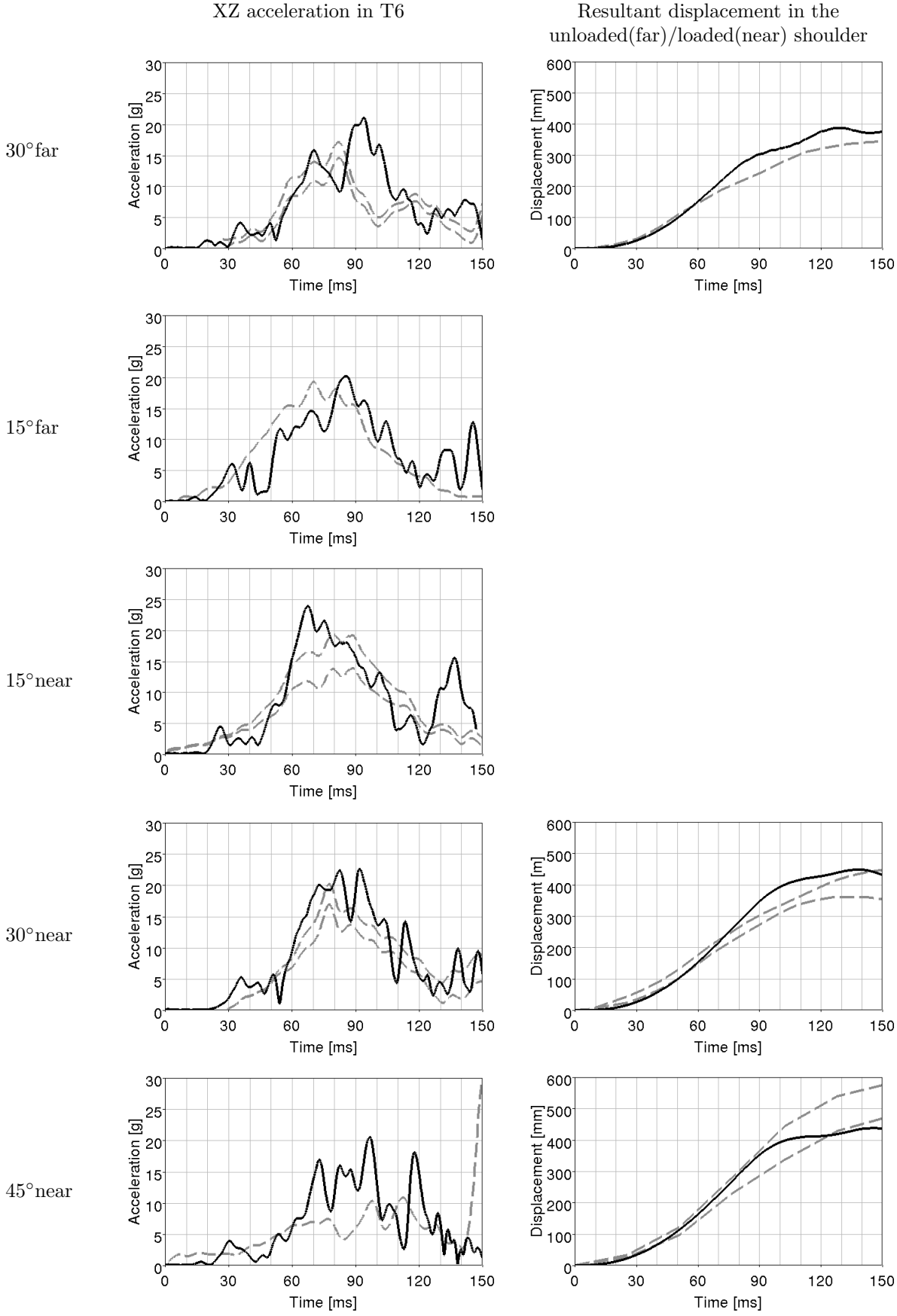


Figure 3.3.5: *The accelerations and displacements of THUMS in the Heidelberg simulation compared to the measured data from the mechanical test (*Unpublished material from the Heidelberg test *2012).*

# 4 Discussion

Both sled simulation models are considered to give realistic responses. The geometry is given. The material data in the seat does not affect the kinematics significantly. The belt data is given for the Graz belt and a similar high stretch belt is used in Heidelberg. Finally the contact frictions are not dependent on the test subject and are therefore not directly connected to the sled reliability. This is discussed further in chapter 4.1.

During the evaluation of THUMS in oblique frontal collisions it is judged that THUMS captured post mortem human behaviour, but there are some issues worth noting. THUMS appears to be stiffer than the PMHS and the contacts between THUMS and the belt creates problems in the simulation. In chapter 4.2 the evaluation of THUMS is discussed further.

Differences in THUMS kinematics compared to PMHS kinematics does not necessarily mean that THUMS kinematics differ in the same manner, compared to living humans. No research is done in this project concerning differences between PMHS and humanís kinematics and it is therefore not possible to say if THUMS behaves more or less like a PMHS or a human.

The parameter variations during the sled validations and THUMS evaluation show which parameters that affect the test subject's kinematics significantly. The frictions between the subject and the seat, the location of the belt across the subject's chest and shoulder, which Shaw et al. (2005) means is important when measuring belt forces and how the belt is tightened are all important to the kinematics. The acceleration signals are less dependent on the belt situation than the belt forces.

The accelerometers in the mechanical tests were mounted with x forward. However, it is not known how exact the mounting was and there might be a difference in the rotation around the y axis. Therefore it is relevant to look at the resultant XZ accelerations and Y accelerations when comparing the test and the simulation results.

Since it is unknown where the lap belt force measure devices were positioned in the mechanical tests, they is assumed to be located at the lower anchor point of the belts in both test setups, since it is not visible at any other place on the belts in the pictures. If it is not positioned there, we are comparing forces that are not originating at the same part of the belt, and the adjustments of frictions and springs are not correct. However it is likely that the forces are measured at the end of the belts since that are the only places along the belt where it is not pressing against the dummy or the sled.

Since there is no documented procedure for how the seat belts were routed, it is assume that there were none. This can cause different slacks in the belts and as a result, the belt force is offset in time. The spring elements that are added in the belt anchors are used to compensate for this. For example in 15° far side collision in the Heidelberg sled a 43 mm spring gives approximately a 6 ms delay 1 kN. In general the springs are chosen to make the simulated force curve reach 1 kN at the same time as the test force. The 1 kN level is chosen sufficiently high to tighten the belt system completely. In some simulations choosing springs this way makes the simulations reach maximum force up to 25 ms earlier than the maximum force is reached in the tests. In these simulations the springs are chosen according to the best visible choice to create conformity between the simulation and test results.

## 4.1 Validation of the Sled Environments

The sled and seat geometry from the mechanical tests are specified and the sleds are built according to this information. The sled geometries should therefore not differ between the mechanical tests and the simulations. However, the material data are not fully known for either sled but when the seat material data are varied during the sled validation it turns out that this does not affect the kinematics significantly.

There is an issue with the 30° and 45° far side simulation angles. The shoulder belt slides of the HIII simulation models shoulder which can be seen in both the shoulder belt forces and the spine accelerations. This does not

occur in the mechanical test and the kinematic data can therefore not be compared after this happens. To test if it is possible to prevent the belt from sliding of the shoulder the shoulder belt is moved closer to the neck. The frictions in the contacts are also changed. Neither of these modifications gives successful results. The reason the belt slips of the shoulder can be that the simulation models is coarsely meshed and the chest can therefore not deform as it does on the physical dummy. In the mechanical tests the belt pressed onto the torso giving a local depression so that the belt stayed in place. In the simulation the torso is locally too stiff and the belt slides off.

Differences in the shoulder geometry are also relevant when looking at belt forces according to Shaw et al. (2005) and the coarse mesh in the HIII simulation model gives some differences in the shoulder geometry, seen in figure 4.1.2 and 4.1.1, which could affect the belt slip as well as the belt forces. It is not possible to position the arms of the HIII simulation model as the arms of the HIII crash dummy. However, moving the arm in the simulation model does not affect the shoulder geometry which can be seen in figure 4.1.2. It is possible that the arm position affects how the shoulders move, which could affect the belt slip. The influence the arms have on the belt slip is not evaluated.

Figure 4.1.1: *The shoulder of the HIII crash dummy. From* Humanetics *(2012).*

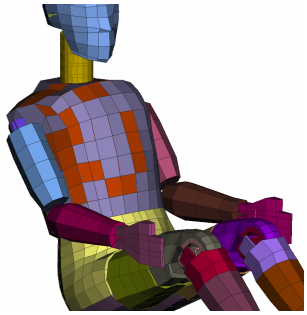

Figure 4.1.2: *The shoulder of the HIII simulation model.*

### 4.1.1 Validation of the Graz Sled Environment

When validating the Graz sled environment it is noticed that the lap belt force in the 30° near side mechanical dummy test is low. It is approximately half the amplitude of the simulated lap belt force as well as the lap belt forces in the mechanical tests in the other directions. It is therefore probable that the low test force curve is the result of the HIII dummy interacting with the belt force measuring device in the mechanical test. Since the device is not visible in the movies, we cannot tell if the dummy interacts with the device and therefore not determine if that is the reason for the low lap belt forces. In this validation it is assumed that the lap belt force is low due to measuring errors. The large difference between the test data and the simulation data is probably due to other issues as well. The hip displacement is approximately 4 cm shorter in the simulation than in the mechanical test, which could be the result of the lap belt force being too high in the simulation.

The high friction in the HIII belt interaction in the Graz sled validation is chosen due to that the HIII dummy did not wear any clothing in the mechanical test and the videos show that the belt did not slide along the dummies chest.

The Young's modulus for plywood normally ranges from 7.9-20 GPa. The plywood used in the Graz sled has a calculated Young's modulus of 1.23 GPa, calculated in chapter 2.2.1. This is probably due to that the plywood only has three layers, which makes the direction of the fibres important. The outer layers of the plywood in the sled are directed in the weaker direction which gives a low stiffness of the material. Another reason for the low Young's modulus can be that the measured plywood has been used in the tests and therefore might have internal micro cracks. Cracks would have evolved during the testing which would create small differences in Young's modulus between the tests. The plywood material data is varied in the validation of the sled which shows that the plywood does not have a significant effect on the kinematics.

### 4.1.2 Validation of the Heidelberg Sled Environment

There are also some issues with the kinematic responses in the Heidelberg simulations. The belt force curves in the 15° and 30° near side simulations are very similar to the test curves until 90 ms. After that the shoulder belt forces in the mechanical tests decreases while those in the simulations stays loaded. The opposite situation occurs in the lap belt where the test curves stay loaded while the simulation curves decreases. The issue with the simulated lap belt force decreasing before the test lap belt force occurs in the 15° far side angle as well.

Varying parameters during the sled validation does not eliminate these problems. It is possible that the belt force-elongation curve used in the simulation model does not correspond to the force-elongation curve from the actual belt. A 17% elongation belt might not be an exact scaling of a 16% elongation belt curve. The belts are different in all the tests as they have been previously used in cars. The usage might have caused different frictions in the belts, both in the slipring and between the belt and the HIII. This could also affect the lap belt force. Finally this could be due to belt positioning or HIII posture which, as explained above, is significant for the belt forces. The simulated accelerations are however similar to the test accelerometer signals which shows that the total response from the sled is satisfying.

There is an optional explanation for the issues above. If the belt force signals from the mechanical tests were switched, due to an error in the test setup, this would give better conformity in all angles. The original and switched belt forces for the 15° near side angle is seen in figure 4.1.3. If the belt force measuring device were switched in one angle, it is probable that they were switched in all angles as all tests were carried out in a sequence. However the evidence is not fully convincing in the all angles and the original force data are therefore used in the validation.

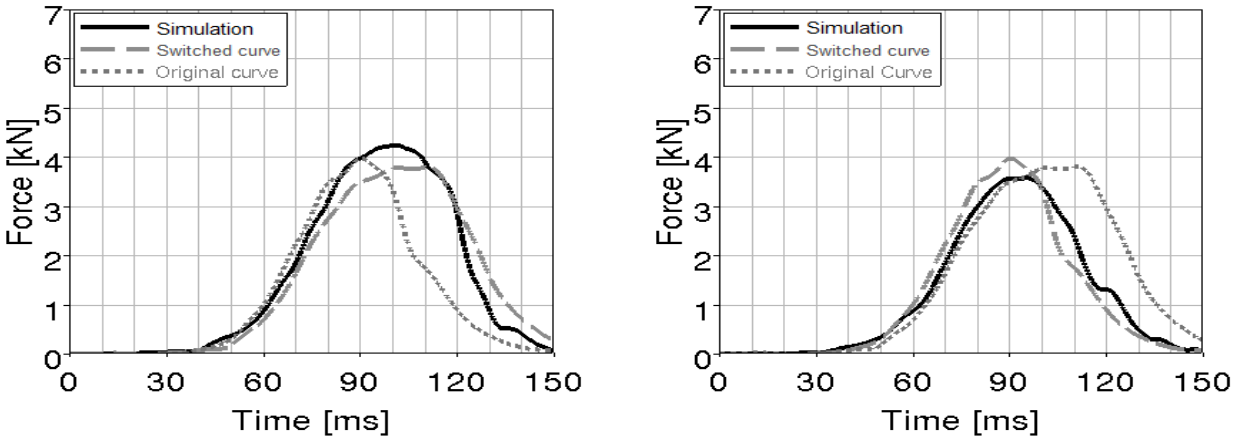


Figure 4.1.3: *Belt forces from the Heidelberg simulation in 15° near side angle. Right: Shoulder belt, Left: Lap belt.*

## 4.2 Evaluation of THUMS

THUMS captures post mortem human kinematics in the upper body. However, only one accelerometer on the spine, and tracking of the shoulders, is not particularly much information to use when evaluating the kinematics of a subject. Thus it is not possible to validate THUMS but only to evaluate it. Without any accelerometer or tracking on the pelvis or legs only the upper body movements can be evaluated. Tracking is not performed on the PMHS lower bodies since the videos are dark and 3D markers are not present there. What best shows that THUMS upper body moves similar to PMHS are the shoulder displacements. Comparing the displacements from the tests and the simulations, show a very close similarity with a difference of a few cm in most angles. In the cases where the simulated shoulder displacements differ from the mechanical test shoulder displacement, the shoulder belt force is also higher, up to 0.8 kN too high, which would explain the shorter shoulder movements.

It is complicated to determine within what range of the PMHS test THUMS should be to qualify as having well coinciding kinematics to a PMHS. The scaling used for the PMHS test data (Mertz, 1984), is based on the response of the thorax. The thorax is simplified to a mass-spring system where only the mass and depth of the chest are considered. A sled test is more complicated and the scaling might overlook many differences between PMHS that might be relevant in this case. However, it is necessary to scale the data since there are large length and weight differences between the cadavers.

In several angles of the Heidelberg test there are only one PMHS tested. It is not possible to draw any conclusions from such a comparison since the PMHS kinematics could be far from a mean PMHS kinematics. An example is the 15° far side test in the Heidelberg sled. There is a large difference between the belt forces of the simulation and the test data. This could be because the PMHS responded uniquely to that collision. That PMHS was probably tighter belted which results in the belt forces increasing earlier than in all the other tests. Even in the cases where there are two PMHS the corridor is most likely narrower than if there were more PMHS included in the tests.

The Graz sled has a fictive door structure. In Törnvall et al. (2008b) it is noticed that, out of the three PMHS tested, only PMHS 3 hits the car door in the 30° near side test. Since PMHS 3 is closer to a 50th percentile male than the other PMHS in the Graz test, Törnvall states that a 50th percentile male would hit the door. THUMS, which is a 50th percentile male, hits the door in this angle and confirms Törnvalls hypothesis.

Some issues can be seen in the kinematic comparison as well as during the simulations. In all the THUMS simulations, in both sled setups, all angles and both seat belt systems, the shoulder belt force increases steeper than in the PMHS tests. This could be due to that THUMS is stiffer than the PMHS. The acceleration signals from the THUMS simulations are also very noisy. They are filtered with SAE60 like all other signals but some of the noise remains. This makes the comparison complicated since the signals fluctuate a lot.

In the simulations there are problems with entanglement between THUMS and the belt. The shoulder belt presses hard into THUMS chest, which causes the elements in the chest to wrap around the belt and the elements get entangled and the belt get stuck, see figure 4.2.1. Another numerical problem is that the belt gets stuck in THUMS neck in the simulations of the Heidelberg sled in near side collisions. The fact that it only occurs in the Heidelberg sled is due to the positions of the belt attachment points. The problem is partly adjusted using null elements between the neck and the shoulder but it does not solve the problem completely. This might cause the shoulder belt force to increase and could then explain why the shoulder belt in 30° near side simulation is higher than expected.

## 4.3 Sources of Error and Limitations

The primary use of the PMHS test series, when performed may years ago was not to compare the test data with simulations. This has caused a lack of information that is useful in a simulation and several estimates have to be made. The information missing is listed below:

- Dynamic data for some of the sled materials.
- Information on when the bolt and the aluminium extension at the upper belt anchor of the Graz sled was deformed. This might have happened during a test, when it was built or during transport. This information could lead to important dynamic data on the materials. Most likely the aluminium extension was deformed when the bolt was tightened and the bolt was deformed during a test. Either way, the spring elements added in the belt anchor of the simulation model also compensate for the flexibility in the bolt and aluminium extension.
- There is inconsistent information regarding belt anchor positions in the Heidelberg sled. Figure 2.1.5 shows that both the buckle and the lower anchor are located on the same x and z coordinates. However it is also stated in Törnvall et al. (2005) that the original buckle is used and this is not located at the same x and y coordinates as the figure shows. The location of the buckle is chosen as the original seat buckle.

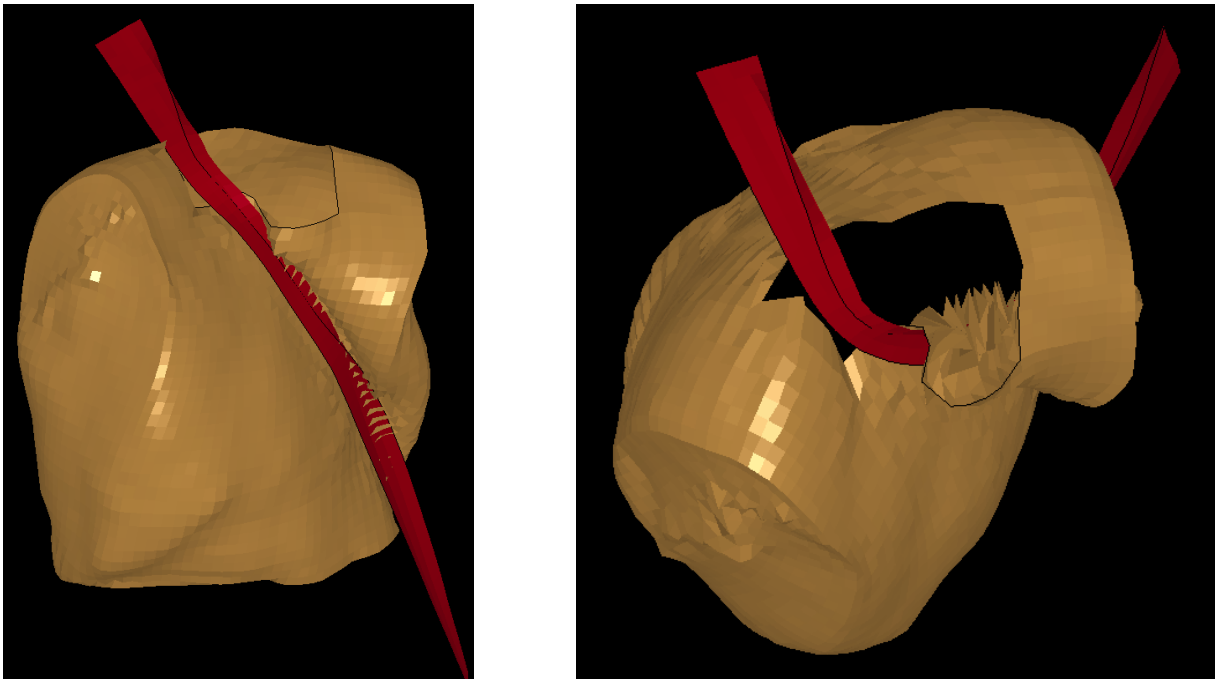

Figure 4.2.1: *THUMS chest interacting with the belt.*

- Detailed information on the back angle of the test subjects. This could cause differences in the position between the test subjects in the mechanical tests and in the simulations, which might cause some differences in the kinematics.
- Information about the way the test subjects were strapped in the belts, how tight they were fastened and where the belt was strapped over the chest and shoulder.
- Information about the location of the lap belt force measuring device.
- A flash to mark time 0 in the videos of the Graz test. This might have caused the timing on the hip tracking to be off.
- Accelerations of the lower part of the body. This makes it impossible to evaluate THUMS kinematics fully.
- The accelerometers in the original Heidelberg test only measured accelerations in the directions, x and z. This means that the movement in y direction, important since the tests are in oblique angles, is unknown and cannot be evaluated.
- Accelerometers and force measuring devices were not calibrated to 0 in the Heidelberg dummy tests. They are therefore offset in this project to start at 0, which is done by hand.

There are some issues that have occurred during the work of reproducing the mechanical sled tests. These are listed below.

- The HIII dummies were positioned with their hands on the laps, but the arms of the simulation models does not reach that far.
- The foam used in the Graz sled simulation model is of the same material and density as the foam used in the Graz mechanical sled, but it has unknown cell structure. The foam used in the Graz sled is a closed cell structure. If the foams have different cell structure this might affect the force-deflection curve. However, the curve is varied during the sled validation without any significant effect on the responses. With this information the material model for the foam is seen as sufficiently good.

- The HIII dummy does not wear any clothing in the Graz test, which made it necessary to re-evaluate the frictions in the Graz sled between the sled validation and THUMS evaluation.
- The sled tests performed at Chalmers using the HIII dummy were not run with the same sled as the original Heidelberg sled tests were. The steel rig differs some and new golf Mk1 seats and seat belts, as in the original Heidelberg setup, could not be found and used seats and seat belts were used instead. The foam in the seat might therefore have behaved differently. It is also possible that new and old belts have different loading curves and different friction coefficients. This means that the sled optimized in the sled validation does not necessarily have the same response as the original sled.
- The belt curve used in the simulation material is taken from a 16% elongation seat belt and then scaled to a 17 % elongation seat belt. This scaled belt curve might differ from the actual belt curve. There might also be a difference in the belt curve between a used belt and a new belt.

## 4.4 Recommendations

Further work is recommended in order to validate THUMS in oblique frontal sled tests. Research on how to scale PMHS kinematic test data in order of comparing the data with THUMS kinematic data is needed. The scaling methods available today are not developed in order of scaling sled test data. Scaling THUMS kinematic data to sizes of the PMHS is another tool that would be useful.

In order of validating THUMS further in these angles, new sled tests need to be performed with the objective to simulate them. In order for the tests to be simulated properly, documentation of the dynamic belt data is needed for the force and velocity span of the test. The belt position along the chest and shoulder as well as the test subject posture needs to be documented and/or photographed. The procedure used when tightening the belt must be documented. Document where the belt force measuring devices are positioned and make sure that the test subject does not interact with the measuring devices. Finally in order of comparing the kinematic response of the entire THUMS model body accelerometers needs to be attached to both the upper and lower parts of the spine. Measuring equipment on the chest would also be useful. When filming mechanical tests, use a flash to mark time 0. This makes it easy to compare tracking from the videos with accelerometer signals and simulation signals. Use good light when filming and photographing. Use several cadavers in each test angle. If cadavers of a 50th percentile male cannot be used, spread cadaver sizes (length, weight) over all tests angles. This gives a corridor for each angle within which most cadavers sizes should fit.

During the numerical work of a validation it is useful to do a full DOE on all uncertain parameters. In this project the focus is on the material parameters and contacts due to the simplicity of evaluating these parameters. Including more variations in seating position, belt position and tightening of the belt would give more answers to how important these parameters are.

# 5 Conclusion

The THUMS model generally shows realistic kinematics in the upper body when compared to PMHS. However, the model appears to be stiffer than the PMHS in the upper body. Problems with THUMS in the simulations include the belt entangling with the chest elements and wedging down in the neck. Another problem is that the accelerometer signals from THUMS are very noisy. This evaluation should only be seen as an indication of THUMS post mortem human kinematics and therefore more validations of THUMS need to be done in oblique frontal collisions.

# References


*ANSA* (2011). *CAE Pre-processor*. Version 13.2.1. Beta CAE Systems SA. URL: http://www.beta-cae.gr/ansa.htm.

*Britannica* (June 10, 2012a). *Human rib cage*. URL: http://www.britannica.com/EBchecked/media/138380/Human-rib-cage.

*Britannica* (June 10, 2012b). *Vertebral column*. URL: http://www.britannica.com/EBchecked/topic/626589/vertebral-column.

*Bultens teknikhandbok* (1999). IDÉ bild. URL: www.bulten.com.

Chawla, A et al. (2005). "Vaidation of the Cervical Spine Model in THUMS". In:

Guha, S. et al. (Oct. 30, 2008). "LSTC Hybrid III Dummies. Positioning & Post-Processing. Dummy Version: LSTC.H3.103008$_v$1.0". In: *Materials and Science in Sports*, pp. 105–117.

*Humanetics* (June 3, 2012). *Hybrid III 50th Male Dummy 78051-218X*. Humanetics. URL: http://www.humaneticsatd.com/sites/default/files/PC-H3-50th.pdf.

*HyperGraph* (2011). *Post-Processor*. Version 11. Altair HyperWorks. URL: http://www.altairhyperworks.com/Product,5,HyperGraph.aspx.

Iwarmoto, M. et al. (2002). "Development of a Finete Element Model of the Total Human Model For Safety (THUMS) and Application to Injury Reconstruction". In: *IRCOBI Conference Munich(Germany), September 2002*.

Kallieris, D. (1982). "Thoraxbelastung und Verletzungsmuster bei der Schrägkollision". In: *Beitr Gerichtl Med* XL, pp. 275–81.

Kang, S. and P. Xiao (2008). "Comparison of Hybrid III Rigid Body Dummy Models". In: *10th International LS-DYNA Users Conference*.

*LS-DYNA* (2012). *Occupant safety simulations*. Version Dyna version. Livermore Software Technology Corporation. URL: http://www.lstc.com/.

*LSTC. LSTC.H3.103008.V1.0.RigidFE.50th*. URL: http://www.lstc.com/.

*MAKROCLEAR* (Jan. 31, 2012). *Polycarbonate sheet*. Arla Plast AB. URL: http://www.arlaplast.se/GetDoc.ashx?p=72&t=0&s=8.

Mattson, B. S. (2001). *Aluminium SIS handbok 12:2001*. SIS Förlag AB, pp. 332, 345.

Mertz, H. J. (1984). "A Procedure for Normalizing Impact Response Data". In: *SAE Technical Paper*, pp. 1159–1166.

*MetaPost* (2011). *Post-processor*. Version 6.7.0. Beta CAE Systems SA. URL: http://www.beta-cae.gr.

Mills, N. and G. Lyn (2001). "Design of Foam Padding for Rugby Posts". In: *Materials and Science in Sports*, pp. 105–117.

Oshita, F. et al. (2002). "Development of a Finite Element Model of the Human Body". In: *7th International LS-DYNA Users Conference*.

Pipkorn, B. and R. Kent (2011). "Validation of a Human Body Thorax Model and its Use for Force, Energy and Strain Analysis in Various Loading Conditions". In: *IRCOBI*.

*Plastmästarn* (Jan. 31, 2012). *Correspondence with glenn@plastmastarn.se*. URL: http://www.plastmastan.se.

Ragland, C et al. (2001). "Evaluation of Frontal Offset/Oblique Crach Test Conditions". In: *17th International Yechnical Conference on the Enhanced Safety of Vehicles*.

*SAE J211* (Oct. 1970). *Surface Vehicle Recommended Practice: Instrumentation for Impact Test - part 1 - Electronic Instrumentation*. Version REV.MAR95. SAE International.

Serifi, E. et al. (2008). "Modelling of Foams using MAT83 - Preperation and Evaluation of Experimental Data." In: $4^{th}$ *European LS-DYNA Users Conference*.

Shaw, G. et al. (2005). "Dummy Torso Response to Anterior Quasi-Static Loading". In:

Sundström, B. and others. (1998). *Handbok och formelsamling i Hållfasthetslära*. Fingraf AB, pp. 332,345.

*Toyota Central R&D Labs*. URL: http://www.tytlabs.co.jp/eindex.html.

*Transportstyrelsen* (May 15, 2012). *Dödade och svårt skadade efter färdsätt*. Transportstyrelsen. URL: http://www.transportstyrelsen.se/sv/Press/Statistik/Vag/Olycksstatistik/Olycksstatistik-vag/Nationell-statistik1/Arsvis-statistik/Historik-fardsatt/.

Törnvall, F. V. et al. (2005). "Frontal Impact Dummy Kinematics in Oblique Frontal Collisions: Evaluation Against Post Mortem Human Subject Test Data". In: *Traffic Injury Prevention* 6, pp. 340–350.

Törnvall, F. V. et al. (2008a). "Evaluation of Dummy shoulder Kinematics in Oblique Frontal Collisions". In: *IRCOBI*, pp. 195–210.

Törnvall, F. V. et al. (2008b). "Post Mortem Human Subject Kinematics in Oblique Frontal Collision: Shoulder Complex Emphasized". In:

*Unpublished material from the Graz test* (2012). *Data received from Chalmers Division of Vehicle Safey through Johan Davidsson.*

*Unpublished material from the Heidelberg test* (2012). *Data received from Chalmers Division of Vehicle Safey through Mats Y Svensson.*

*Version 2.21-040407* (2005). *Labs, T.C.R.D. THUMS (Total HUman Model for Safety) Occupant Model.*

# A Material Cards and Contact Cards in Graz Simulation Model

## A.1 Material Cards

```
*MAT_LOW_DENSITY_FOAM_TITLE
Seat foam
       1    3.5E-8   0.00035      9992     1.E20      0.01              0.05
      7.       0.0      0.0        0.       0.        0.        1.
*MAT_RIGID_TITLE
Rigid sled material lock
       2   7.85E-6      210.       0.3       0.        0.        0.
     1.0        5.       7.
       0.       0.       0.        0.       0.        0.
*MAT_RIGID_TITLE
Rigid sled material
       3   7.85E-6      210.       0.3       0.        0.        0.
     0.0
       0.       0.       0.        0.       0.        0.
*MAT_ELASTIC_TITLE
PC
       4    1.2E-6       2.3       0.3       0.        0.        0.
*MAT_ELASTIC_TITLE
Plywood
     120   5.71E-7      1.23       0.3       0.        0.        0.
*MAT_PIECEWISE_LINEAR_PLASTICITY_TITLE
Aluminium 6083 T6 EN755_2 1997
       6    2.7E-6       69.       0.3                 0.     1.E20        0.
       0.       0.     9993                  0.
       0.       0.       0.        0.       0.        0.        0.        0.
       0.       0.       0.        0.       0.        0.        0.        0.
*MAT_PIECEWISE_LINEAR_PLASTICITY_TITLE
steel screw 8.8 bultens_teknikhandbok
       7   7.85E-6      210.       0.3                 0.     1.E20        0.
       0.       0.        4                  0.
       0.       0.       0.        0.       0.        0.        0.        0.
       0.       0.       0.        0.       0.        0.        0.        0.
*MAT_RIGID_TITLE
Default MAT20 MAT_RIGID buckle
     100   1.12E-6      206.       0.3       0.        0.        0.
     0.0
       0.       0.       0.        0.       0.        0.
*MAT_RIGID_TITLE
Default MAT20 MAT_RIGID buckle
     101   7.83E-6      206.       0.3       0.        0.        0.
     0.0
       0.       0.       0.        0.       0.        0.
*MAT_SPRING_GENERAL_NONLINEAR_TITLE
Default MAT205 MAT_SPRING_GENERAL_NONLINEAR buckle
     102       24       25        0.       0.        0.
*MAT_RIGID_TITLE
Default MAT20 MAT_RIGID buckle
     103   7.85E-6      210.       0.3       0.        0.        0.
     0.0
       0.       0.       0.        0.       0.        0.
*MAT_SPRING_INELASTIC_TITLE
Default MAT207 MAT_SPRING_INELASTIC_uppe
     104       22        0.      -1.0
*MAT_SPRING_INELASTIC_TITLE
Default MAT207 MAT_SPRING_INELASTIC_nere
     105       23        0.      -1.0
*MAT_SEATBELT_TITLE
MAT_SEATBELT 1D
    1000    0.0002       10       10      4.9



*MAT_SEATBELT_TITLE
Mat seatbelt shells
    1001    0.0002       10       10      1.2       2.
*MAT_FABRIC_TITLE
Seatbelt fabric
    1002     2.E-7     4.58                    0.2
                                                      0.05
                            0.       0.0       0.0
```

## A.2 Material Curves

```
*DEFINE_CURVE_TITLE
Screw_88 bolt
      4       0       1.    1000.       0.       0.
             0.             0.64
          0.109            0.896
*DEFINE_CURVE_TITLE
Loading_curve_belt
     10       0       1.       1.       0.       0.
             0.             0.
       0.003358           0.125
        0.00709         0.416667
       0.009701         0.833333
       0.012687         1.208333
       0.014552              1.5
       0.016045             1.75
       0.017537         2.041667
       0.020896         2.541667
       0.023881         2.833333
          0.025         2.916667
       0.026119         3.083333
       0.028358             3.25
       0.031343         3.458333
       0.031716         3.583333
       0.035821         3.833333
       0.037687         3.958333
       0.040672            4.125
       0.045522            4.375
       0.061194            5.125
       0.079851               6.
       0.087687             6.25
       0.097388         6.666667
       0.105597         7.041667
       0.113433            7.375
       0.118657         7.583333
       0.123881         7.833333
       0.126493         7.958333
       0.135448         8.416667
       0.141791         8.833333
       0.150746         9.291667
       0.159701            9.875
       0.164552            10.25
       0.171642         10.58333
       0.178358         11.04167
       0.182836         11.41667
       0.186567         11.66667
       0.188433         12.04167
*DEFINE_CURVE_TITLE
80022  RIGHT ANCH END PART _spring
     22       0      4*.       1.       0.       0.                    * Scale factor, changed between the tests.
             0.             0.
            4.8             1.
            6.4             2.
```

```
           7.04                3.
           8.                  8.
           8.8                 20.
*DEFINE_CURVE_TITLE
80022  RIGHT ANCH END PART _spring
      23        0       6*.       1.       0.       0.                    * Scale factor, changed between the tests.
             0.                  0.
             4.8                 1.
             6.4                 2.
             7.04                3.
             8.                  8.
             8.8                 20.
*DEFINE_CURVE_TITLE
DEFINE_CURVE_00000491_buckle
      24        0       1.       1.       0.       0.
           -0.57            -10000.
           -0.55              -0.1
             0.                  0.
            0.41                0.1
            0.43               10000.
*DEFINE_CURVE_TITLE
DEFINE_CURVE_00000492buckle
      25        0       1.       1.       0.       0.
           -0.02            -10000.
             0.                  0.
            0.02               10000.
*DEFINE_CURVE_TITLE
PE_FOAM
    9992        0       1.    0.001       0.       0.
             0.                  0.
         0.002165            0.003053
         0.012351            0.006107
         0.024236             0.01145
         0.034423            0.016794
         0.046307            0.022901
         0.051401            0.026718
         0.056494            0.033588
         0.068379            0.040458
         0.073472            0.045802
         0.080263            0.051908
         0.088752            0.057252
         0.095543            0.064885
         0.114219            0.077863
         0.127801            0.082443
         0.146477             0.08626
         0.166851             0.09084
         0.171944             0.09313
         0.540365            0.167939
         0.547156              0.1694
         0.557156            0.171587
         0.567156            0.173946
         0.577156            0.176496
```

```
        0.587156          0.179256
        0.597156          0.182251
        0.607156          0.185506
        0.617156          0.189052
        0.627156          0.192925
        0.637156          0.197163
        0.647156          0.201813
        0.657156          0.206929
        0.667156          0.212574
        0.677156           0.21882
        0.687156          0.225755
        0.697156          0.233479
        0.707156          0.242114
        0.717156          0.251806
        0.727156          0.262728
        0.737156          0.275092
        0.747156          0.289156
        0.757156          0.305237
        0.767156          0.323727
        0.777156           0.34512
        0.787156          0.370035
        0.797156          0.399269
        0.807156          0.433846
        0.817156          0.475111
        0.827156          0.524851
        0.837156          0.585476
        0.857156          0.753982
*DEFINE_CURVE_TITLE
Aluminium_curve
    9993       0       1.      1.      0.      0.
              0.              0.24
          0.0725              0.31
```

## A.3 Contact Cards in the Sled

```
*CONTACT_AUTOMATIC_SURFACE_TO_SURFACE_ID
1       *CONTACT_door_rigg_window
       3       4       2       2                       0       0
     0.3                             20.       0

*CONTACT_AUTOMATIC_SINGLE_SURFACE_ID
2       *CONTACT_belt_attachment
       7       0       1       0                       0       0
     0.3                                     0

*CONTACT_TIED_SURFACE_TO_SURFACE_OFFSET_ID
3       *CONTACT_foam_sits
       5       6       2       2                       0       0
     0.3                             20.       0

*CONTACT_AUTOMATIC_SURFACE_TO_SURFACE_ID
4       *CONTACT_belt_foam
       9       6       2       2                       0       0
     0.3                             20.       0

       2      0.1           1.025       0.       2       10       1
      0.       0       0       0       0       0      0.       0.
```

## A.4 Contact Cards in the HIII Simulation

```
*CONTACT_AUTOMATIC_SURFACE_TO_SURFACE_ID
1       Contact lap belt
   100082       7       2       2                       1       1
     0.9                               20.       0

       2      0.1           1.025       0.       2       10       1
      0.       0       0       0       0
*CONTACT_AUTOMATIC_SURFACE_TO_SURFACE_ID
2       CONTACT_leg_leg
   100077   100078       2       2                       0       0
     0.3                                     0

*CONTACT_AUTOMATIC_SURFACE_TO_SURFACE_ID
3       *CONTACT_gubbe_foam
       7       8       2       2                       0       0
     0.3                               20.       0

*CONTACT_AUTOMATIC_SURFACE_TO_SURFACE_ID
5       *CONTACT_feet_rigg
   100006      100       2       2                       0       0
     0.4                               20.       0

*CONTACT_AUTOMATIC_SURFACE_TO_SURFACE_ID
6       Contact_feet_belt
   100073   100070       2       2                       1       1
     0.3                               20.       0

       2      0.1           1.025       0.       2       10       1
      0.       0       0       0       0
*CONTACT_AUTOMATIC_SURFACE_TO_SURFACE_ID
10      Contact shoulder belt
   100083   100089       2       2                       1       1
     0.9                               20.       0

       2      0.1           1.025       0.       2       10       1
      0.       0       0       0       0
*CONTACT_AUTOMATIC_SURFACE_TO_SURFACE_ID
100008   *CONTACT_gubbe_door
   100002       10       2       2                       0       0
     0.2                               20.       0

*CONTACT_AUTOMATIC_SURFACE_TO_SURFACE_ID
100005   *CONTACT_gubbe_ryggstod
   100086   100084       2       2                       0       0
```

## A.5 Contact Cards in the THUMS Simulation

```
*CONTACT_AUTOMATIC_SURFACE_TO_SURFACE_ID
10       *CONTACT_THUMS_FOAM
  8980003        6        2        2                         0        0
      0.6                               20.        0

       1      0.1             1.025       0.        2       10        1
      0.        0        0        0        0
*CONTACT_AUTOMATIC_SURFACE_TO_SURFACE_ID
11       *CONTACT_lap_belt
       11   8980003        2        2                         0        0
      0.6                               20.        0

       2      0.1             1.025       0.        2       10        1
      0.        0        0        0        0
*CONTACT_AUTOMATIC_SURFACE_TO_SURFACE_ID
12       *CONTACT_feet_belt
       12       100        2        2                         0        0
      0.3                               20.        0

*CONTACT_AUTOMATIC_SURFACE_TO_SURFACE_ID
13       *CONTACT_shoulder_belt
       10       101        2        2                         0        0
      0.6                               20.        0

       2      0.1             1.025       0.        2       10        1
      0.        0        0        0        0
*CONTACT_AUTOMATIC_SURFACE_TO_SURFACE_ID
14       *CONTACT_Head_arms
  8710009       102        2        2                         0        0
      0.2                               20.        0

       2      0.1             1.025       0.        2       10        1
      0.        0        0        0        0
```

# B Material Cards and Contact Cards in Heidelberg Simulation Model

## B.1 Material Cards

```
*MAT_PIECEWISE_LINEAR_PLASTICITY_TITLE
 Docol 200 rate
       1    7.8E-6      210.       0.3        0.        0.        0.
                        1                1.


*MAT_LOW_DENSITY_FOAM_TITLE
Seat_foam
        2    6.7E-8  0.000276         2     1000.       0.1     8000.      0.02
       2.       0.0       0.0        0.       0.        0.        1.
*MAT_RIGID_TITLE
Seat_back_rigid
        3   7.85E-6      210.       0.3        0.        0.        0.
      0.0
       0.        0.        0.        0.        0.        0.
*MAT_NULL_TITLE
Seat null mat
       10   7.85E-6        0.        0.        0.        0.      210.       0.3
*MAT_SPRING_GENERAL_NONLINEAR_TITLE
Belt_attachment_spring
      802     80024     80025        0.        0.        0.
*MAT_RIGID_TITLE
belt_attachment_anchor_rigid
      803   7.85E-6      210.       0.3        0.        0.        0.        0.
      0.0
       0.        0.        0.        0.        0.        0.
*MAT_RIGID_TITLE
Rigid sled
     1000   7.85E-6      210.       0.3        0.        0.        0.
       1.0        5.        7.
       0.        0.        0.        0.        0.        0.
*MAT_RIGID_TITLE
Belt_anchor_rigid
     1001   7.85E-6      210.       0.3        0.        0.        0.        0.
      0.0
       0.        0.        0.        0.        0.        0.
*MAT_SEATBELT_TITLE
MAT_SEATBELT 1D
    80012    0.0002       10        10       4.9
*MAT_SEATBELT_TITLE
Mat seatbelt shells
    80013    0.0002       10        10       1.2        2.
*MAT_SPRING_INELASTIC_TITLE
Upper spring
    80021     80021        0.      -1.0
*MAT_SPRING_INELASTIC_TITLE
Lower spring
    80022     80022        0.      -1.0
*MAT_FABRIC_TITLE
Seat fabric
  2000500   6.91E-7      0.41      0.41      0.41       0.3       0.3       0.3
     0.038     0.038     0.038         1.       0.5       0.3       0.5      0.05
       0.0        0.        0.        0.       0.0       0.0                 0.
```

## B.2 Material Curves

```
*DEFINE_CURVE_TITLE
80021 RIGHT ANCH END PART
   80021       0     16*.      1.      0.      0.                  * Scale factor, changed between the tests.
            0.              0.
           4.8              1.
           6.4              2.
          7.04              3.
           8.              8.
           8.8             20.
*DEFINE_CURVE_TITLE
80021 RIGHT ANCH END PART
   80022       0      6*.      1.      0.      0.                  * Scale factor, changed between the tests.
            0.              0.
           4.8              1.
           6.4              2.
          7.04              3.
           8.              8.
           8.8             20.
*DEFINE_CURVE_TITLE
Belt_spring
   80024       0      1.    1000.      0.      0.
         -0.57          -10000.
         -0.55            -0.1
            0.              0.
          0.41             0.1
          0.43           10000.
*DEFINE_CURVE_TITLE
Belt_spring
   80025       0      1.    1000.      0.      0.
         -0.02          -10000.
            0.              0.
          0.02           10000.
*DEFINE_CURVE_TITLE
retractor loading curve
   80026       0      1.      1.      0.      0.
            0.            0.01
            1.            100.
*DEFINE_CURVE_TITLE
retractor unloading curve
   80027       0      1.      1.      0.      0.
            0.              0.
           15.             12.
*DEFINE_TABLE_TITLE
Docol 200 steel
      11
   1.E-8
  0.0001
   0.001
    0.01
     0.1
      1.
```

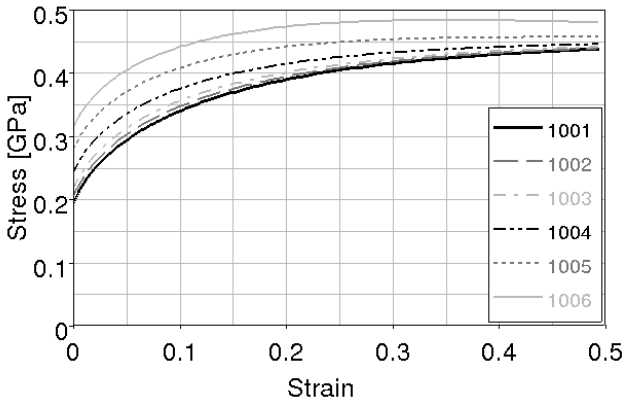


Figure B.2.1: *Material curves for Docol 200 steel in the simulated seat model.*

```
*DEFINE_CURVE_TITLE
Loading_curve seat belt
     10       0    1.06       1.       0.       0.
             0.              0.
       0.003358          0.125
        0.00709        0.416667
       0.009701        0.833333
       0.012687        1.208333
       0.014552             1.5
       0.016045            1.75
       0.017537        2.041667
       0.020896        2.541667
       0.023881        2.833333
          0.025        2.916667
       0.026119        3.083333
       0.028358            3.25
       0.031343        3.458333
       0.031716        3.583333
       0.035821        3.833333
       0.037687        3.958333
       0.040672            4.125
       0.045522            4.375
       0.061194            5.125
       0.079851               6.
       0.087687            6.25
       0.097388        6.666667
       0.105597        7.041667
       0.113433            7.375
       0.118657        7.583333
       0.123881        7.833333
       0.126493        7.958333
       0.135448        8.416667
       0.141791        8.833333
       0.150746        9.291667
       0.159701            9.875
       0.171642        10.58333
       0.178358        11.04167
       0.182836        11.41667
       0.186567        11.66667
       0.188433        12.04167


*DEFINE_CURVE_TITLE
Seat_foam
     1000       0       1.       1.       0.       0.
```

Curve 1000 is seen in figure 2.2.8 with the legend Heidelberg.

## B.3 Contact Cards in the Sled

```
*CONTACT_AUTOMATIC_SURFACE_TO_SURFACE_ID
1         Seat_foam
         1       2       2       2                       0       0
       0.3                             20.       0

         1      0.1            1.025       0.       2       0       0
*CONTACT_AUTOMATIC_SURFACE_TO_SURFACE_ID
2         Pipes_seat
         3       1       2       2                       0       0
       0.1                                     0

*CONTACT_AUTOMATIC_SURFACE_TO_SURFACE_ID
3         Pipes_foam
         2       3       2       2                       0       0
       0.3                             20.       0

*CONTACT_AUTOMATIC_SURFACE_TO_SURFACE_ID
10        Belt_foam
        34       21       2       2                       0       0
        0.                             20.       0

         2      0.1            1.025       0.       2      10       1
*CONTACT_AUTOMATIC_SURFACE_TO_SURFACE_ID
11        Buckle_plate
        41       40       2       2                       0       0
       0.1                             20.       0
```

## B.4 Contact Cards in the HIII Simulation

```
*CONTACT_AUTOMATIC_SURFACE_TO_SURFACE_ID
4         Leg_contact
         7       8       2       2                       0       0
                                              0

*CONTACT_AUTOMATIC_SURFACE_TO_SURFACE_ID
5         Feet_sled
        11       12       2       2                       0       0
       0.1                                     0

*CONTACT_AUTOMATIC_SURFACE_TO_SURFACE_ID
6         Bottom_foam
        13       21       2       2                       0       0
      0.23                              20.       0

         2      0.1            1.025       0.       2      10       1
*CONTACT_AUTOMATIC_SURFACE_TO_SURFACE_ID
7         Belt_lap
        17       15       2       2                       0       0
       0.1                             20.       0

         2      0.1            1.025       0.       5       3       1
*CONTACT_AUTOMATIC_SURFACE_TO_SURFACE_ID
8         Belt_Shoulder
        16       27       2       2                       0       0
       0.1                             20.       0

         2      0.1            1.025       0.       5       3       1
*CONTACT_SURFACE_TO_SURFACE_ID
9         Feet_belt
    100113   100114       2       2                       0       0
       0.1                             20.       0
```

## B.5 Contact Cards in the THUMS Simulation

```
*CONTACT_AUTOMATIC_SURFACE_TO_SURFACE_ID
6       Bottom_seat
  8980003       2       2       2                       0       0
    0.23                            20.       0

       2      0.1           1.025       0.       2       10       1
*CONTACT_SURFACE_TO_SURFACE_ID
7       Feet_belt
 18980038  18980037       2       2                       0       0
     0.1                            20.       0

*CONTACT_AUTOMATIC_SURFACE_TO_SURFACE_ID
8       chest_belt
      35       28       2       2                       0       0
     0.1                            20.       0
                              1.
       2      0.1           1.025       0.       5       3       1
*CONTACT_AUTOMATIC_SURFACE_TO_SURFACE_ID
9       Lap_belt
      36       29       2       2                       0       0
     0.1                            20.       0
                              1.
       2      0.1           1.025       0.       5       3       1
*CONTACT_AUTOMATIC_SURFACE_TO_SURFACE_ID
10      Feet_floor
 18980037       39       2       2                       0       0
     0.1                            20.       0

       2      0.1           1.025       0.       2       10       1
*CONTACT_AUTOMATIC_SURFACE_TO_SURFACE_ID
11      Head_arms
  8000004   8710009       2       2                       0       0
                                        0

       2      0.1           1.025       0.       2       10       1
```

# C Simulations of the Graz Sled with HIII

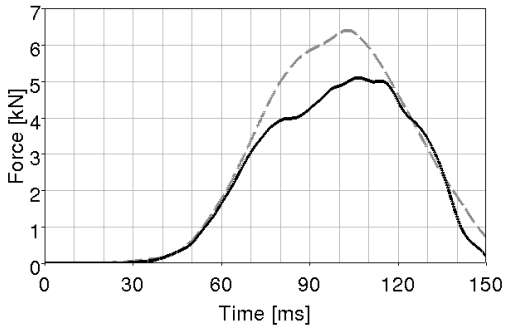


Figure C.0.1: *Shoulder belt force in* 45° *far side collision with HIII, Graz. From Törnvall et al. (2008a).*

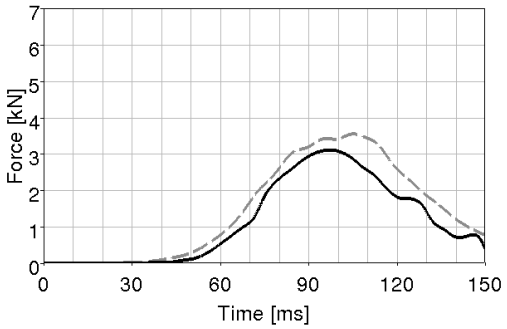


Figure C.0.2: *Lap belt force in* 45° *far side collision with HIII, Graz. From Törnvall et al. (2008a).*

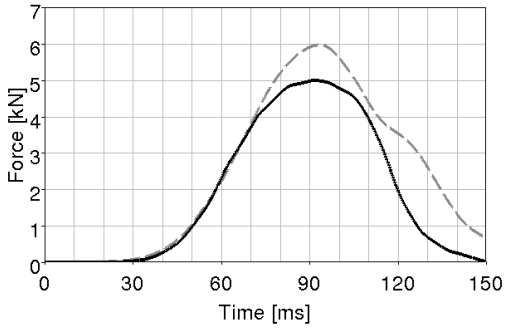


Figure C.0.3: *Shoulder belt force in* 0° *collision with HIII, Graz. From Törnvall et al. (2008a).*

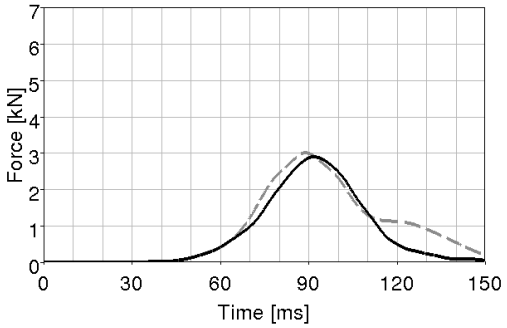


Figure C.0.4: *Lap belt force in* 0° *collision with HIII, Graz. From Törnvall et al. (2008a).*

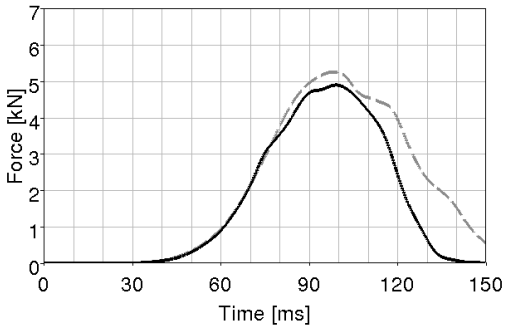


Figure C.0.5: *Shoulder belt force in* 30° *near side collision with HIII, Graz. From Törnvall et al. (2008a).*

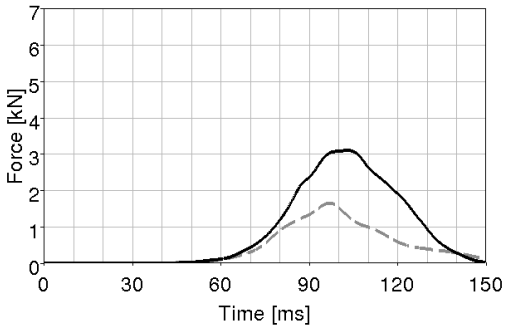


Figure C.0.6: *Lap belt force in* 30° *near side collision with HIII, Graz. From Törnvall et al. (2008a).*

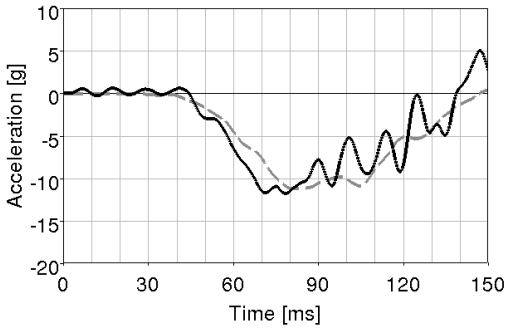


Figure C.0.7: *X acceleration in T1 in* 45° *far side collision with HIII, Graz. From Törnvall et al. (2008a).*

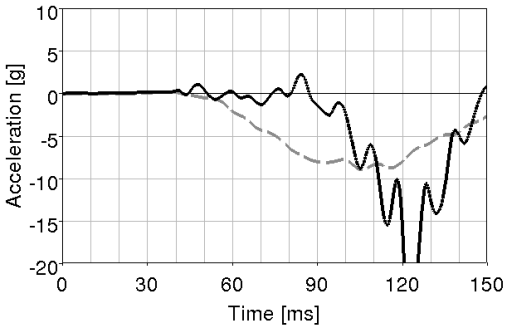


Figure C.0.8: *Y acceleration in T1 in* 45° *far side collision with HIII, Graz. From Törnvall et al. (2008a).*

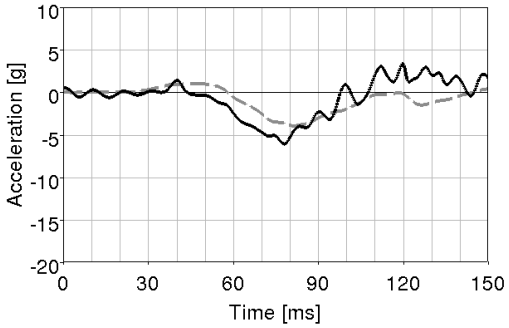


Figure C.0.9: *Z acceleration in T1 in* 45° *far side collision with HIII, Graz. From Törnvall et al. (2008a).*

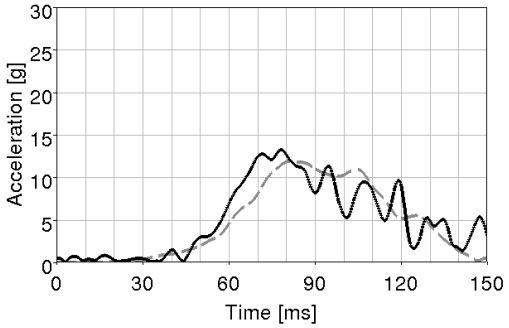


Figure C.0.10: *XZ acceleration in T1 in* 45° *far side with HIII, Graz. From Törnvall et al. (2008a).*

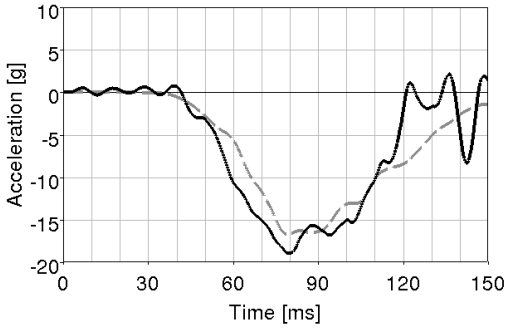


Figure C.0.11: *X acceleration in T1 in* 0° *collision with HIII, Graz. From Törnvall et al. (2008a).*

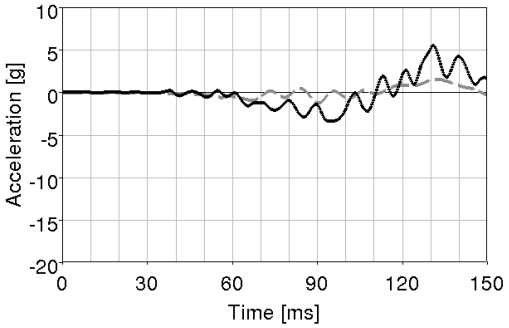


Figure C.0.12: *Y acceleration in T1 in* 0° *collision with HIII, Graz. From Törnvall et al. (2008a).*

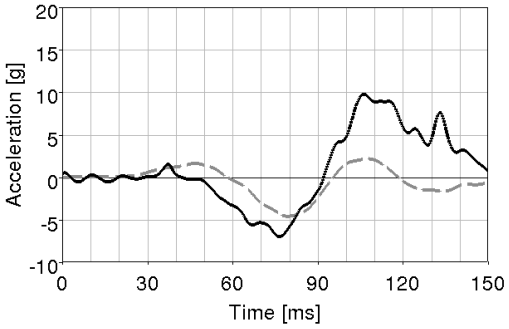


Figure C.0.13: *Z acceleration in T1 in* 0° *collision with HIII, Graz. From Törnvall et al. (2008a).*

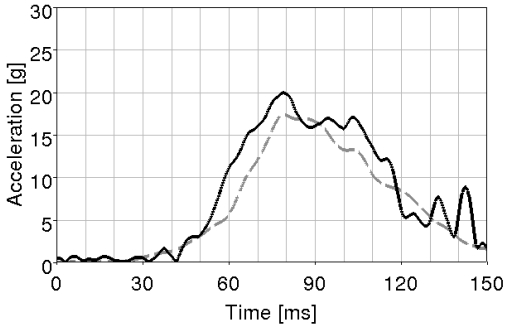


Figure C.0.14: *XZ acceleration in T1 in* 0° *collision with HIII, Graz. From Törnvall et al. (2008a).*

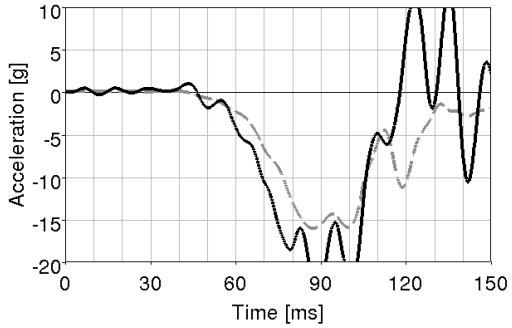


Figure C.0.15: *X acceleration in T1 in* 30° *near side collision with HIII, Graz. From Törnvall et al. (2008a).*

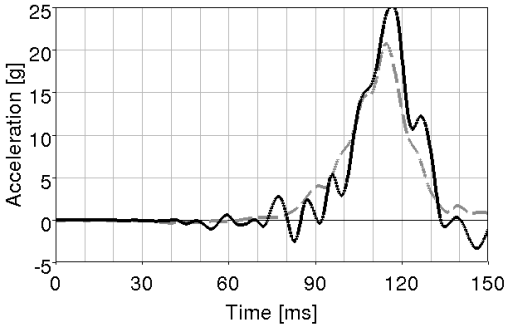


Figure C.0.16: *Y acceleration in T1 in* 30° *near side with HIII, Graz. From Törnvall et al. (2008a).*

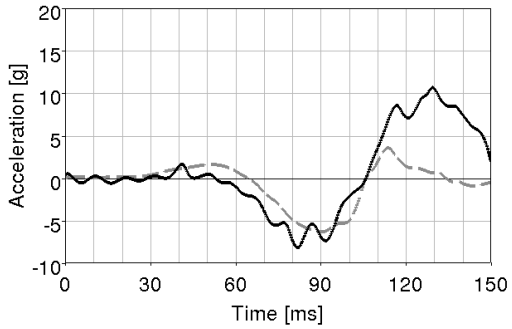


Figure C.0.17: *Z acceleration in T1 in* 30° *near side collision with HIII, Graz. From Törnvall et al. (2008a).*

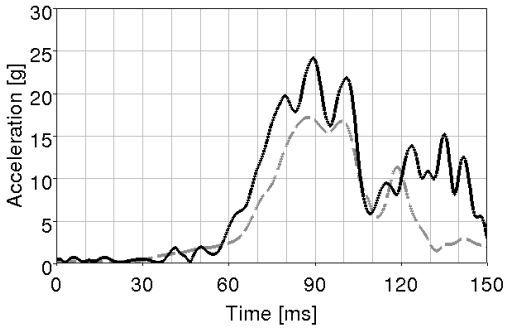


Figure C.0.18: *XZ acceleration in T1 in* 30° *near side collision with HIII, Graz. From Törnvall et al. (2008a).*

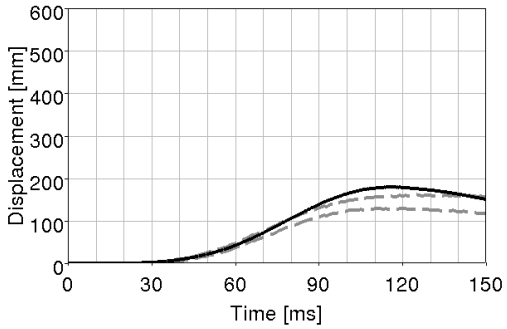


Figure C.0.19: *X displacement in the hip in 45° far side collision with HIII, Graz. From Törnvall et al. (2008a).*

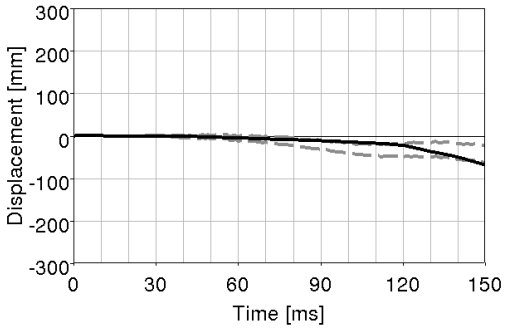


Figure C.0.20: *Y displacement in the hip in 45° far side collision with HIII, Graz. From Törnvall et al. (2008a).*

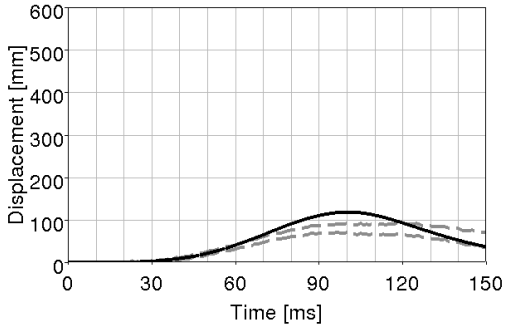


Figure C.0.21: *X displacement of the hip in 0° collision with HIII, Graz. From Törnvall et al. (2008a).*

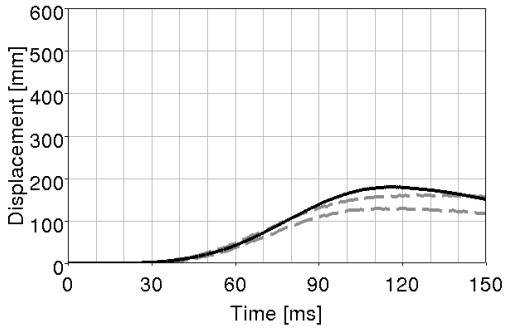


Figure C.0.22: *X displacement in the hip in 30° near side collision with HIII, Graz. From Törnvall et al. (2008a).*

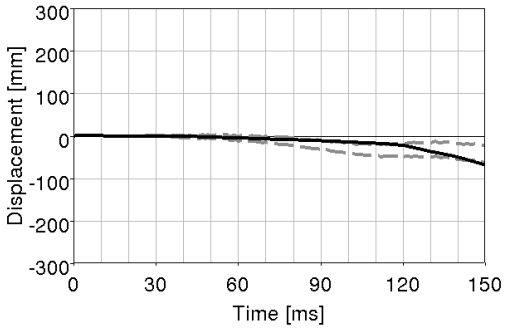


Figure C.0.23: *Y displacement in the hip in 30° near side collision with HIII, Graz. From Törnvall et al. (2008a).*

# D Simulation of the Heidelberg Sled with HIII

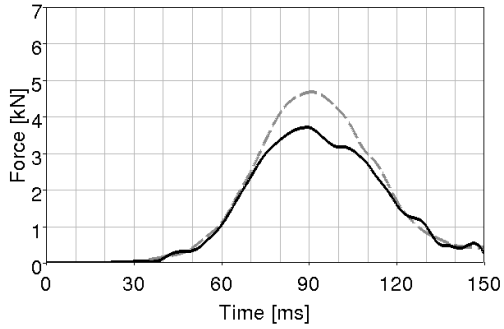


Figure D.0.1: *Shoulder belt force in 30° far side collision with HIII, Heidelberg. From* Unpublished material from the Heidelberg test *(2012).*

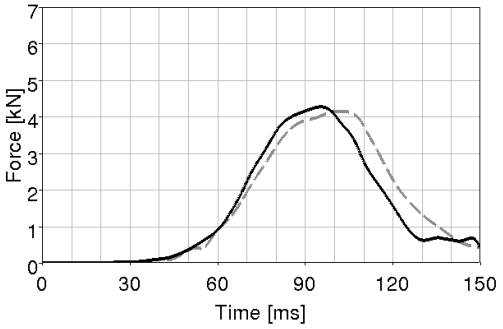


Figure D.0.2: *Lap belt force in 30° far side collision with HIII, Heidelberg. From* Unpublished material from the Heidelberg test *(2012).*

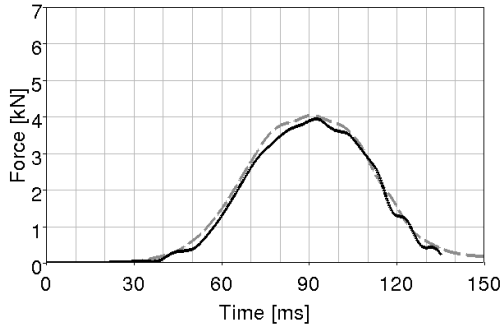


Figure D.0.3: *Shoulder belt force in 15° far side collision with HIII, Heidelberg. From* Unpublished material from the Heidelberg test *(2012).*

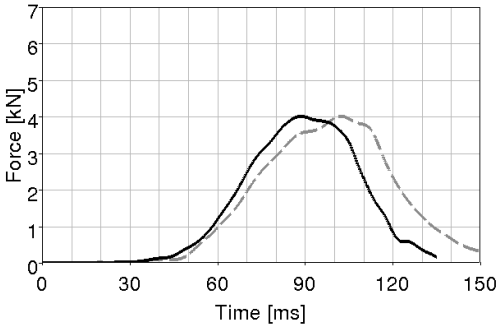


Figure D.0.4: *Lap belt force in 15° far side collision with HIII, Heidelberg. From* Unpublished material from the Heidelberg test *(2012).*

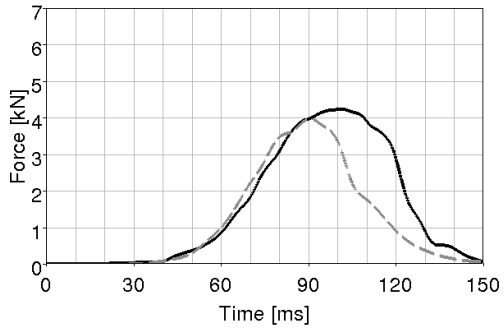


Figure D.0.5: *Shoulder belt force in 15° near side collision with HIII, Heidelberg. From* Unpublished material from the Heidelberg test *(2012).*

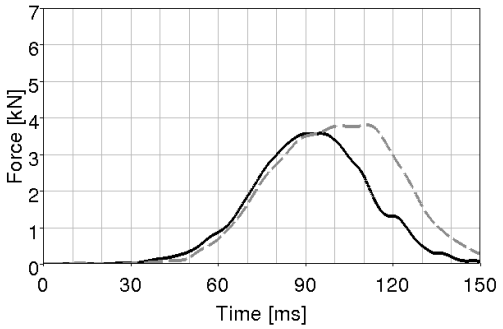


Figure D.0.6: *Lap belt force in 15° near side collision with HIII, Heidelberg. From* Unpublished material from the Heidelberg test *(2012).*

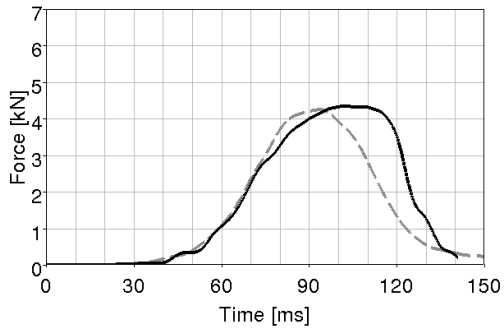


Figure D.0.7: *Shoulder belt force in 30° near side collision with HIII, Heidelberg. From* Unpublished material from the Heidelberg test *(2012).*

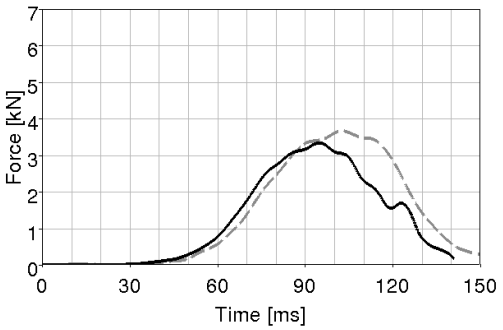


Figure D.0.8: *Lap belt force in 30° near side collision with HIII, Heidelberg. From* Unpublished material from the Heidelberg test *(2012).*

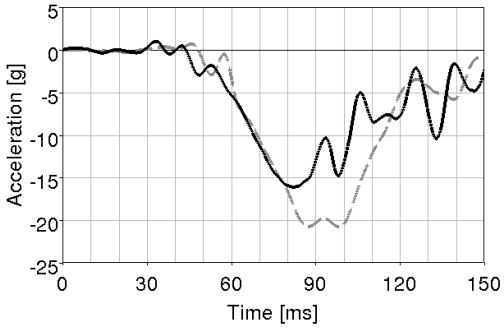


Figure D.0.9: *X acceleration of T1 in 30° far side collision with HIII, Heidelberg. From* Unpublished material from the Heidelberg test *(2012).*

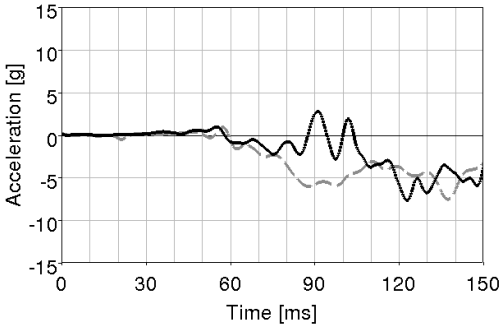


Figure D.0.10: *Y acceleration in T1 in 30° far side collision with HIII, Heidelberg. From* Unpublished material from the Heidelberg test *(2012).*

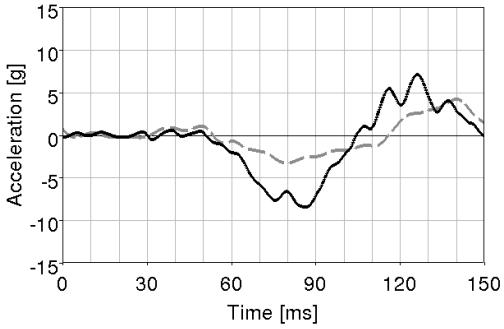


Figure D.0.11: *Z acceleration in T1 in 30° far side collision with HIII, Heidelberg. From* Unpublished material from the Heidelberg test *(2012).*

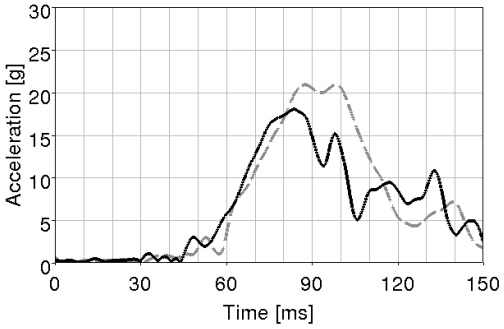


Figure D.0.12: *XZ acceleration in T1 30° far side collision with HIII, Heidelberg. From* Unpublished material from the Heidelberg test *(2012).*

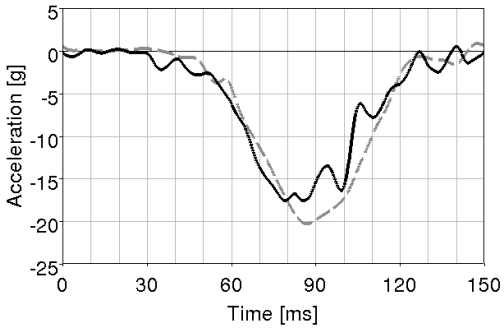


Figure D.0.13: *X acceleration of T6 in 30° far side collision with HIII, Heidelberg. From* Unpublished material from the Heidelberg test *(2012).*

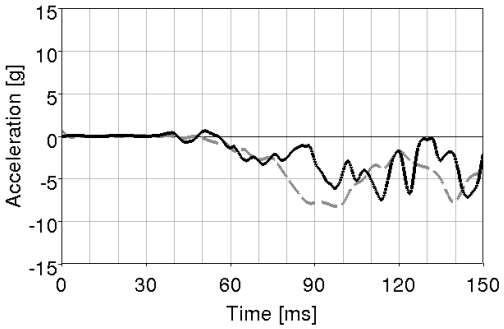


Figure D.0.14: *Y acceleration in T6 in 30° far side collision with HIII, Heidelberg. From* Unpublished material from the Heidelberg test *(2012).*

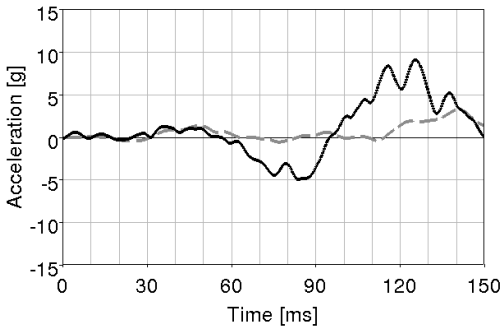


Figure D.0.15: *Z acceleration in T6 in 30° far side collision with HIII, Heidelberg. From* Unpublished material from the Heidelberg test *(2012).*

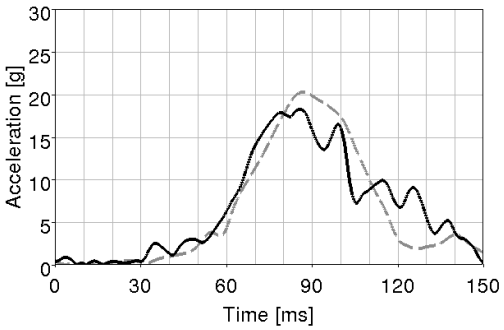


Figure D.0.16: *XZ acceleration in T6 in 30° far side collision with HIII, Heidelberg. From* Unpublished material from the Heidelberg test *(2012).*

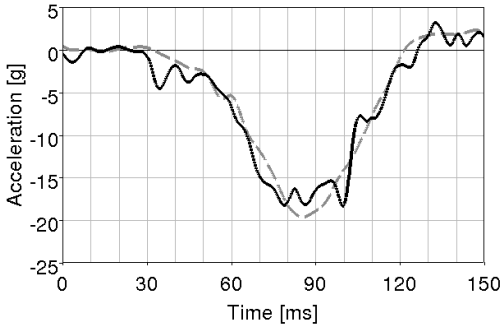


Figure D.0.17: *X acceleration of T12 in 30° far side collision with HIII, Heidelberg. From* Unpublished material from the Heidelberg test *(2012).*

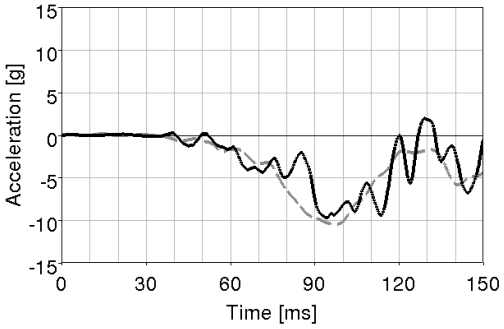


Figure D.0.18: *Y acceleration in T12 in 30° far side collision with HIII, Heidelberg. From* Unpublished material from the Heidelberg test *(2012).*

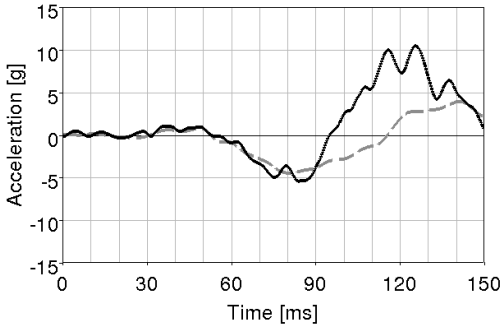


Figure D.0.19: *Z acceleration in T12 in 30° far side collision with HIII, Heidelberg. From* Unpublished material from the Heidelberg test *(2012).*

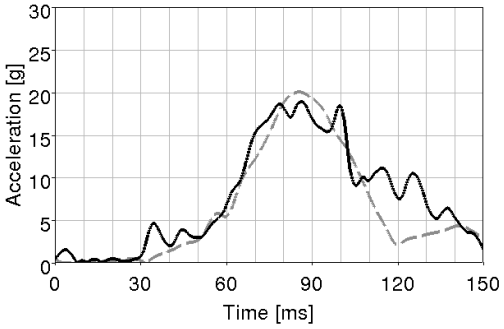


Figure D.0.20: *XZ acceleration in T12 in 30° far side collision with HIII, Heidelberg. From* Unpublished material from the Heidelberg test *(2012).*

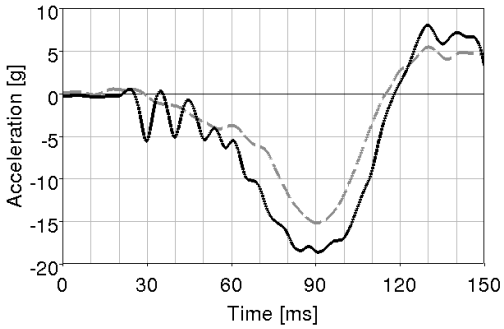


Figure D.0.21: *X acceleration of pelvis in 30° far side collision with HIII, Heidelberg. From* Unpublished material from the Heidelberg test *(2012).*

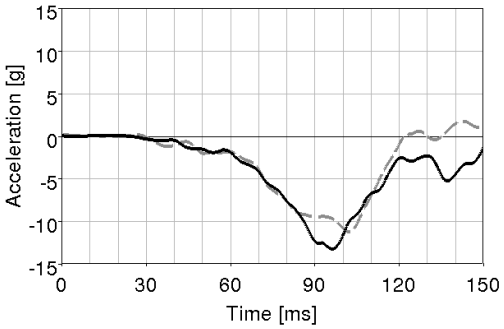


Figure D.0.22: *Y acceleration in pelvis in 30° far side collision with HIII, Heidelberg. From* Unpublished material from the Heidelberg test *(2012).*

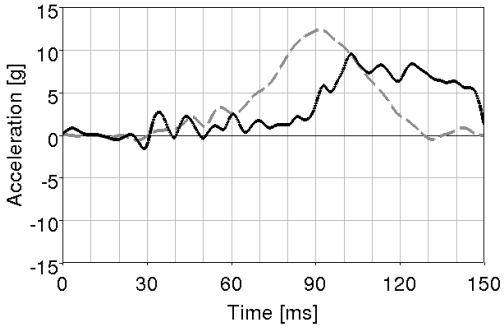


Figure D.0.23: *Z acceleration in pelvis in 30° far side collision with HIII, Heidelberg. From* Unpublished material from the Heidelberg test *(2012).*

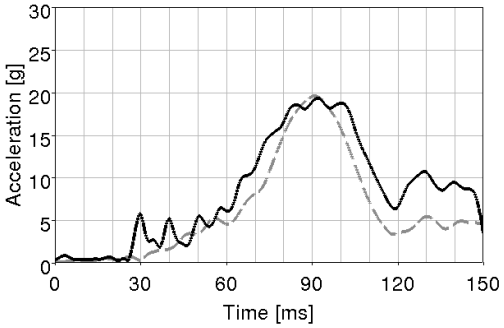


Figure D.0.24: *XZ acceleration in pelvis in 30° far side collision with HIII, Heidelberg. From* Unpublished material from the Heidelberg test *(2012).*

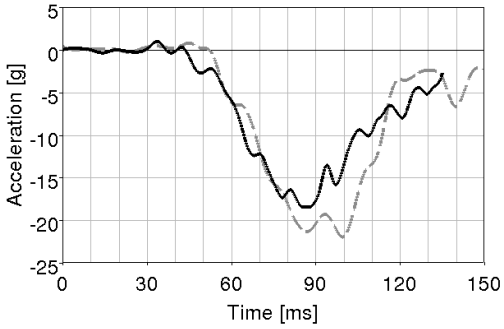


Figure D.0.25: *X acceleration of T1 in 15° far side collision with HIII, Heidelberg. From* Unpublished material from the Heidelberg test *(2012).*

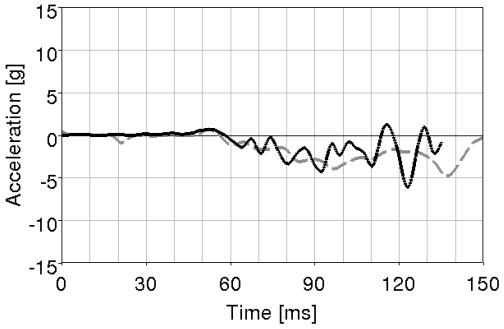


Figure D.0.26: *Y acceleration in T1 in 15° far side collision with HIII, Heidelberg. From* Unpublished material from the Heidelberg test *(2012).*

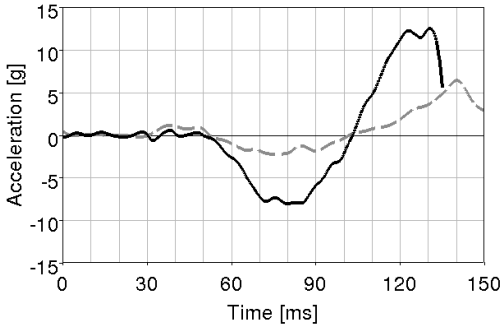


Figure D.0.27: *Z acceleration in T1 in 15° far side collision with HIII, Heidelberg. From* Unpublished material from the Heidelberg test *(2012).*

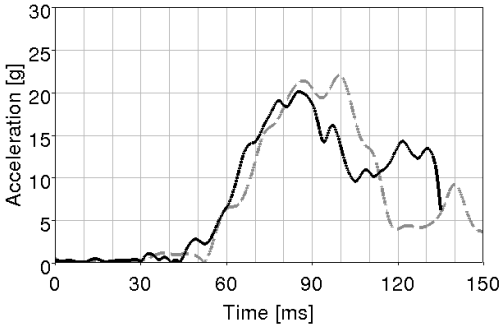


Figure D.0.28: *XZ acceleration in T1 15° far side collision with HIII, Heidelberg. From* Unpublished material from the Heidelberg test *(2012).*

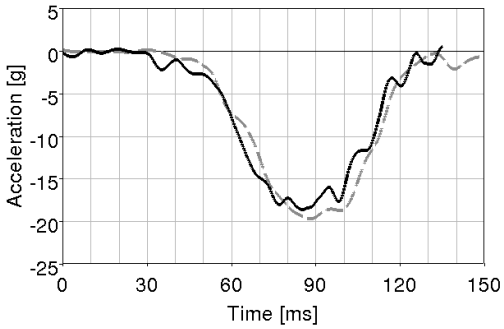


Figure D.0.29: *X acceleration of T6 in 15° far side collision with HIII, Heidelberg. From* Unpublished material from the Heidelberg test *(2012).*

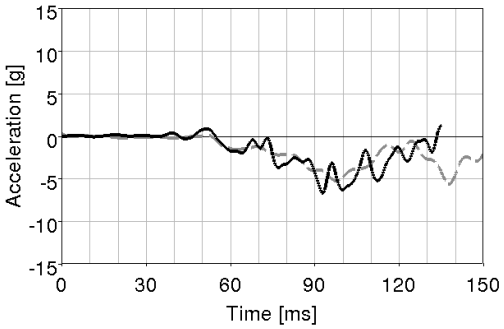


Figure D.0.30: *Y acceleration in T6 in 15° far side collision with HIII, Heidelberg. From* Unpublished material from the Heidelberg test *(2012).*

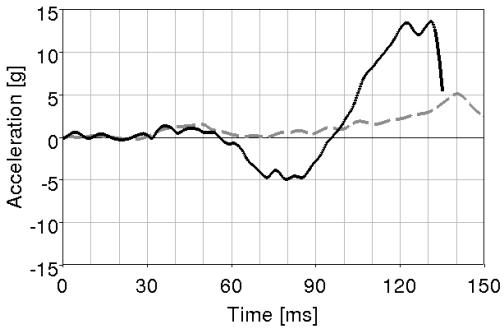


Figure D.0.31: *Z acceleration in T6 in 15° far side collision with HIII, Heidelberg. From* Unpublished material from the Heidelberg test *(2012).*

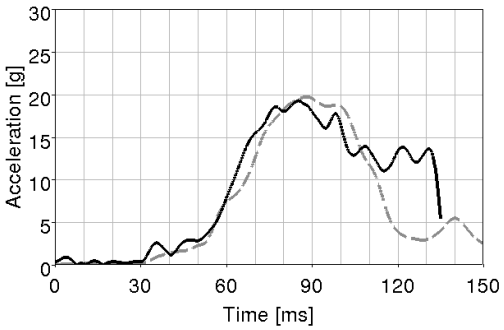


Figure D.0.32: *XZ acceleration in T6 in 15° far side collision with HIII, Heidelberg. From* Unpublished material from the Heidelberg test *(2012).*

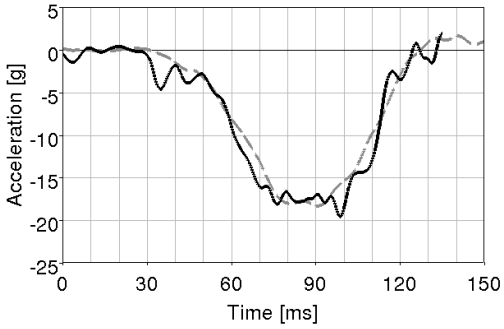


Figure D.0.33: *X acceleration of T12 in 15° far side collision with HIII, Heidelberg. From* Unpublished material from the Heidelberg test *(2012).*

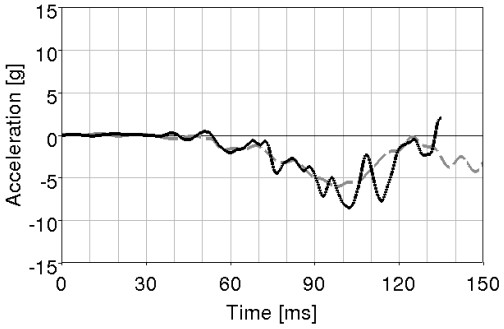


Figure D.0.34: *Y acceleration in T12 in 15° far side collision with HIII, Heidelberg. From* Unpublished material from the Heidelberg test *(2012).*

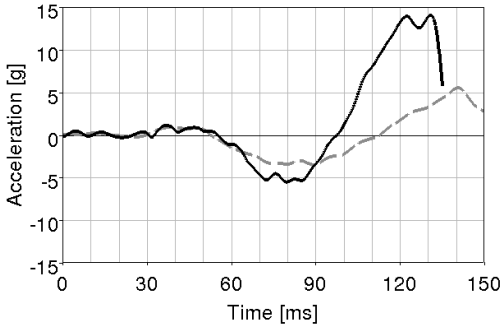


Figure D.0.35: *Z acceleration in T12 in 15° far side collision with HIII, Heidelberg. From* Unpublished material from the Heidelberg test *(2012).*

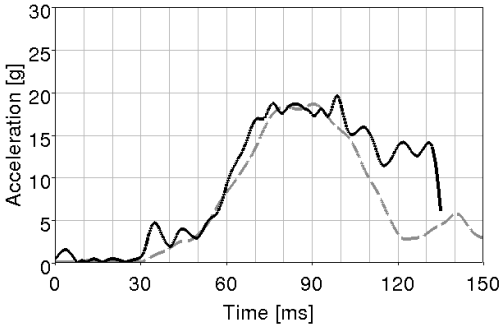


Figure D.0.36: *XZ acceleration in T12 in 15° far side collision with HIII, Heidelberg. From* Unpublished material from the Heidelberg test *(2012).*

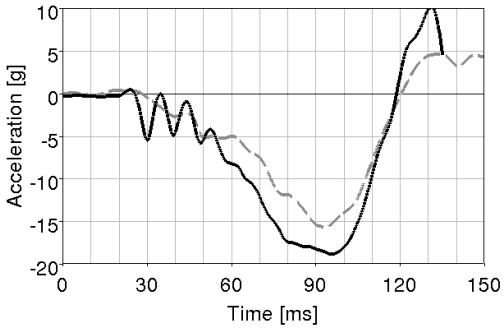


Figure D.0.37: *X acceleration of pelvis in 15° far side collision with HIII, Heidelberg. From* Unpublished material from the Heidelberg test *(2012).*

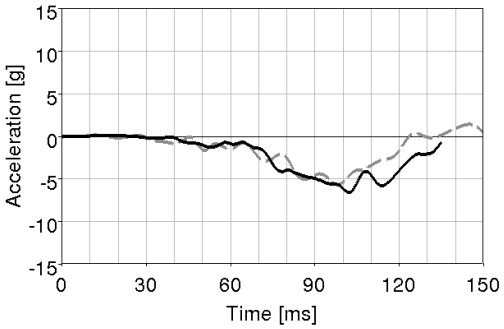


Figure D.0.38: *Y acceleration in pelvis in 15° far side collision with HIII, Heidelberg. From* Unpublished material from the Heidelberg test *(2012).*

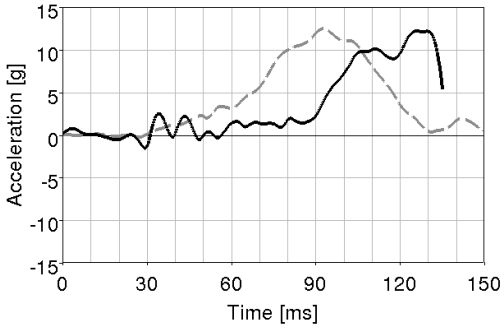


Figure D.0.39: *Z acceleration in pelvis in 15° far side collision with HIII, Heidelberg. From* Unpublished material from the Heidelberg test *(2012).*

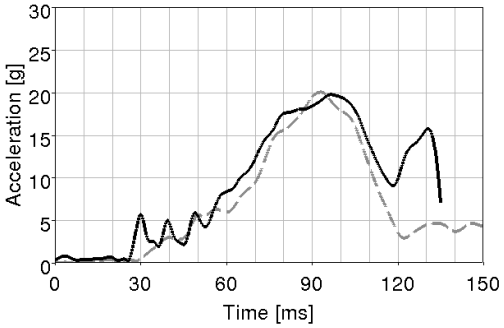


Figure D.0.40: *XZ acceleration in pelvis in 15° far side collision with HIII, Heidelberg. From* Unpublished material from the Heidelberg test *(2012).*

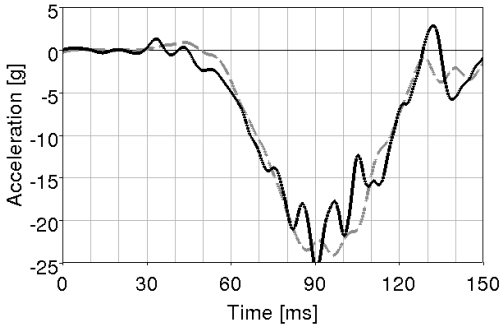


Figure D.0.41: *X acceleration of T1 in 15° near side collision with HIII, Heidelberg. From* Unpublished material from the Heidelberg test *(2012).*

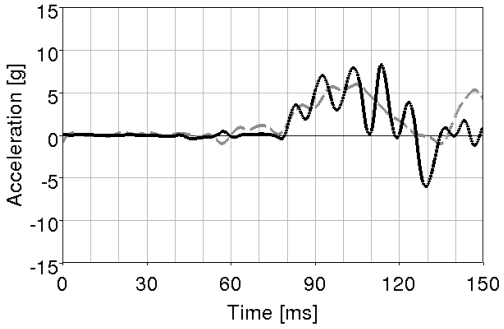


Figure D.0.42: *Y acceleration in T1 in 15° near side collision with HIII, Heidelberg. From* Unpublished material from the Heidelberg test *(2012).*

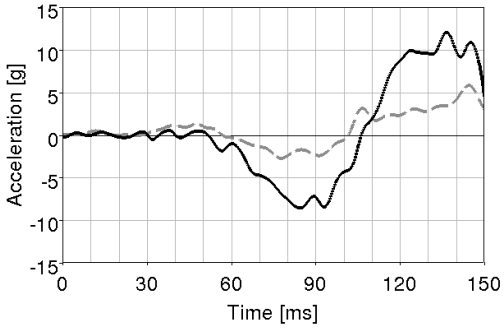


Figure D.0.43: *Z acceleration in T1 in 15° near side collision with HIII, Heidelberg. From* Unpublished material from the Heidelberg test *(2012).*

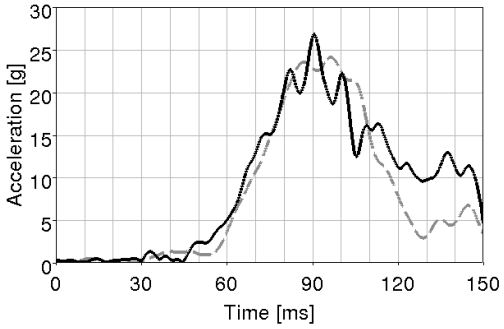


Figure D.0.44: *XZ acceleration in T1 15° near side collision with HIII, Heidelberg. From* Unpublished material from the Heidelberg test *(2012).*

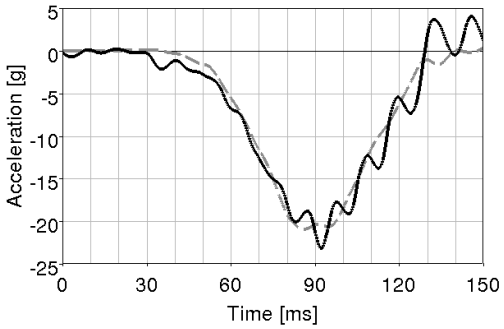


Figure D.0.45: *X acceleration of T6 in 15° near side collision with HIII, Heidelberg. From* Unpublished material from the Heidelberg test *(2012).*

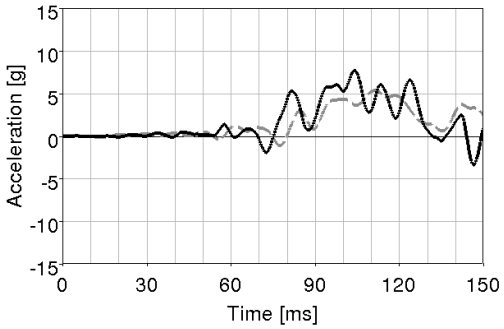


Figure D.0.46: *Y acceleration in T6 in 15° near side collision with HIII, Heidelberg. From* Unpublished material from the Heidelberg test *(2012).*

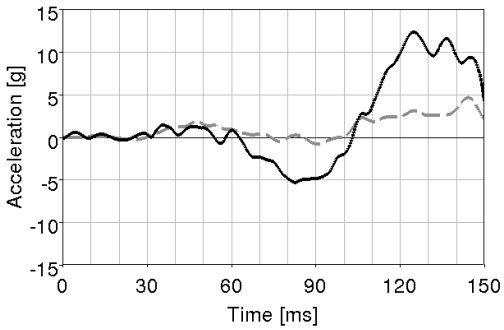


Figure D.0.47: *Z acceleration in T6 in 15° near side collision with HIII, Heidelberg. From* Unpublished material from the Heidelberg test *(2012).*

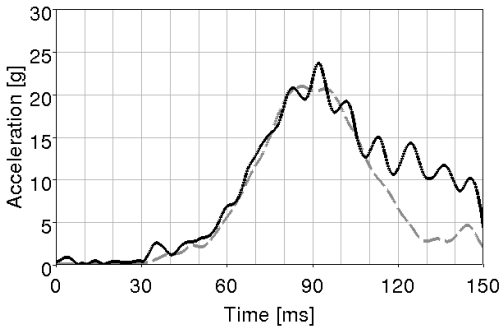


Figure D.0.48: *XZ acceleration in T6 in 15° near side collision with HIII, Heidelberg. From* Unpublished material from the Heidelberg test *(2012).*

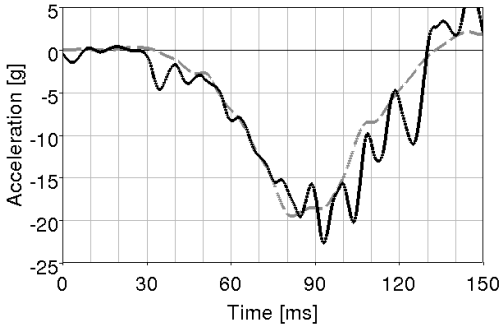


Figure D.0.49: *X acceleration of T12 in 15° near side collision with HIII, Heidelberg. From* Unpublished material from the Heidelberg test *(2012).*

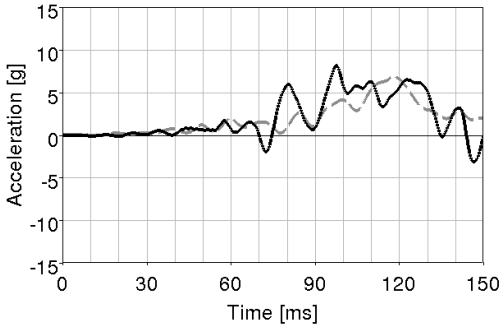


Figure D.0.50: *Y acceleration in T12 in 15° near side collision with HIII, Heidelberg. From* Unpublished material from the Heidelberg test *(2012).*

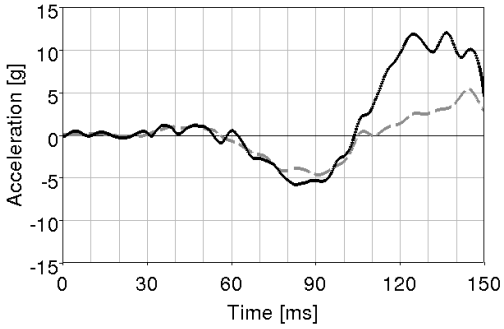


Figure D.0.51: *Z acceleration in T12 in 15° near side collision with HIII, Heidelberg. From* Unpublished material from the Heidelberg test *(2012).*

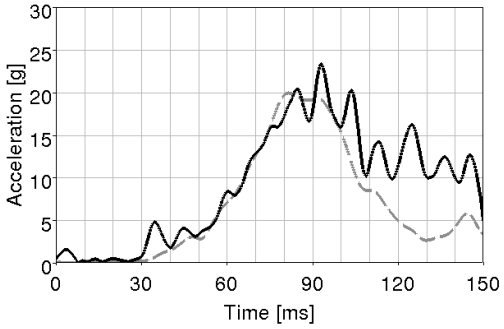


Figure D.0.52: *XZ acceleration in T12 in 15° near side collision with HIII, Heidelberg. From* Unpublished material from the Heidelberg test *(2012).*

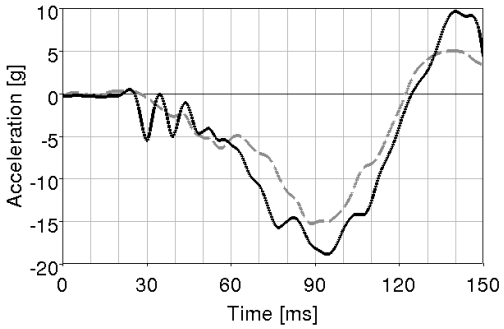


Figure D.0.53: *X acceleration of pelvis in 15° near side collision with HIII, Heidelberg. From* Unpublished material from the Heidelberg test *(2012).*

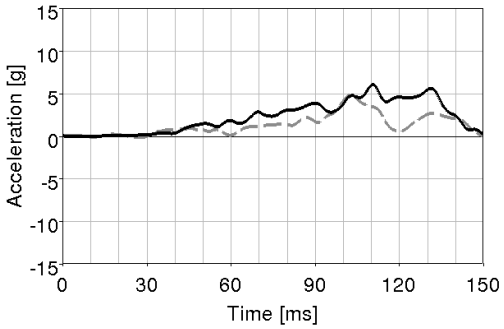


Figure D.0.54: *Y acceleration in pelvis in 15° near side collision with HIII, Heidelberg. From* Unpublished material from the Heidelberg test *(2012).*

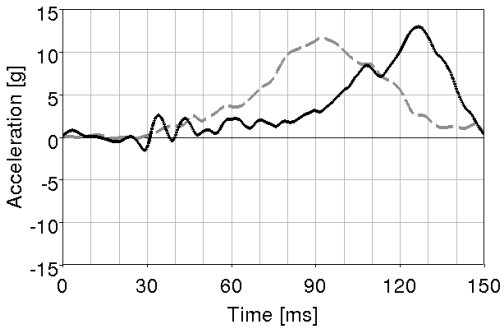


Figure D.0.55: *Z acceleration in pelvis in 15° near side collision with HIII, Heidelberg. From* Unpublished material from the Heidelberg test *(2012).*

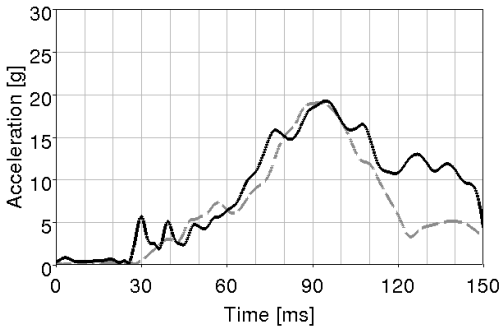


Figure D.0.56: *XZ acceleration in pelvis in 15° near side collision with HIII, Heidelberg. From* Unpublished material from the Heidelberg test *(2012).*

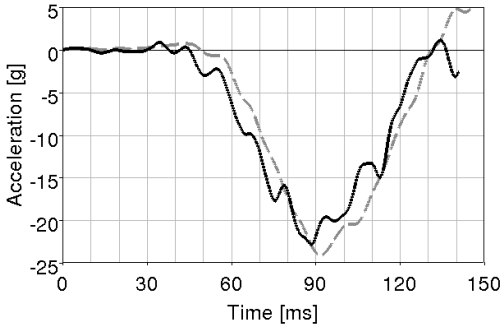


Figure D.0.57: *X acceleration of T1 in 30° near side collision with HIII, Heidelberg. From* Unpublished material from the Heidelberg test *(2012).*

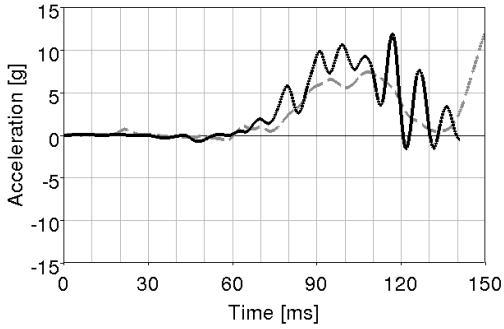


Figure D.0.58: *Y acceleration in T1 in 30° near side collision with HIII, Heidelberg. From* Unpublished material from the Heidelberg test *(2012).*

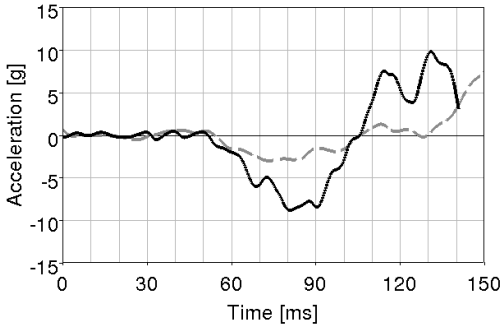


Figure D.0.59: *Z acceleration in T1 in 30° near side collision with HIII, Heidelberg. From* Unpublished material from the Heidelberg test *(2012).*

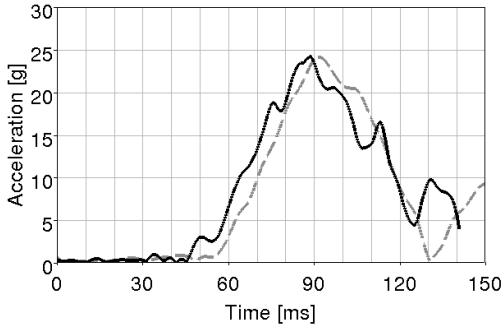


Figure D.0.60: *XZ acceleration in T1 30° near side collision with HIII, Heidelberg. From* Unpublished material from the Heidelberg test *(2012).*

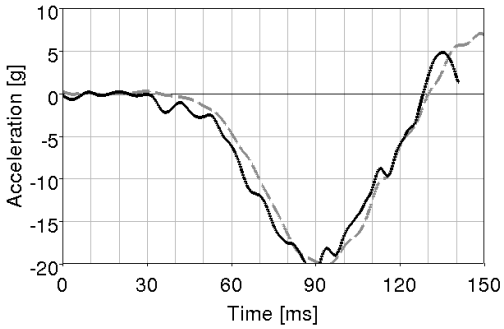


Figure D.0.61: *X acceleration of T6 in 30° near side collision with HIII, Heidelberg. From* Unpublished material from the Heidelberg test *(2012).*

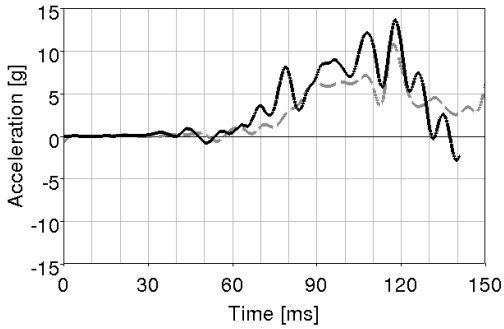


Figure D.0.62: *Y acceleration in T6 in 30° near side collision with HIII, Heidelberg. From* Unpublished material from the Heidelberg test *(2012).*

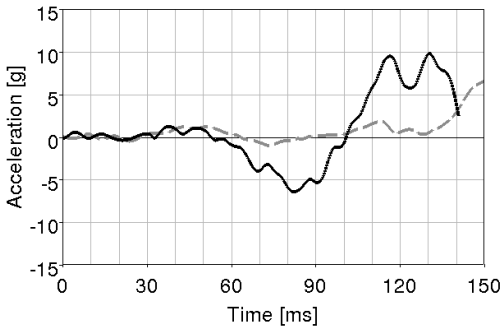


Figure D.0.63: *Z acceleration in T6 in 30° near side collision with HIII, Heidelberg. From* Unpublished material from the Heidelberg test *(2012).*

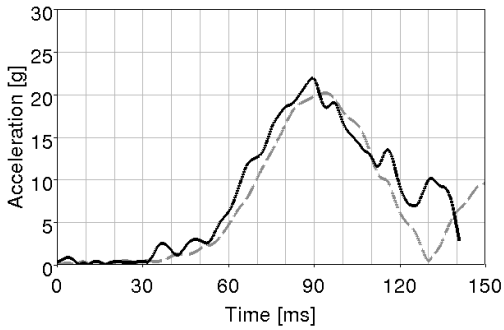


Figure D.0.64: *XZ acceleration in T6 in 30° near side collision with HIII, Heidelberg. From* Unpublished material from the Heidelberg test *(2012).*

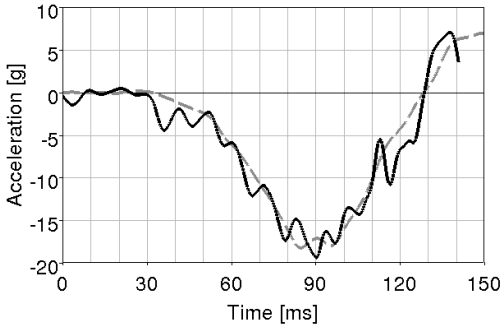


Figure D.0.65: *X acceleration of T12 in 30° near side collision with HIII, Heidelberg. From* Unpublished material from the Heidelberg test *(2012).*

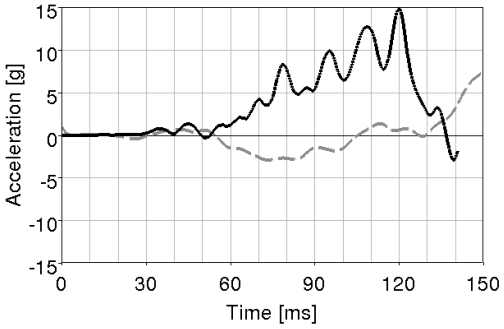


Figure D.0.66: *Y acceleration in T12 in 30° near side collision with HIII, Heidelberg. From* Unpublished material from the Heidelberg test *(2012).*

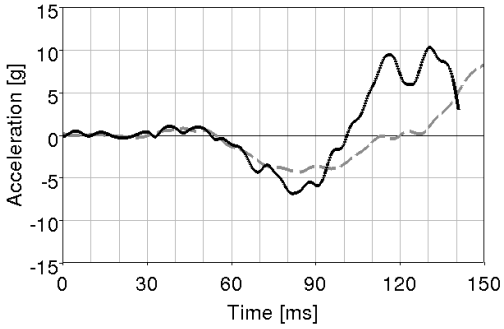


Figure D.0.67: *Z acceleration in T12 in 30° near side collision with HIII, Heidelberg. From* Unpublished material from the Heidelberg test *(2012).*

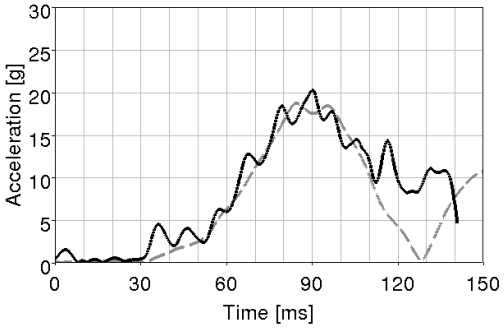


Figure D.0.68: *XZ acceleration in T12 in 30° near side collision with HIII, Heidelberg. From* Unpublished material from the Heidelberg test *(2012).*

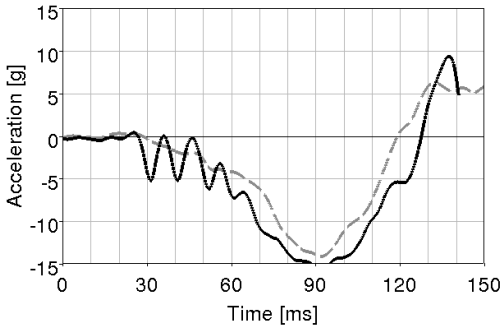


Figure D.0.69: *X acceleration of pelvis in 30° near side collision with HIII, Heidelberg. From* Unpublished material from the Heidelberg test *(2012).*

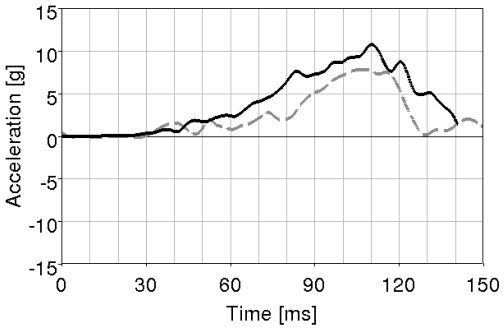


Figure D.0.70: *Y acceleration in pelvis in 30° near side collision with HIII, Heidelberg. From* Unpublished material from the Heidelberg test *(2012).*

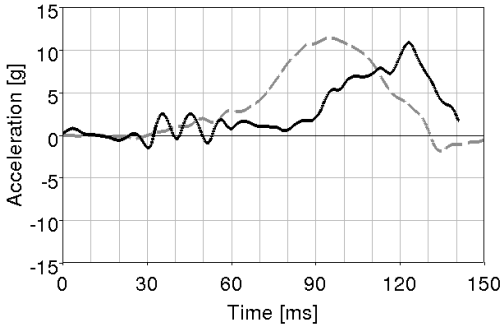


Figure D.0.71: *Z acceleration in pelvis in 30° near side collision with HIII, Heidelberg. From* Unpublished material from the Heidelberg test *(2012).*

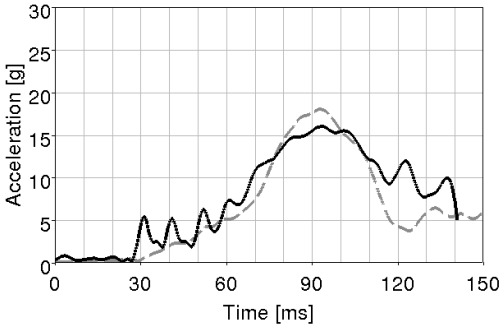


Figure D.0.72: *XZ acceleration in pelvis in 30° near side collision with HIII, Heidelberg. From* Unpublished material from the Heidelberg test *(2012).*

# E Simulation of the Graz sled with THUMS

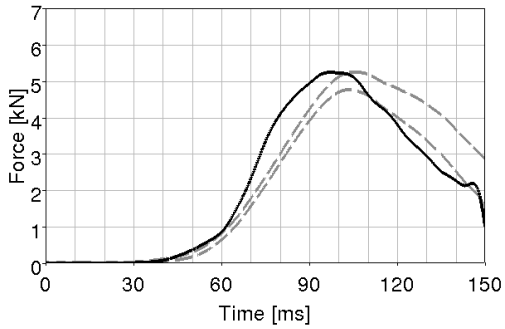


Figure E.0.1: *Shoulder belt force in* 45° *far side collision with THUMS, Graz. From Törnvall et al. (2008b).*

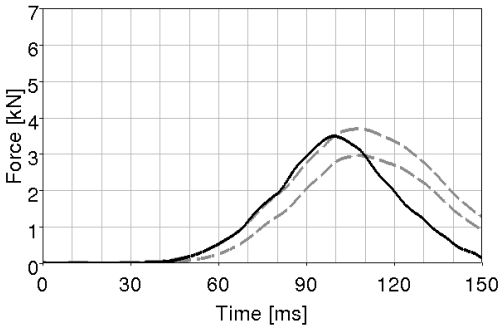


Figure E.0.2: *Lap belt force in* 45° *far side collision with THUMS, Graz. From Törnvall et al. (2008b).*

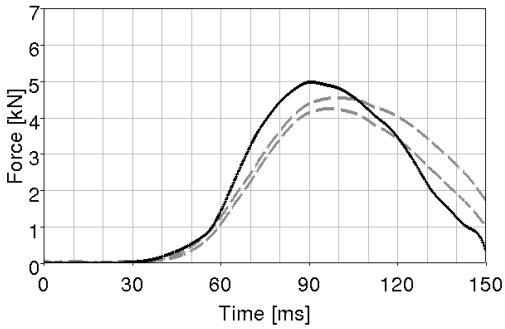


Figure E.0.3: *Shoulder belt force in* 0° *collision with THUMS, Graz. From Törnvall et al. (2008b).*

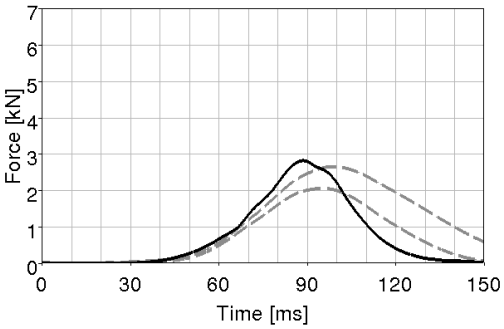


Figure E.0.4: *Lap belt force in* 0° *collision with THUMS, Graz. From Törnvall et al. (2008b).*

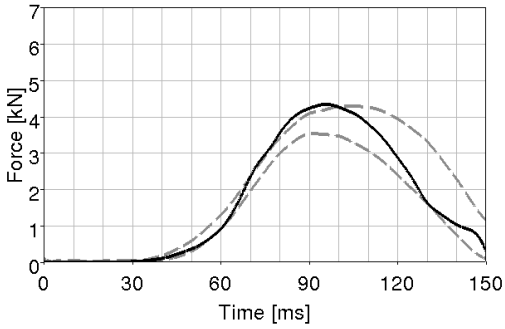


Figure E.0.5: *Shoulder belt force in* 30° *near side collision with THUMS, Graz. From Törnvall et al. (2008b).*

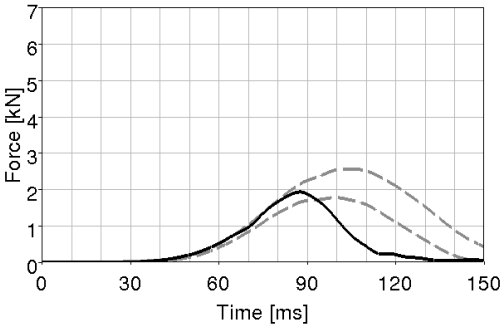


Figure E.0.6: *Lap belt force in* 30° *near side collision with THUMS, Graz. From Törnvall et al. (2008b).*

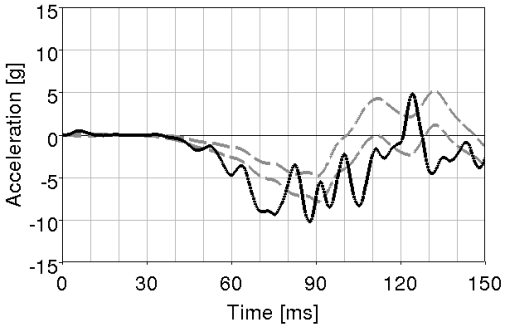


Figure E.0.7: *X acceleration in T1 in* 45° *far side collision with THUMS, Graz. From Törnvall et al. (2008b).*

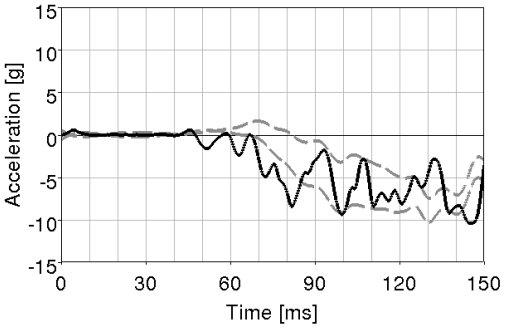


Figure E.0.8: *Y acceleration in T1 in* 45° *far side collision with THUMS, Graz. From Törnvall et al. (2008b).*

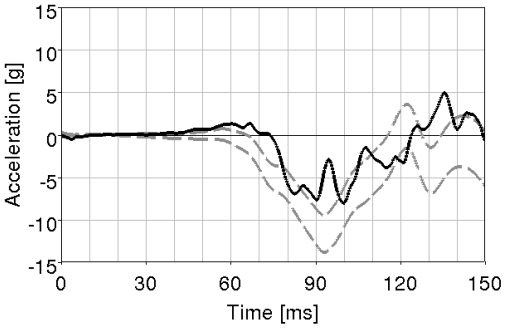


Figure E.0.9: *Z acceleration in T1 in* 45° *far side collision with THUMS, Graz. From Törnvall et al. (2008b).*

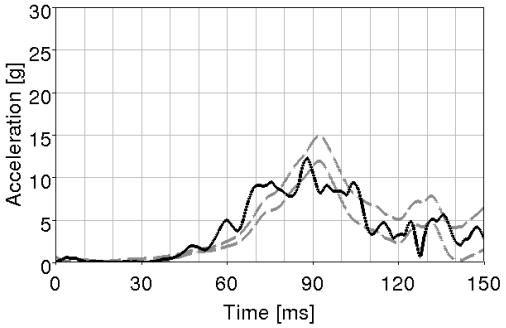


Figure E.0.10: *XZ acceleration in T1 in* 45° *far side collision with THUMS, Graz. From Törnvall et al. (2008b).*

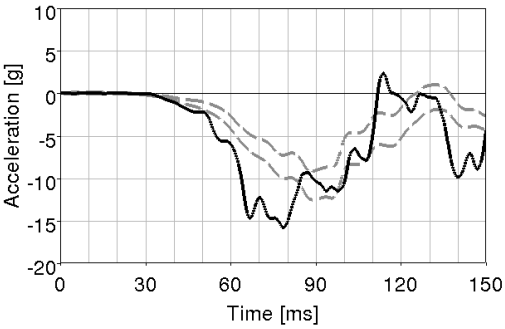


Figure E.0.11: *X acceleration in T1 in* 0° *collision with THUMS, Graz. From Törnvall et al. (2008b).*

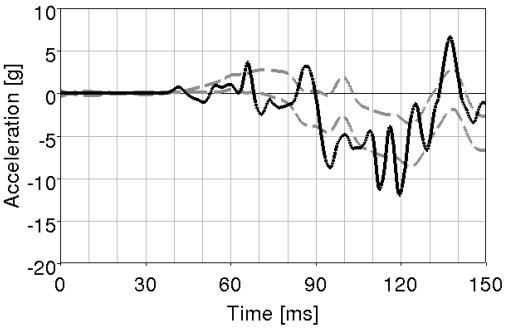


Figure E.0.12: *Y acceleration in T1 in* 0° *collision with THUMS, Graz. From Törnvall et al. (2008b).*

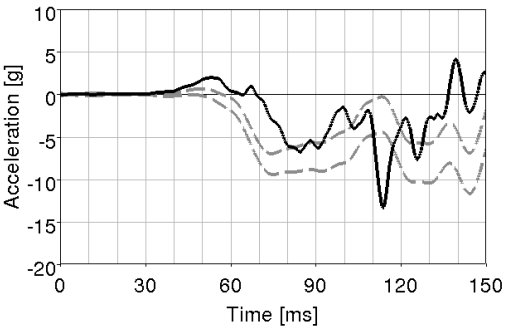


Figure E.0.13: *Z acceleration in T1 in* 0° *collision with THUMS, Graz. From Törnvall et al. (2008b).*

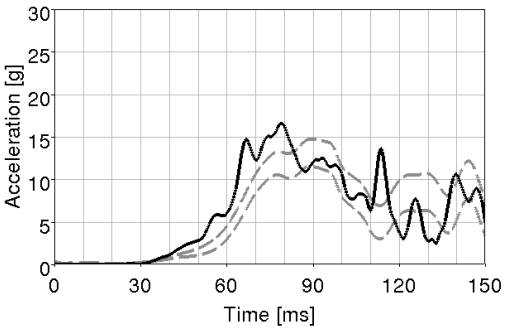


Figure E.0.14: *XZ acceleration in T1 in* 0° *collision with THUMS, Graz. From Törnvall et al. (2008b).*

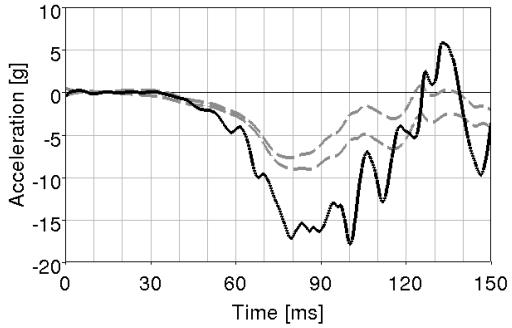


Figure E.0.15: *X acceleration in T1 in* 30° *near side collision with THUMS, Graz. From Törnvall et al. (2008b).*

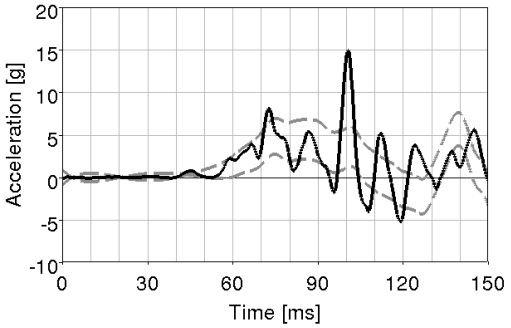


Figure E.0.16: *Y acceleration in T1 in* 30° *near side collision with THUMS, Graz. From Törnvall et al. (2008b).*

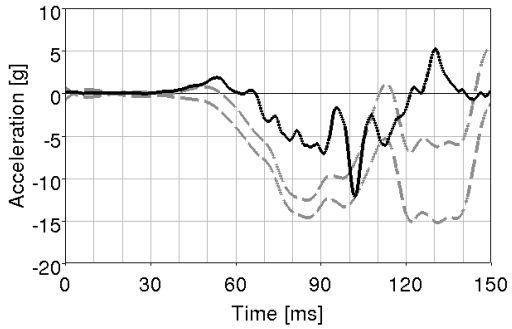


Figure E.0.17: *Z acceleration in T1 in* 30° *near side collision with THUMS, Graz. From Törnvall et al. (2008b).*

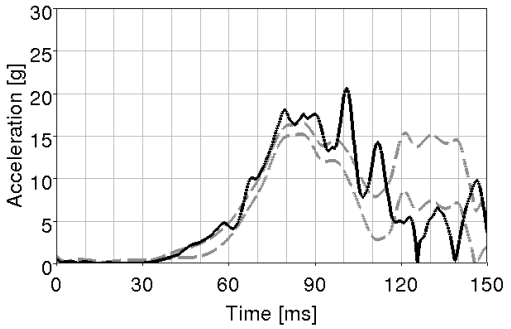


Figure E.0.18: *XZ acceleration in T1 in* 30° *near side collision with THUMS, Graz. From Törnvall et al. (2008b).*

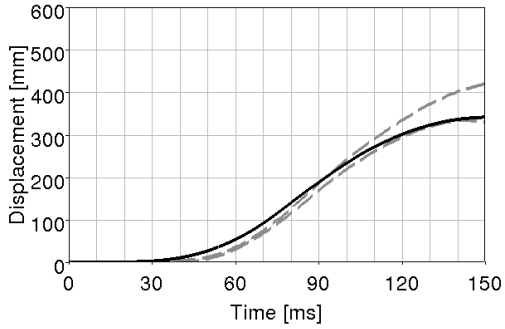


Figure E.0.19: *X displacement in the unloaded shoulder in* 45° *far side collision with THUMS, Graz. From Törnvall et al. (2008b).*

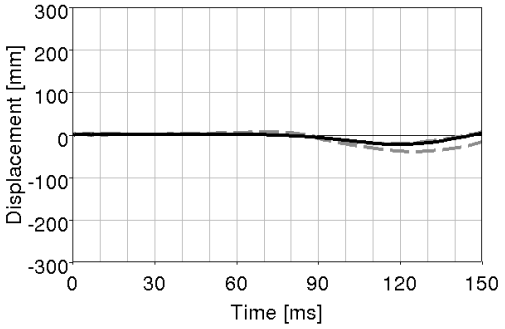


Figure E.0.20: *Y displacement in the unloaded shoulder in* 45° *far side collision with THUMS, Graz. From Törnvall et al. (2008b).*

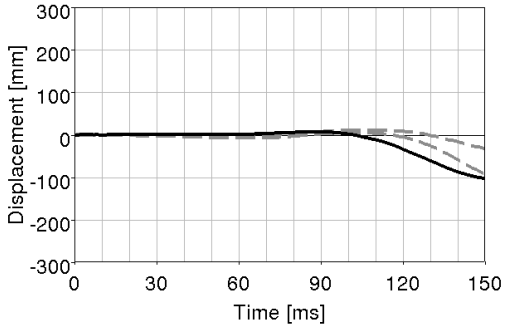


Figure E.0.21: *Z displacement in the unloaded shoulder in* 45° *far side collision with THUMS, Graz. From Törnvall et al. (2008b).*

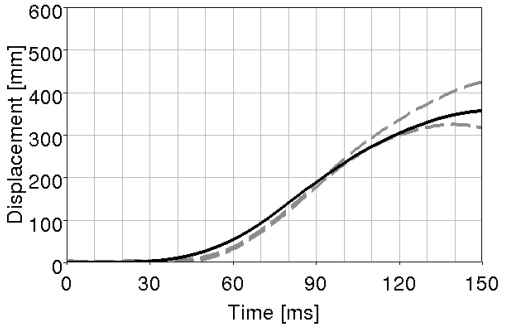


Figure E.0.22: *XZ displacement in the unloaded shoulder in* 45° *far side collision with THUMS, Graz. From Törnvall et al. (2008b).*

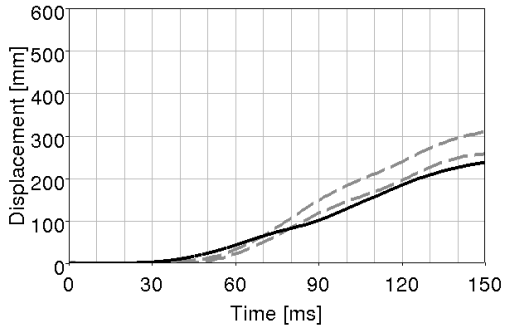


Figure E.0.23: *X displacement in the loaded shoulder in* 45° *far side collision with THUMS, Graz. From Törnvall et al. (2008b).*

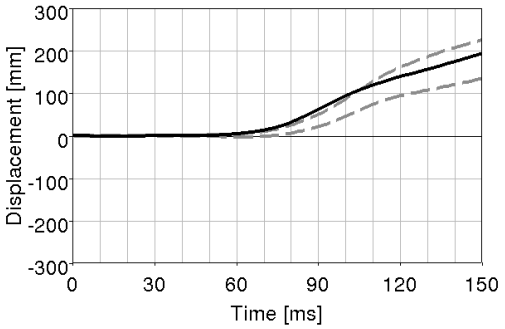


Figure E.0.24: *Y displacement in the loaded shoulder in* 45° *far side collision with THUMS, Graz. From Törnvall et al. (2008b).*

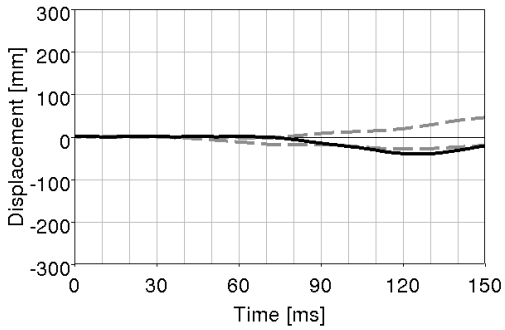


Figure E.0.25: *Z displacement in the loaded shoulder in* 45° *far side collision with THUMS, Graz. From Törnvall et al. (2008b).*

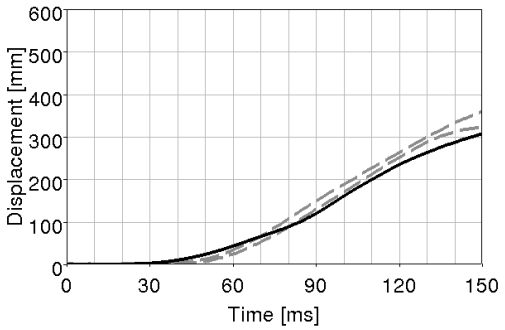


Figure E.0.26: *XZ displacement in the loaded shoulder in* 45° *far side collision with THUMS, Graz. From Törnvall et al. (2008b).*

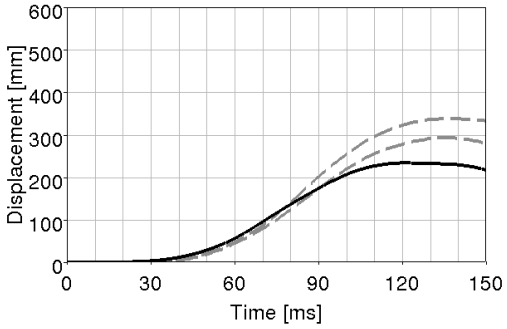


Figure E.0.27: *X displacement in the unloaded shoulder in* 0° *collision with THUMS, Graz. From Törnvall et al. (2008b).*

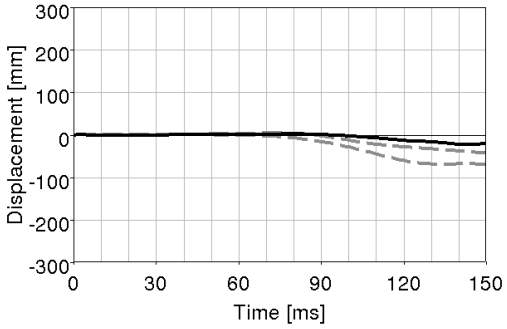


Figure E.0.28: *Y displacement in the unloaded shoulder in* 0° *collision with THUMS, Graz. From Törnvall et al. (2008b).*

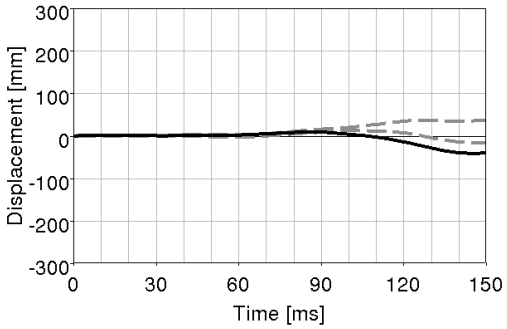


Figure E.0.29: *Z displacement in the unloaded shoulder in* 0° *collision with THUMS, Graz. From Törnvall et al. (2008b).*

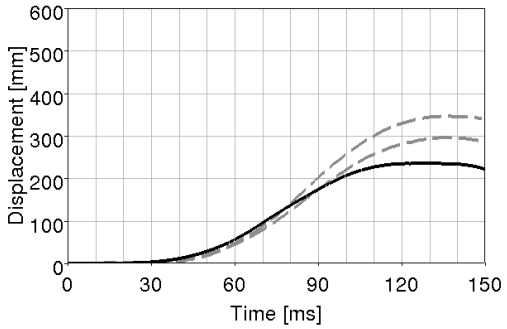


Figure E.0.30: *XZ displacement in the unloaded shoulder in* 0° *collision with THUMS, Graz. From Törnvall et al. (2008b).*

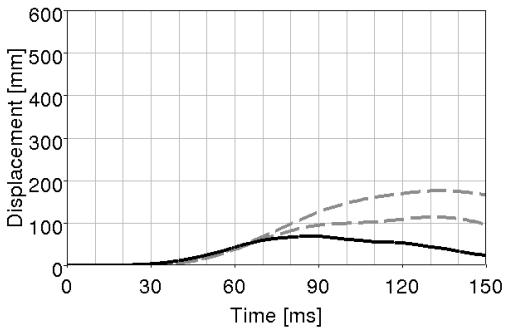


Figure E.0.31: *X displacement in the loaded shoulder in* 0° *collision with THUMS, Graz. From Törnvall et al. (2008b).*

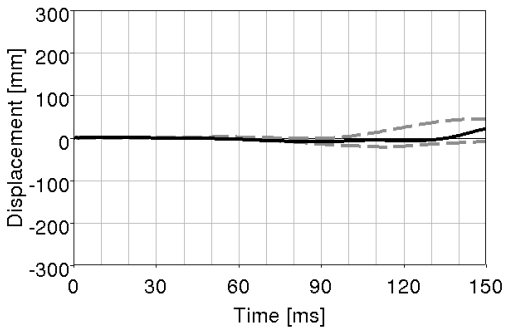


Figure E.0.32: *Y displacement in the loaded shoulder in* 0° *collision with THUMS, Graz. From Törnvall et al. (2008b).*

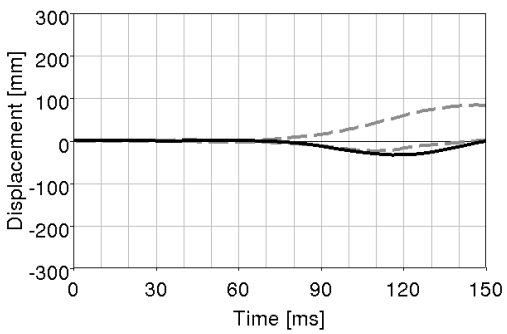


Figure E.0.33: *Z displacement in the loaded shoulder in* 0° *collision with THUMS, Graz. From Törnvall et al. (2008b).*

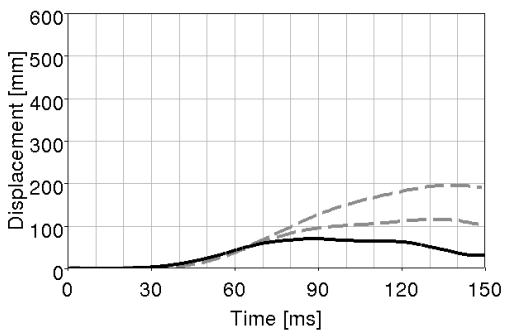


Figure E.0.34: *XZ displacement in the loaded shoulder in* 0° *collision with THUMS, Graz. From Törnvall et al. (2008b).*

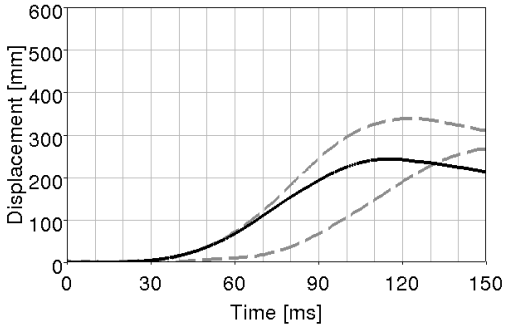


Figure E.0.35: *X displacement in the unloaded shoulder in* 30° *near side collision with THUMS, Graz. From Törnvall et al. (2008b).*

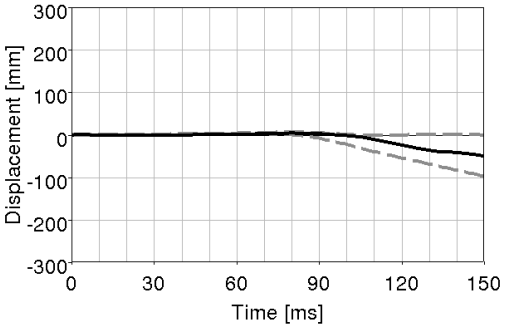


Figure E.0.36: *Y displacement in the unloaded shoulder in* 30° *near side collision with THUMS, Graz. From Törnvall et al. (2008b).*

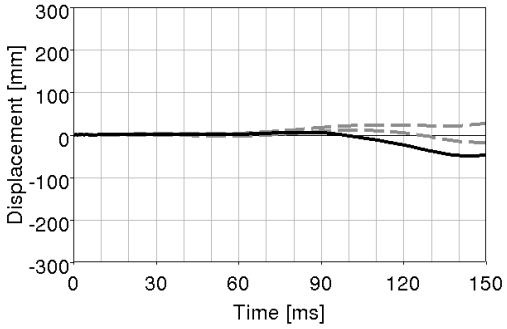


Figure E.0.37: *Z displacement in the unloaded shoulder in* 30° *near side collision with THUMS, Graz. From Törnvall et al. (2008b).*

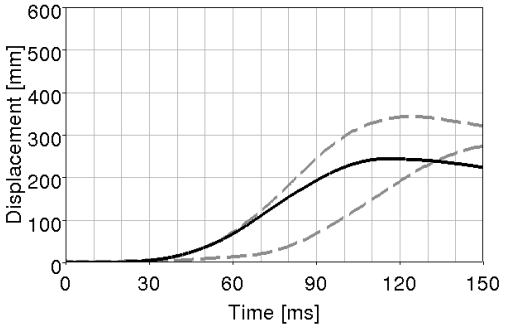


Figure E.0.38: *XZ displacement in the unloaded shoulder in* 30° *near side collision with THUMS, Graz. From Törnvall et al. (2008b).*

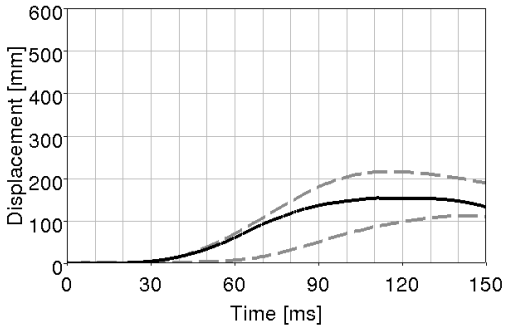


Figure E.0.39: *X displacement in the loaded shoulder in* 30° *near side collision with THUMS, Graz. From Törnvall et al. (2008b).*

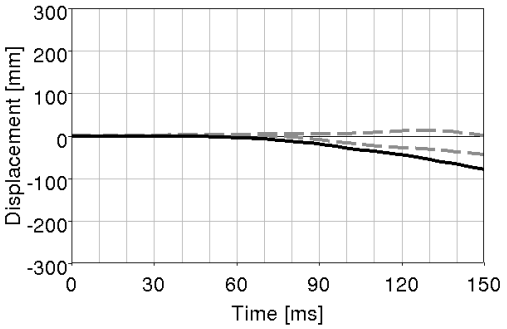


Figure E.0.40: *Y displacement in the loaded shoulder in* 30° *near side collision with THUMS, Graz. From Törnvall et al. (2008b).*

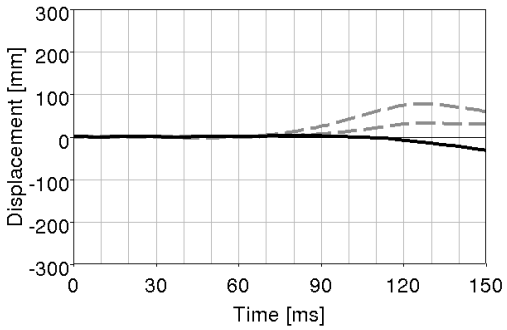


Figure E.0.41: *Z displacement in the loaded shoulder in* 30° *near side collision with THUMS, Graz. From Törnvall et al. (2008b).*

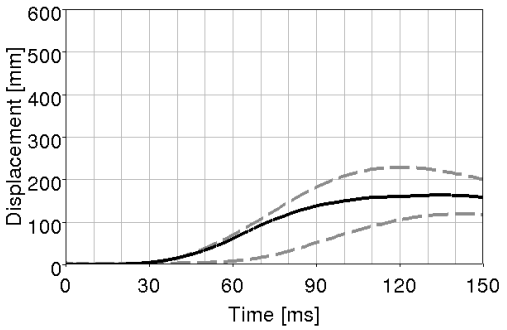


Figure E.0.42: *XZ displacement in the loaded shoulder in* 30° *near side collision with THUMS, Graz. From Törnvall et al. (2008b).*

# F Simulations of the Heidelberg Sled with THUMS

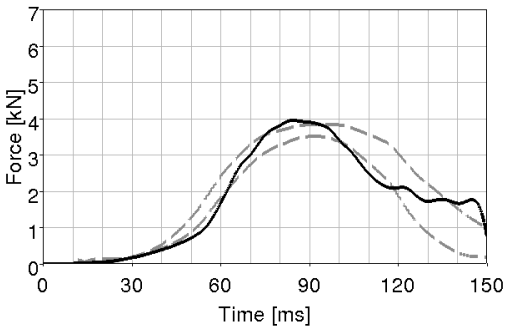


Figure F.0.1: *Shoulder belt force in 30° far side collision with THUMS, Heidelberg. From* Unpublished material from the Heidelberg test *(2012).*

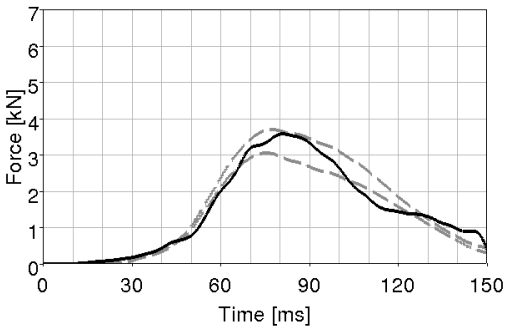


Figure F.0.2: *Lap belt force in 30° far side collision with THUMS, Heidelberg. From* Unpublished material from the Heidelberg test *(2012).*

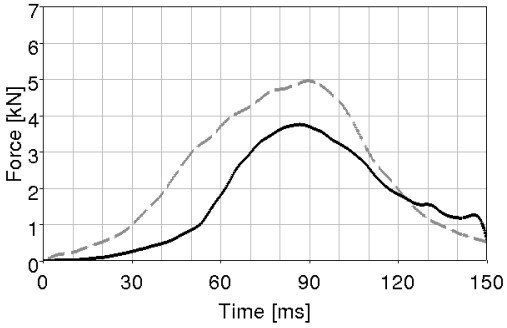


Figure F.0.3: *Shoulder belt force in 15° far side collision with THUMS, Heidelberg. From* Unpublished material from the Heidelberg test *(2012).*

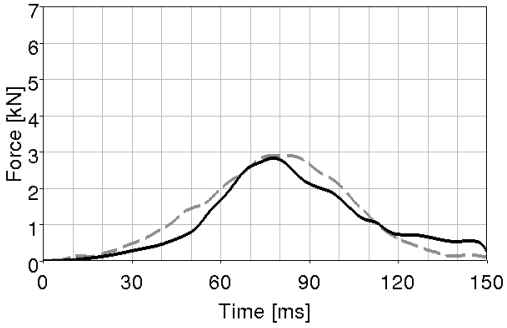


Figure F.0.4: *Lap belt force in 15° far side collision with THUMS, Heidelberg. From* Unpublished material from the Heidelberg test *(2012).*

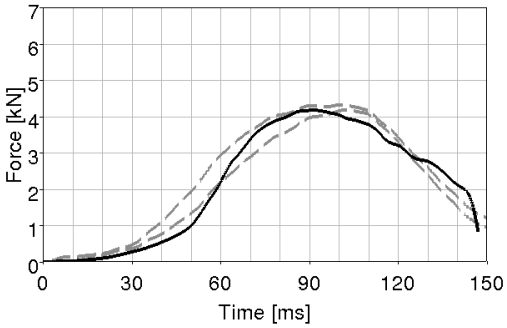


Figure F.0.5: *Shoulder belt force in 15° near side collision with THUMS, Heidelberg. From* Unpublished material from the Heidelberg test *(2012).*

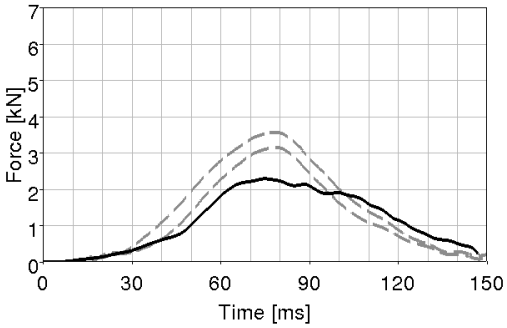


Figure F.0.6: *Lap belt force in 15° near side collision with THUMS, Heidelberg. From* Unpublished material from the Heidelberg test *(2012).*

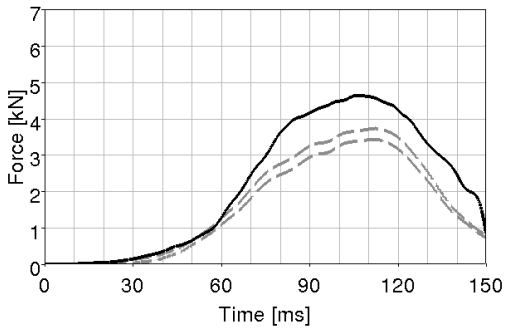


Figure F.0.7: *Shoulder belt force in 30° near side collision with THUMS, Heidelberg. From* Unpublished material from the Heidelberg test *(2012).*

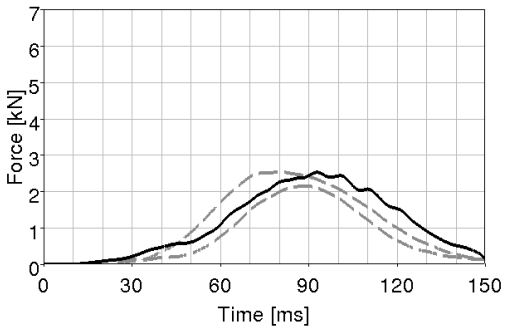


Figure F.0.8: *Lap belt force in 30° near side collision with THUMS, Heidelberg. From* Unpublished material from the Heidelberg test *(2012).*

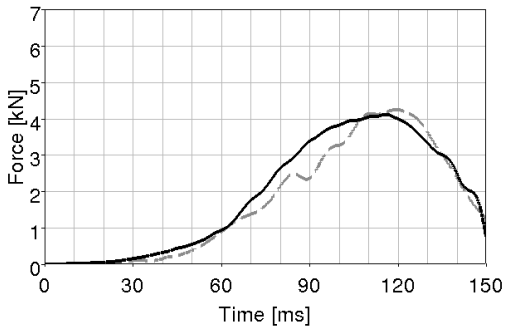


Figure F.0.9: *Shoulder belt force in 45° near side collision with THUMS, Heidelberg. From* Unpublished material from the Heidelberg test *(2012).*

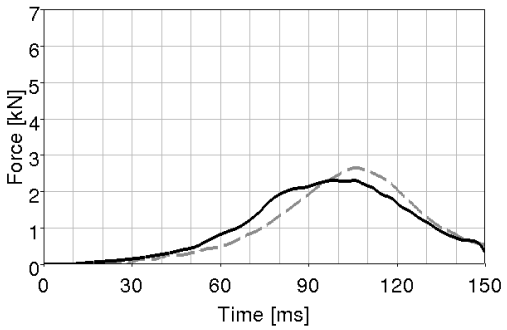


Figure F.0.10: *Lap belt force in 45° near side collision with THUMS, Heidelberg. From* Unpublished material from the Heidelberg test *(2012).*

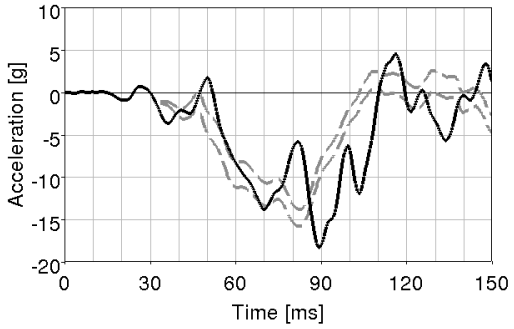


Figure F.0.11: *X acceleration in T6 in 30° far side collision with THUMS, Heidelberg. From* Unpublished material from the Heidelberg test *(2012).*

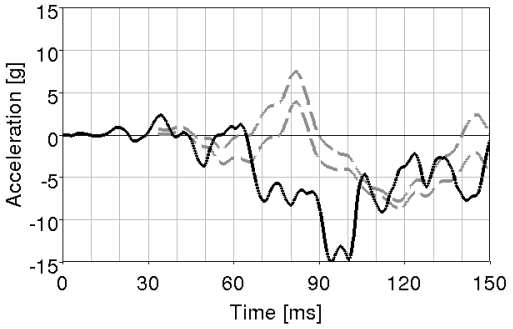


Figure F.0.12: *Z acceleration in T6 in 30° far side collision with THUMS, Heidelberg. From* Unpublished material from the Heidelberg test *(2012).*

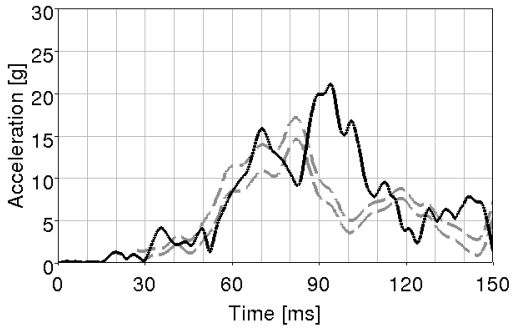


Figure F.0.13: *XZ acceleration in T6 in 30° far side collision with THUMS, Heidelberg. From* Unpublished material from the Heidelberg test *(2012).*

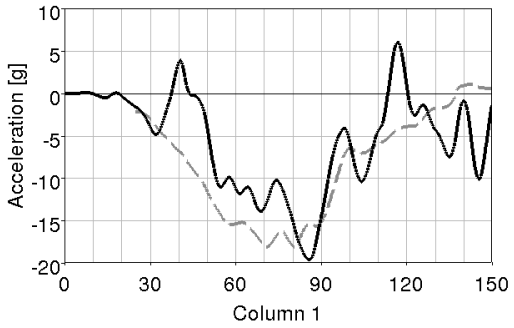


Figure F.0.14: *X acceleration in T6 in 15° far side collision with THUMS, Heidelberg. From* Unpublished material from the Heidelberg test *(2012).*

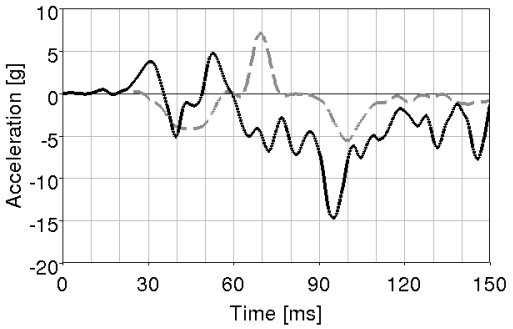


Figure F.0.15: *Z acceleration in T6 in 15° far side collision with THUMS, Heidelberg. From* Unpublished material from the Heidelberg test *(2012).*

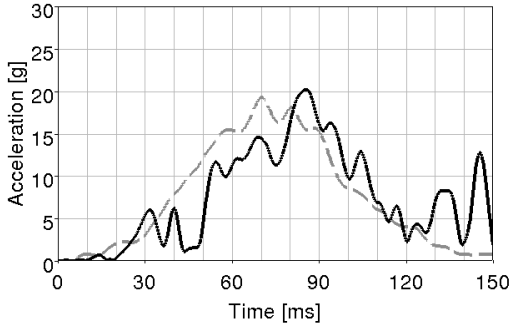


Figure F.0.16: *XZ acceleration in T6 in 15° far side collision with THUMS, Heidelberg. From* Unpublished material from the Heidelberg test *(2012).*

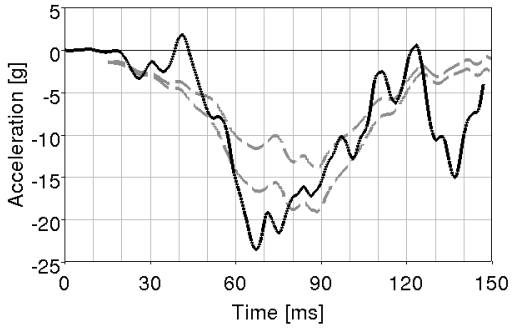


Figure F.0.17: *X acceleration in T6 in 15° near side collision with THUMS, Heidelberg. From* Unpublished material from the Heidelberg test *(2012).*

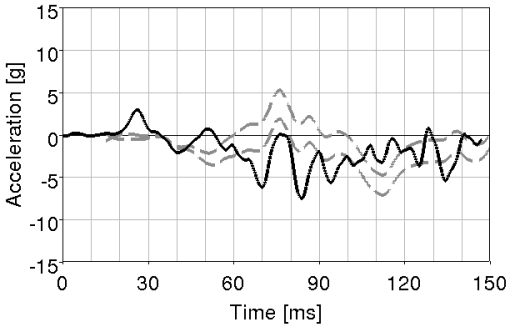


Figure F.0.18: *Z acceleration in T6 in 15° near side collision with THUMS, Heidelberg. From* Unpublished material from the Heidelberg test *(2012).*

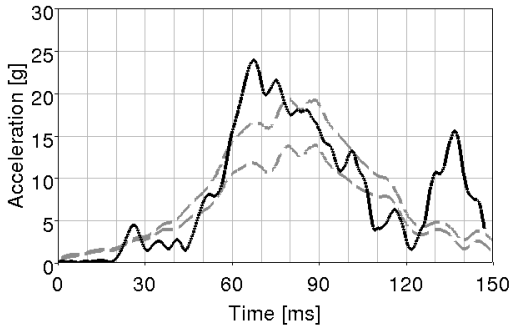


Figure F.0.19: *XZ acceleration in T6 in 15° near side collision with THUMS, Heidelberg. From* Unpublished material from the Heidelberg test *(2012).*

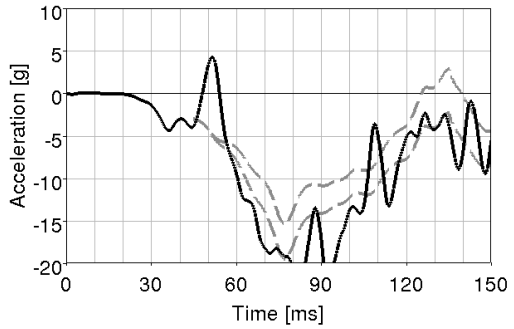


Figure F.0.20: *X acceleratione in T6 in 30° near side collision with THUMS, Heidelberg. From* Unpublished material from the Heidelberg test *(2012).*

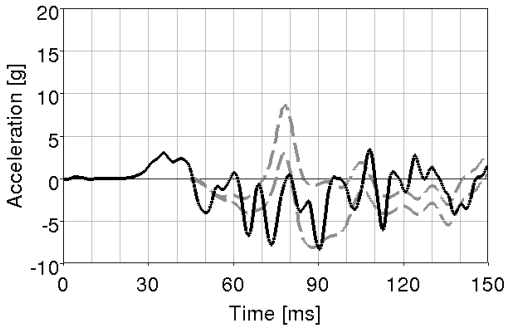


Figure F.0.21: *Z acceleratione in T6 in 30° near side collision with THUMS, Heidelberg. From* Unpublished material from the Heidelberg test *(2012).*

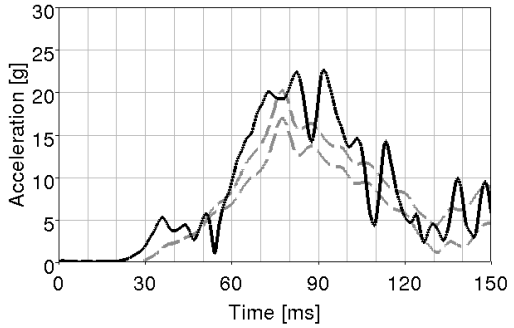


Figure F.0.22: *XZ acceleration in T6 in 30° near side collision with THUMS, Heidelberg. From* Unpublished material from the Heidelberg test *(2012).*

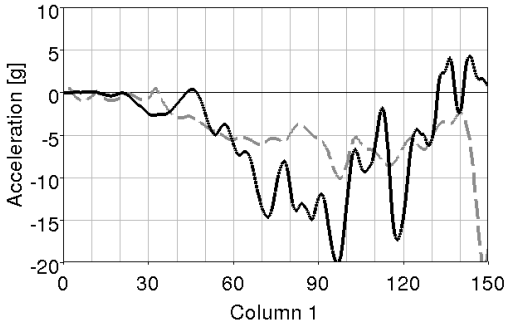


Figure F.0.23: *X acceleration in T6 in 45° near side collision with THUMS, Heidelberg. From* Unpublished material from the Heidelberg test *(2012).*

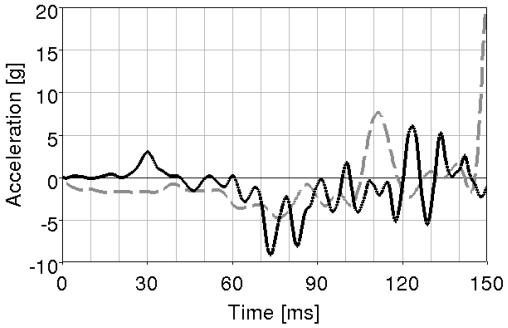


Figure F.0.24: *Z acceleration in T6 in 45° near side collision with THUMS, Heidelberg. From* Unpublished material from the Heidelberg test *(2012).*

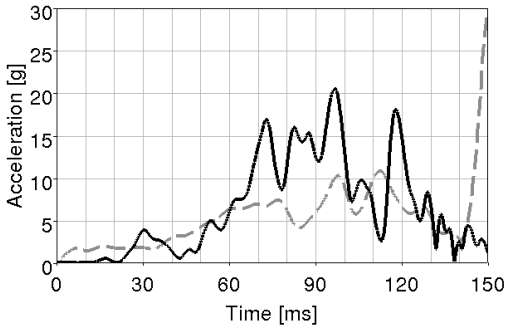


Figure F.0.25: *XZ acceleration in T6 in 45° near side collision with THUMS, Heidelberg. From* Unpublished material from the Heidelberg test *(2012).*

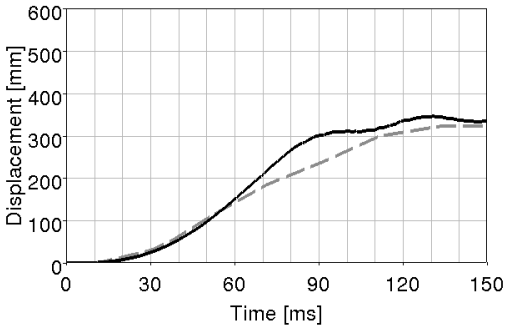


Figure F.0.26: *X displacement of loaded shoulder in 30° far side collision with THUMS, Heidelberg. From* Unpublished material from the Heidelberg test *(2012).*

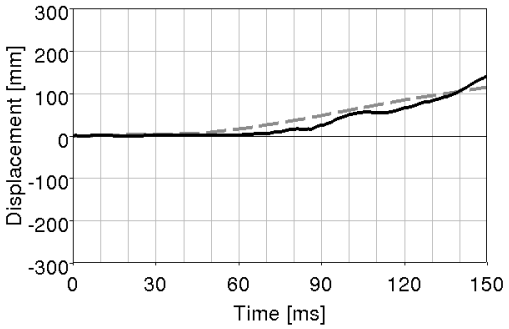


Figure F.0.27: *Y displacement of loaded shoulder in 30° far side collision with THUMS, Heidelberg. From* Unpublished material from the Heidelberg test *(2012).*

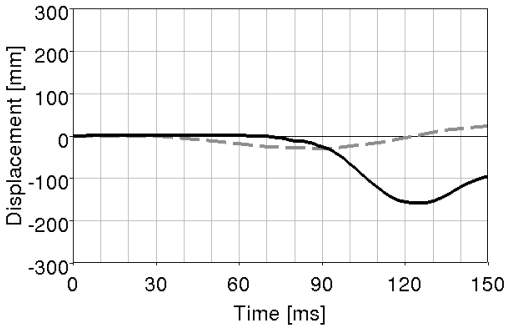


Figure F.0.28: *Z displacement of loaded shoulder in 30° far side collision with THUMS, Heidelberg. From* Unpublished material from the Heidelberg test *(2012).*

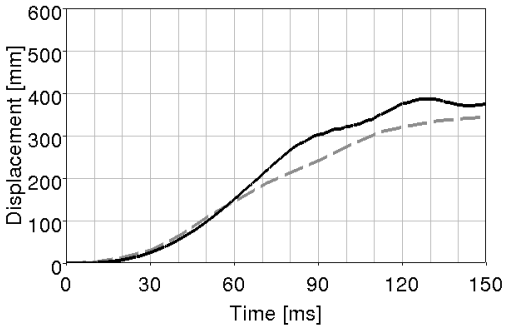


Figure F.0.29: *XYZ displacement of loaded shoulder in 30° far side collision with THUMS, Heidelberg. From* Unpublished material from the Heidelberg test *(2012).*

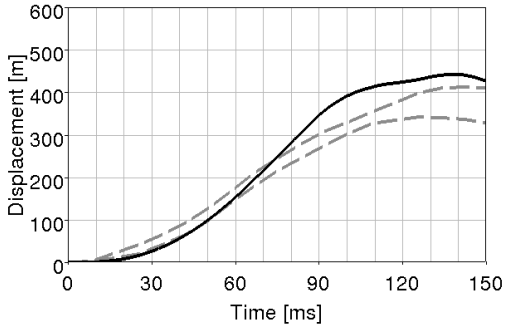


Figure F.0.30: *X displacement of unloaded shoulder in 30° near side collision with THUMS, Heidelberg. From* Unpublished material from the Heidelberg test *(2012).*

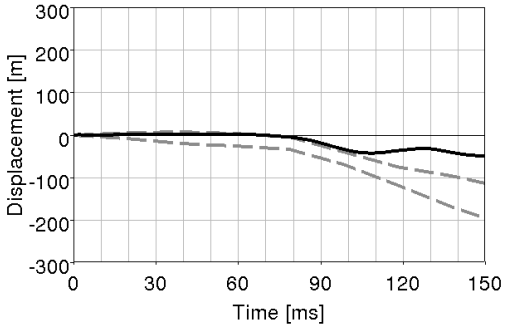


Figure F.0.31: *Y displacement of unloaded shoulder in 30° near side collision with THUMS, Heidelberg. From* Unpublished material from the Heidelberg test *(2012).*

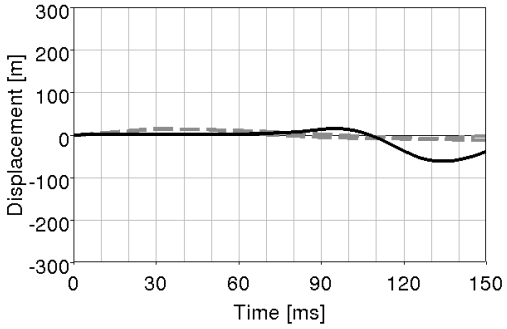


Figure F.0.32: *Z displacement of unloaded shoulder in 30° near side collision with THUMS, Heidelberg. From* Unpublished material from the Heidelberg test *(2012).*

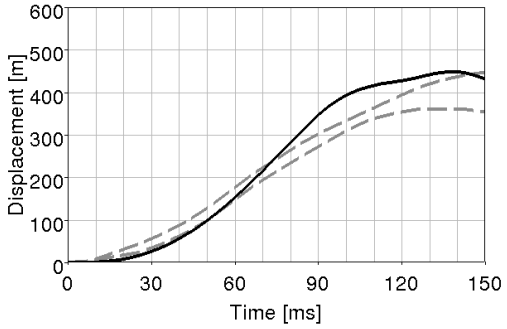


Figure F.0.33: *XYZ displacement of unloaded shoulder in 30° near side collision with THUMS, Heidelberg. From* Unpublished material from the Heidelberg test *(2012).*

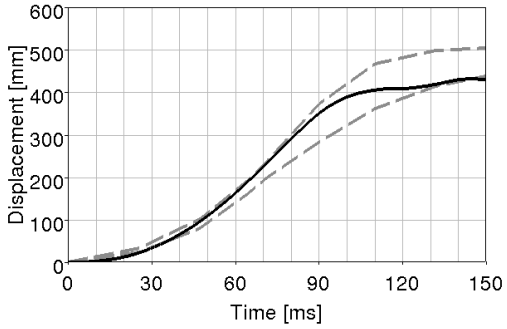


Figure F.0.34: *X displacement of unloaded shoulder in 45° near side collision with THUMS, Heidelberg. From* Unpublished material from the Heidelberg test *(2012).*

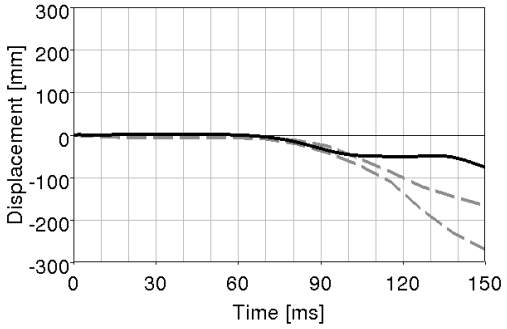


Figure F.0.35: *Y displacement of unloaded shoulder in 45° near side collision with THUMS, Heidelberg. From* Unpublished material from the Heidelberg test *(2012).*

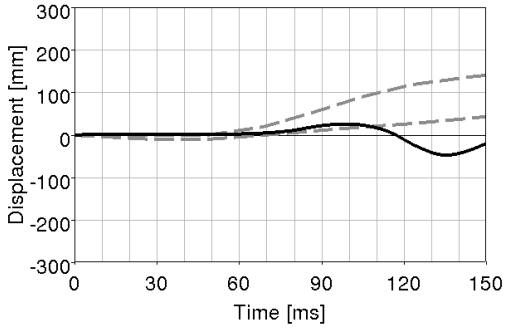


Figure F.0.36: *Z displacement of unloaded shoulder in 45° near side collision with THUMS, Heidelberg. From* Unpublished material from the Heidelberg test *(2012).*

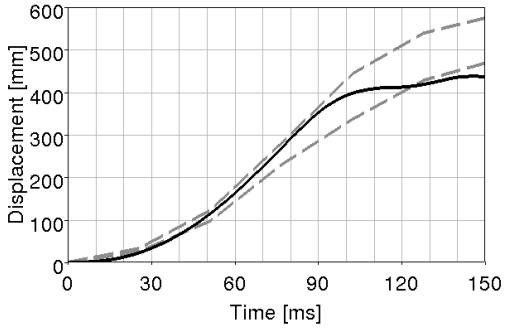


Figure F.0.37: *XYZ displacement of unloaded shoulder in 45° near side collision with THUMS, Heidelberg. From* Unpublished material from the Heidelberg test *(2012).*